Green Energy and Technology

Carlo Giavarini
Keith Hester

Gas Hydrates

Immense Energy Potential and Environmental Challenges

Springer

Green Energy and Technology

For further volumes:
http://www.springer.com/series/8059

Carlo Giavarini · Keith Hester

Gas Hydrates

Immense Energy Potential and Environmental Challenges

Springer

Carlo Giavarini
Department of Ingegneria Chimica
University of Rome La Sapienza
Via Eudossiana 18
00184 Rome
Italy
e-mail: giavarini2@interfree.it

Keith Hester
S Quaker Ave 4514
Tulsa, OK 74105
USA
e-mail: ketone303@gmail.com

ISSN 1865-3529
e-ISSN 1865-3537
ISBN 978-0-85729-955-0
e-ISBN 978-0-85729-956-7
DOI 10.1007/978-0-85729-956-7
Springer London Dordrecht Heidelberg New York

British Library Cataloguing in Publication Data
A catalogue record for this book is available from the British Library

Cover design: eStudio Calamar, Berlin/Figueres

Printed on acid-free paper

Springer is part of Springer Science+Business Media (www.springer.com)

Foreword

The scientific community has known and studied gas hydrates for decades. However, most people do not know of this "strange" material so common on the Earth. At the international level, it seems that a text is missing for non-experts in gas hydrates. This book aims to fill this gap, in the simplest way possible, by explaining in a strictly scientific manner what gas hydrates are and highlighting the important energy and environmental aspects related to them. Are gas hydrates a huge source of energy or an environmental challenge to humanity, or both?

Our ambition is to make the main issues and implications of gas hydrates accessible to a general technical audience, while providing enough detail to be useful for the practicing scientist or engineer. In large part, the various chapters have been designed so they can be read independently of each other, without compromising overall understanding. The use of equations, formulas, and complicated graphs has been limited as much as possible. Non-technical readers may gloss over some of the more specific discussions without losing the overall message presented. For the experts, some parts may seem elementary. However, it is hoped that this does not jeopardize the general idea of the work.

The field of gas hydrates is fascinating and covers virtually all disciplines ranging from chemistry to geology to biology. From the engineering of energy production and transportation to environmental science and climatology, gas hydrates present difficult challenges and exciting possibilities.

For more in-depth specific knowledge of the various scientific and engineering aspects related to gas hydrates, we direct the reader to now classic works on gas hydrates by authors such as E. D. Sloan, Y. Makogon, M. Max, J. Carrol, T. Collett, B. Dillon, J. S. Gudmunsson, and others. These texts will be frequently cited in the various chapters of this book.

Contents

Abbreviations

ANG	Adsorbed natural gas
bbl	Barrel
BP	Before present
CNG	Compressed natural gas
DEG	Diethylene glycol
DOE	US Department of Energy
DSC	Differential scanning calorimetry
EO	Ethylene oxide
EPICA	European project for ice coring in Antarctica
FPSO	Floating Production, Storage, and Offloading
GHSZ	Gas hydrate stability zone
GRIP	Greenland ice core project
GTL	Gas-to-liquids
GTW	Gas to wire
H	Hydrate
I (or) Ih	Hexagonal ice
ICGH	International Conference on Gas Hydrates
IFP	French Petroleum Institute
IGCC	Integrated gasification combined cycle
IODP	Integrated ocean drilling program
IPCC	Intergovernmental panel on climate change
IPEV	French Polar Institute Paul-Emile Victor
JAPEX	Japan Petroleum Exploration Co
JIP	Joint industry project
JNOC	Japanese national oil company
KHI	Kinetic hydrate inhibitor
LDHI	Low-dosage hydrate inhibitor
LNG	Liquefied natural gas
L_w	Liquid water
MDSC	Modulated differential scanning calorimetry
MEG	Monoethylene glycol

MES	Mitsui Engineering and Shipbuildings Co.
MeOH	Methanol
MM	Thousand
MMbpd	Million barrels per day
MMcm	Million cubic meters
Mscf	Thousand standard cubic feet
mol%	Mole percent
n	Hydration number
NGH	Natural gas hydrate
NGHP	National gas hydrate program of India
NMR	Nuclear magnetic resonance
OECD	Organization for Economic Co-operation and Development
P	Pressure
P–T	Pressure–Temperature
PNRA	Italian National Antarctic Research Program
PVCap	Polyvinylcaprolactam
PVP	Polyvinyl pyrrolidone
Q_1	Lower quadruple point
Q_2	Upper quadruple point
ROV	Remotely operated vehicle
sI	Type-I or Structure I gas hydrate
sII	Type-II or Structure II gas hydrate
sH	Type-H or Structure H gas hydrate
SEM	Scanning electron microscopy
STP	Standard temperature and pressure
T	Temperature
T-x	Temperature-composition
TCM	Trillion cubic meters
THF	Tetrahydrofuran
TMO	Trimethylene oxide
toe	Tons of oil equivalent
USGS	US Geological Survey
v	Vapor
wt%	Weight percent

Introduction

In 1996, off the coast of California, in the Monterey Bay Canyon, a special remote operated vehicle comes to rest on the ocean floor at over 900 m depth. A controlled amount of methane is injected into the 4°C water and bottom sediments. Within seconds, this mixture of gas and water formed into a solid mass, bright white, and fluffy. In this way, it was experimentally confirmed that methane hydrate formation was not only possible in marine waters but extremely easy and rapid, provided the presence of suitable pressure and temperature conditions.

In November 2000, a fishing trawler off the coast of Vancouver, Canada, pulled up a large block of yellow-stained *ice*. Almost immediately, the catch began to bubble and fizz. The crew had inadvertently discovered a large seafloor deposit of methane hydrate. If a sailor had lit a match, there could have been disaster as the gas hydrates they brought on board were releasing large quantities of hydrocarbon gas as they bubbled away.

The discovery of gas hydrates dates back to 1810. Sir Humphry Davy is given credit for the discovery of hydrates formed from chlorine. These compounds were largely treated as a scientific curiosity until the third decade of the last century, when a connection between hydrates and blockages in oil and gas pipelines was established.

Naturally occurring hydrates were first discovered in the 1960s by Yuri Makogon, where the Russians produced gas from hydrates in the Siberian permafrost. Since that discovery, subsequent research has led to the discovery of vast deposits of hydrates in nature, both in the permafrost and the continental shelves of the World's oceans.

Will gas hydrates become a significant source of energy? Despite the recent acceleration of activities to develop reliable production techniques, it seems unlikely that we will see significant global production within the next 10 to 15 years. However, in certain parts of the world (e.g. Japan and India) with limited resources of conventional energy sources, it is possible that methane hydrates may become an important source of natural gas in the near future.

The recognition that enormous quantities of methane in gas hydrates exist (and have existed) in the subsurface has led to a reconsideration of past climatic events

in the Earth's history. Researchers have hypothesized that former catastrophic releases of methane could have been related with disturbance of gas hydrate deposits. This concern has led environmentalists to consider the current potential of gas hydrates to be involved in future large-scale climate change events.

Undoubtedly, many environmental concerns associated with gas hydrates need to be resolved. For example, the stability of submarine slopes containing hydrates needs to be better understood. A large scale disturbance, such as an earthquake or increasing sea temperatures, could lead to massive release of methane, a potent greenhouse gas, from their icy cages into the atmosphere.

Chapter 1
The Evolution of Energy Sources

1.1 Conventional Fossil Fuels

Coal, oil, and natural gas have served as the traditional energy sources for mankind and have played an enormous role in the development of our modern society. Coal originally displaced wood as the World's major energy supplier, helping spark the Industrial Revolution in the latter part of the eighteenth century. The age of petroleum began in 1859 starting with the first oil well drilled by Colonel Edwin Drake in Titusville, Pennsylvania. Since that time, oil and refined petroleum products have evolved to power transportation over land, sea, and air [2]. It is worth mentioning that the transportation sector relies on oil for 97–98% of its energy and consumes over 50% of the World's oil. Natural gas usage lagged behind oil but is now continually increasing as transportation issues associated with moving a gas versus a liquid are being (at least partially) solved through pipelines and liquefaction techniques.

Despite the decline of coal usage compared to oil and gas, coal reserves far exceed conventional oil and gas and remain an important energy source. This can be seen in Table 1.1, which gives energy consumption by different sources over the last 25 years. Figure 1.1 shows the relative importance of different energy sources over the last century. For comparison purposes, all energy usage has been converted to tons of oil equivalent (toe). Thus, for example, a ton of oil equivalent is about 1,200 m^3 of natural gas.

1.1.1 Crude Oil

Figure 1.2 shows the evolution of oil demand in the period 2006–2010, fluctuating around 86 million barrels/day (MMbpd), or about 4.3 billion tons/year. In contrast to Organization for Economic Co-operation and Development (OECD) member nations, non-OECD countries are steadily increasing their consumption of crude

C. Giavarini and K. Hester, *Gas Hydrates*, Green Energy and Technology,
DOI: 10.1007/978-0-85729-956-7_1, © Springer-Verlag London Limited 2011

Table 1.1 Worldwide energy consumption (in millions of toe)

	1985	1990	1995	2000	2005	2008	% in 2008
Crude oil	2,793	3,172	3,283	3,612	3,892	3,929	34.6
Natural Gas	1,492	1,781	1,914	2,178	2,508	2,768	24.4
Coal	2,089	2,246	2,239	2,247	2,884	3,324	29.3
Nuclear	335	453	526	585	627	620	5.4
Hydro-Geo	448	490	562	601	658	718	6.3
Total	7,157	8,142	8,524	9,223	10,569	11,359	100.0

Source: BP Statistical Review

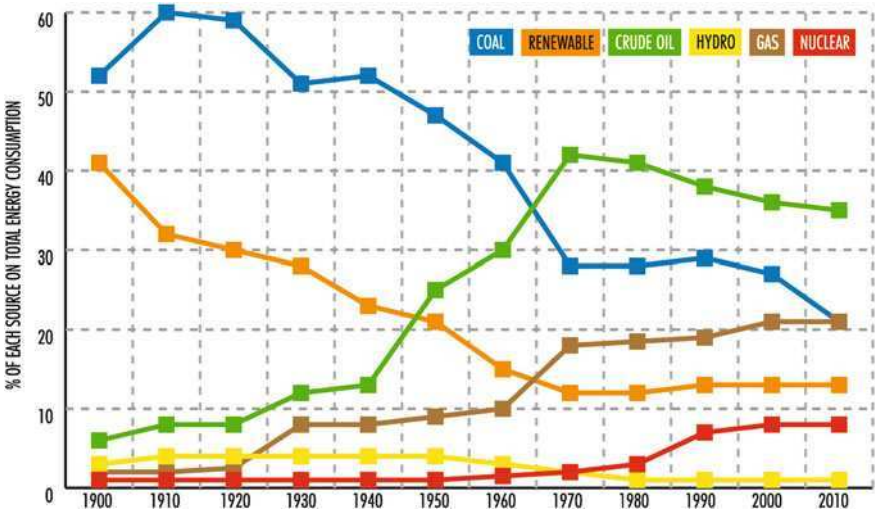

Fig. 1.1 The relative importance of different energy sources in the twentieth century (IEA Data Processing and Aeneas by IIASA-WEC)

oil. China is now a major energy consuming nation, responsible of about one-third of new growth in oil demand.

The future of oil will be likely more influenced by geo-political attitudes than exhaustion of resources. As the Stone Age did not end due to lack of stones, the Age of Oil will likely not end due to lack of the raw material, but for other reasons.

Current estimates of conventional oil (over 160 billon tons) could supply 40 years of demand, at current rates of consumption. One should note that 30 years ago, estimated reserves and "Peak Oil" could then only ensure consumption for three decades or so. In fact, the amount of current new discoveries (though more limited on scale than previous ones) and improved production techniques with higher extraction efficiencies contribute to the continually positive increases in oil reserves. Figure 1.3 shows the estimate from the French Institute of Petroleum, which is similar for other oil companies. Production is expected to reach its peak around 2035 and begin to slowly decline. The increasing forward

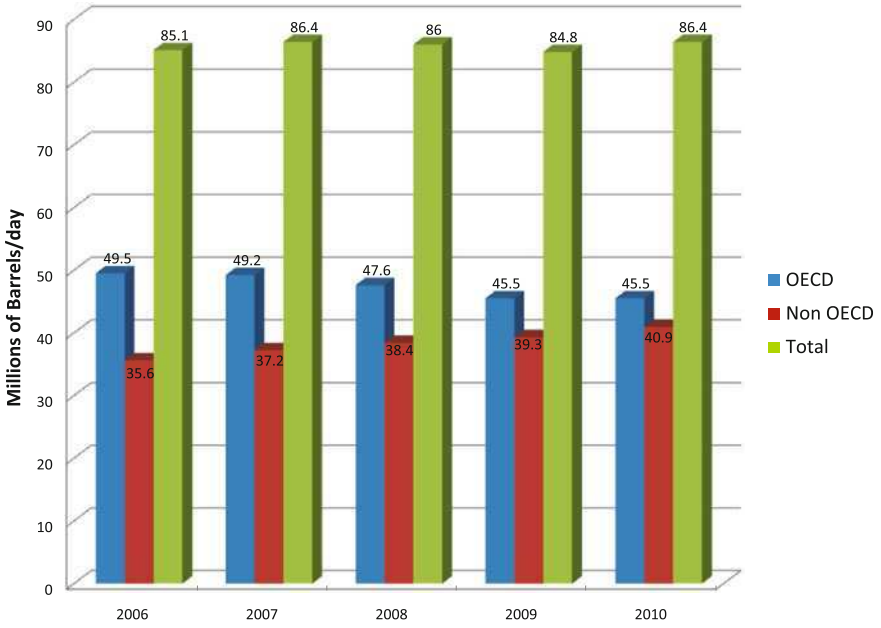

Fig. 1.2 Total oil demand for OECD and non-OECD nations (Source: Hydrocarbon Process, January 2011)

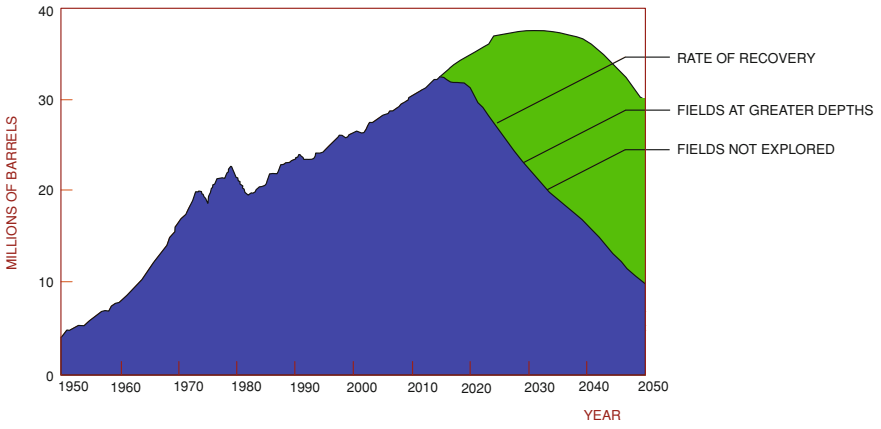

Fig. 1.3 Evolution of oil production. IFP forecast through 2050

estimates of peak oil production is attributed to discovery of new reserves and advancement in oil drilling technology (increase in achievable drilling depths, better drilling techniques, and enhanced oil recovery capabilities, from $\sim$35% to over 50%).

Table 1.2 Typical compositions of dry and wet gases (mol%)

Components	Dry gas	Wet gas
Hydrocarbons		
Methane	70–99	50–92
Ethane	1–10	5–15
Propane	Trace-5	2–14
Butane	Trace-2	1–10
Pentane	Trace-1	Trace-5
Non hydrocarbons		
Nitrogen	Trace-15	Trace-10
CO_2	Trace-1	Trace-14
H_2S	0-Trace	0–6
Helium	0–5	0

* The values here should be considered as averages. There may be gas reservoirs with significantly higher content of individual species, e.g., H_2S

The largest known reserves are held by countries such as Saudi Arabia (nearly 40 billion tons), followed by Iran (just under 20 billion tons), Iraq, Kuwait, UEA, Venezuela, and Russia. While countries such as Norway, Nigeria, and Libya (along with Russia) do not have the largest reserves, they are among the largest worldwide exporters. As we will see later, other petroleum sources, such as oil sands and extra-heavy oils, are moving closer to being considered conventional and the international distribution of known petroleum reserves could see a marked increase.

Oil prices (reported in barrels, equivalent to 159 l) fluctuate greatly depending on events and the International economy. As a historical note for the reader, the use of barrels stems from the first containers used to transport oil: they were wooden barrels originally used to transport whiskey. While the physical metal barrels used today have a greater volume, the barrel unit was standardized at 42 US gallons for commercial and fiscal purposes. To convert between barrels and tons, you can multiply barrels by 0.14 taking into account an average crude oil specific gravity of about 0.85.

1.1.2 Natural Gas

The term *natural gas* is usually reserved for gas from subsurface sediments that is rich in methane, but often contains higher hydrocarbons (primarily ethane and propane). It can also contain higher hydrocarbons and various amounts of acid gases such as carbon dioxide and hydrogen sulfide.

Natural gas is defined as a *wet gas* if it contains relatively significant amounts of higher hydrocarbons compared to methane. The definition of a *sour gas* is one that contains sulfur compounds, particularly hydrogen sulfide. Otherwise, it is known as *sweet gas*. Table 1.2 gives typical ranges for parameters defining the quality of a

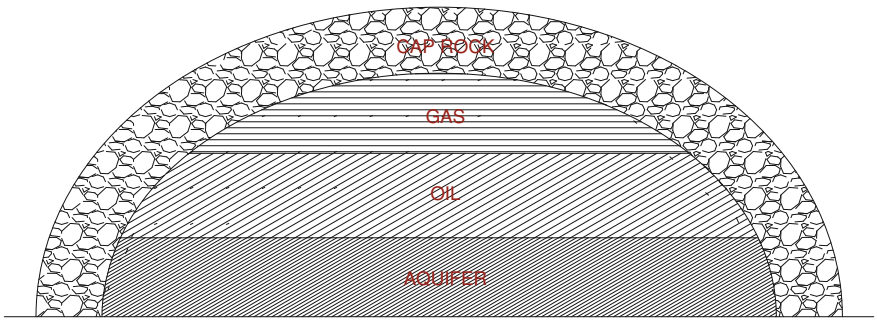

Fig. 1.4 Schematic of a field with associated natural gas

natural gas and their effect on the price it is traded for. A sweet gas typically will sale for a higher price than a sour gas as less processing is needed from raw to final product. Natural gas is often associated with oil production and present in the upper layer of a petroleum deposit (Fig. 1.4).

Conventional natural gas reserves are substantial (about 190 trillion cubic meters, or 160 billion toe), accounting for over 60 years at current rates of consumption. Non-conventional reserves are becoming increasing important (e.g., shale gas and coal bed methane). This could be especially true as natural gas consumption is steadily increasing and anticipated to surpass oil with 10–20 years. The most prevalent deposits are in Russia ($\sim$50,000 MM m^3), Iran, Qatar, Saudi Arabia, UAE, USA, and Algeria. Russia is the World's largest producer, followed by the USA.

The success of natural gas comes from the fact that it can be easily purified and transformed into an almost pure methane product. Methane, which contains only one atom of carbon with four atoms of hydrogen, is the cleanest burning fossil fuel. It is currently the main source for deriving hydrogen gas and will be for the foreseeable future.

Contrasting the simple clean burning nature of methane, because it is a gas, transportation and storage are significantly more complex compared to liquid petroleum products. The relative ease of liquid oil transportation allows access to different markets over the lifetime of producing a well. With natural gas, dedicated infrastructure must be in place, such as a pipeline or liquefied natural gas (LNG) plant, to ensure the gas can reach the market. This is usually stipulated in the contract terms and certain guarantees and certainty is needed before such an economic investment can be made. Much of the proven natural gas reserves are considered *stranded*, meaning they are difficult to reach or far from current markets and not large enough to justify an investment in a pipeline or LNG plant.

Beyond traditional means of transporting natural gas, new technologies are being developed. These include high pressure transportation, gas-to-liquids (GTL) conversion, and in the form of gas hydrates. As further detailed in Chap. 9, these technologies seem particularly well suited for stranded gas fields (Fig. 1.5).

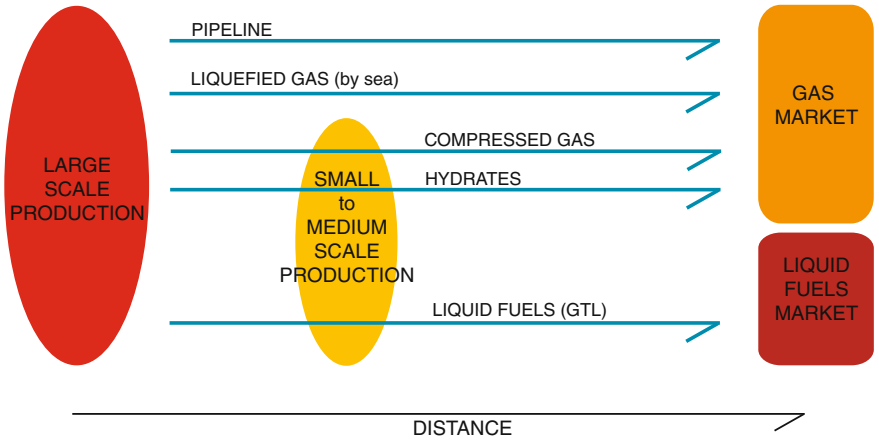

Fig. 1.5 Transportation methods for natural gas

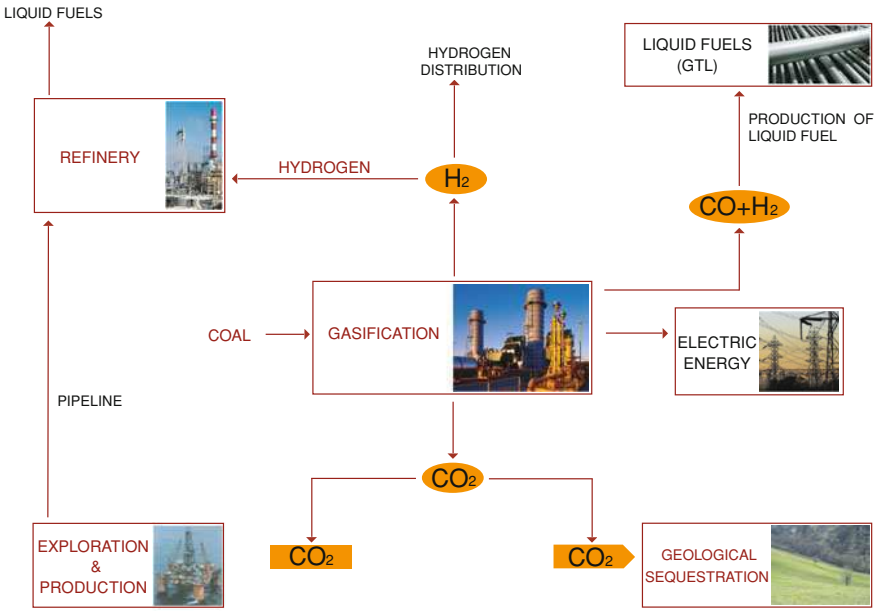

Fig. 1.6 Integration of coal gasification for electricity with hydrogen and liquid fuels production, including separation and sequestration of CO_2

1.1.3 Coal

Excluding gas hydrates, coal reserves are by far the largest of the fossil fuels. They amount to more than 570 billion toe and could provide energy at current rates for

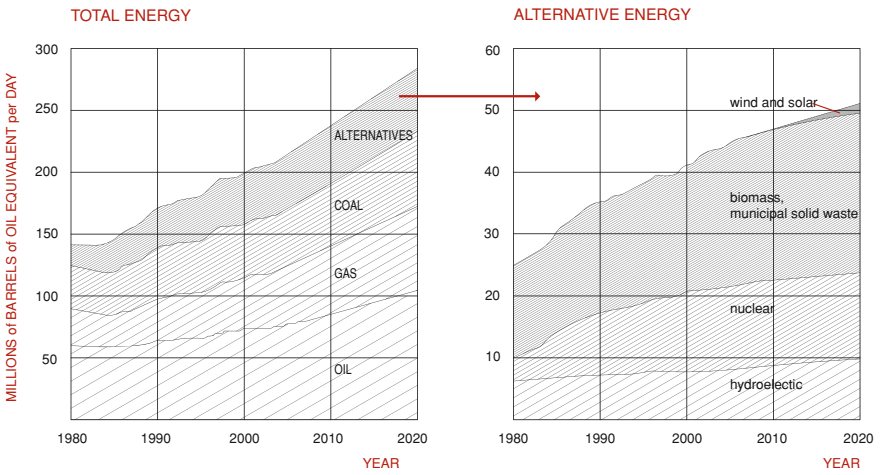

Fig. 1.7 Consumption forecasts for 2020 for nuclear power and renewable energy sources. (Source: Exxon Mobil, 2005)

about 230 years. Although coal usage has long been surpassed by oil, coal consumption is still important. After a period of stagnation, coal consumption again began to increase after 2000 and the most reliable forecasts show a further significant increase particularly from 2010. This is due to a variety of reasons, including strategic, political, and technological ones.

The largest reserves are in locations such as Australia, the United States, Russia, and Europe. Modern technologies, such as gasification or carbon capture, are being developed to allow for much cleaner burning of coal. Figure 1.6 shows a schematic of the modern use of coal, petroleum refining, and the relationship to features of carbon dioxide disposal. The fact remains that coal is harder to extract, transport, store, and use, compared to liquid fuel.

1.2 Nuclear Power and Renewable Energy Sources

1.2.1 Nuclear Power

To meet the increasing demand for energy, a wide portfolio of energy sources and options will be needed in addition to oil, natural gas, and coal. This includes nuclear and renewable energy sources. These contributions are depicted in Fig. 1.7.

Table 1.1 shows the stagnation of energy production from nuclear in recent years, largely driven by concerns over the safety of nuclear power plants and safe disposal of the resulting nuclear product. The usage of nuclear for electricity remains high in many countries, including France ($\sim$76% of electricity produced)

and Germany (30%). The choice to use nuclear power has a higher *rigidity,* even compared to coal, due to the cost and time required to setup, build, and operate new nuclear plants. The latest studies do not show a predicted substantial future increase in the use of nuclear energy, especially after the Japan earthquake in March 2011 and the consequent nuclear plant disaster.

1.2.2 Renewable Energy Sources

The main renewable energy sources are solar, hydroelectric, wind, and biomass. Hydroelectric power was the first of them to be industrially developed. It remains a contributor in many countries and grow is expected. Currently, hydroelectricity accounts for around 20% of the World's electricity and near 90% of electricity derived from renewable sources. However, much of the hydroelectric power possible from water sources above sea level has already been utilized and future sources, such as from waves, are only currently in the development stages.

As shown in the right hand side diagram of Fig. 1.7, solar and wind energy are experiencing double-digit growth, largely thanks to government incentives and technological advances. While growing, the overall contribution from solar and wind is still low and probably will still be less than 0.5% of total electricity production worldwide by 2020.

Biomass includes garbage, wood, landfill gases, and biofuels. First generation biofuels, largely ethanol derived from corn and sugar cane, have experienced controversy from overall energy efficiency to disruption of global food prices. Second generation biofuels, such as those derived directly from cellulose and algae, show greater promise for the future and are currently active areas of research, both academically and industrially.

1.3 Non-Conventional Fossil Fuel Sources

At a time of increased tension between countries rich in oil and gas and those countries heavily dependent on them for energy, there has been great interest in developing *non-conventional* hydrocarbons to reduce foreign energy dependence. The main non-conventional fossil fuels at this time include extra-heavy crudes, tar sands (now called oil sands), oil shales, natural gas in coal beds (coal bed methane) and the shales (shale gas), and methane trapped in gas hydrates.

Figure 1.8 shows how global oil reserves are altered if extra-heavy oil and tar sands (excluding shales) are included. Venezuela and Canada jump to first and third place, respectively, in overall reserves.

Exploitation of these non-conventional sources leads to a host of technical and economical challenges. These reserves are so abundant but so far very difficult to produce. Most are associated with high costs, due to the need to adopt new

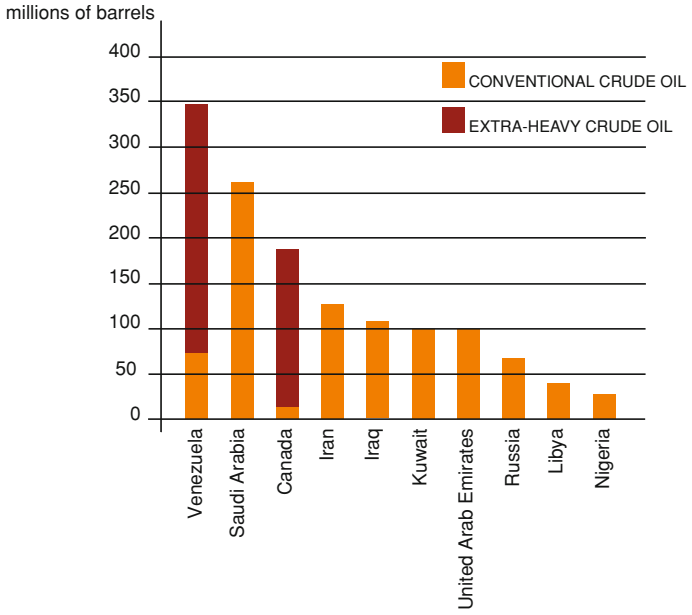

Fig. 1.8 Reserves of conventional crude versus extra-heavy oil sands (Source: B.P., Union Oil, 2006)

complex drilling and production techniques (Fig. 1.9). These new techniques in themselves also pose new environmental concerns which must also be addressed. That being said, due to the rising price of oil, Canada already exports to the USA a large and growing amount of oil extracted from oil sands. The proven reserves of conventional oil and gas were about 300×10^9 toe at the beginning of the third millennium. Non-conventional reserves were around 140×10^{12} toe, with the majority of this number being attributed to methane trapped in gas hydrates. As we well see, even with this large estimated amount of energy available, production from gas hydrates has only occurred on the pilot scale to date.

The quantities of in situ heavy oil and bitumen are also quite substantial: around 600×10^9 toe, equivalent to the remaining conventional oil reserves discovered so far. Approximately 87% of these reserves are found in the oil sands of Canada (Alberta), extra-heavy oils of Venezuela (Orinoco), and Russian heavy oils [4]. Less than 2% of these reserves have been exploited to date. With current technologies, it is estimated that the recoverable amount is about 20%, which is still over five times the oil and gas reserves of Saudi Arabia.

The estimates of gas hydrate reserves have been affected through the years by a large degree of initial uncertainty and only through concerted research efforts, including field drilling and exploration, have the estimates become more refined. While overall amounts have fallen over the years, current consensus places methane in gas hydrate reserves at several orders of magnitude over all other fossil fuels combined. Estimated reserves are $\sim 21 \times 10^{15}$ m^3 or 17,700 toe [1, 3]. This

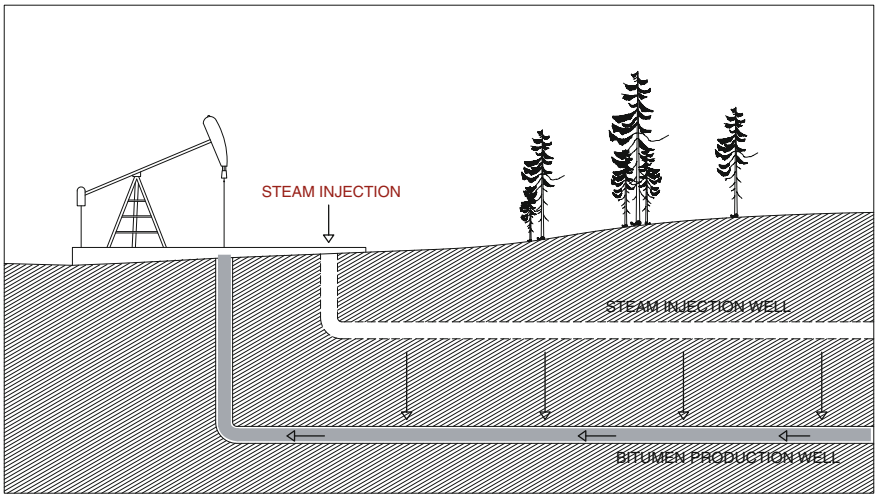

Fig. 1.9 Extraction of bitumen from tar sands in Canada, through a steam stimulation extraction process

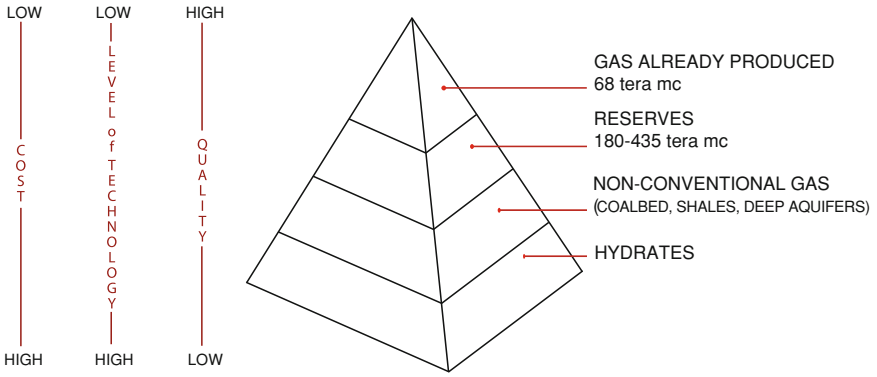

Fig. 1.10 Pyramid of natural gas resources in terms of quantity and accessibility

represents over half of the reserves of organic carbon on Earth. The possible importance of gas hydrates in the World energy scenario can therefore not be ignored, even considering that their distribution is widespread in different areas of the globe.

Figure 1.10 shows the pyramidal shape for conventional and non-conventional gas reserves, both in terms of quantity and accessibility. The conventional reserves are easier to produce but lack the abundance of the more challenging non-conventional reserves. Going from the top of the pyramid to the bottom requires an increase in the level of technology to counter increasing costs in recovery.

1.4 The Evolution of the Global Energy Market

Worldwide, there are sufficient reserves of oil, natural gas, and coal to meet energy demand for many decades to come. The likely decline of conventional oil reserves is being offset by an increase in exploitation of non-conventional reserves. Non-conventional gas reserves are abundant and growing.

However, in the present situation, it is difficult to plan investment and development for conventional resources, mainly oil and gas. Based on the overall size of market demand, operators are having to build larger structures than ever before and explore harsh regions, such as ultra-deep waters, to compete with these emerging economies, where the oil and gas companies are often state controlled.

In the case of oil, the reserve/production ratio over the last 10 years has always fluctuated up to numbers close to 40 years of availability, even when demand in the same period has grown by almost 20%.

The distribution of resources continues to be asymmetric, with the Middle East remaining a vital player in future supply, due to its abundant reserves and low production costs (3–5 US$/bbl, compared to US$12–15 in the USA and Europe). Access to the reserves in these countries has not always easy and, at times, the situation has been dramatically worse. The creation and strengthening of state companies is indicative in this respect. The high degree of uncertainty for the increased risk to capital leads to the search of non-conventional sources, making them an increasing political priority for industrialized countries.

References

1. Collett TS (2003) Natural gas hydrates as a potential energy resource. In: Max MD (ed) Natural gas hydrates in oceanic and permafrost environments. Kluwer Academic Publishers, New York
2. Giavarini C (2006) Structure and schemes of oil refining industry. In: ENI (ed) Encyclopaedia of hydrocarbons, vol 2. Treccani, Rome, pp 3–24
3. Kvenvolden KA, Lorenson TD (2001) The global occurrence of natural gas hydrate. In: Paull CK, Dillon WP (eds) Natural gas hydrates: occurrence, distribution, and detection. American Geophysical Union, Geophysical Monograph Series, vol 124, pp 3–18
4. Sanière A, Argillier TF (2005) Exploitation of heavy oils. Hydrocarbure ENSPM-IFP, vol 234, Paris, pp 11–16

Chapter 2
The Clathrate Hydrates of Gases

2.1 What are Gas Hydrates?

Gas hydrates are crystalline compounds that form when water (or ice) contacts small molecules (called hydrate *guests*) under certain pressure and temperature conditions (Fig. 2.1). The correct chemical name should be *gas clathrate hydrates*, with a clathrate being a compound formed by the inclusion of molecules of one kind in the crystal lattice of another (water in this case). In practice, these compounds are commonly referred to as gas hydrates, clathrate hydrates, or just hydrates. While specific to the particular hydrate guest, gas hydrates are stable typically at high pressures and low temperatures. A wide range of molecules have been shown to form gas hydrates. Those of the most practical interest are light hydrocarbons such as methane, ethane, and propane. Carbon dioxide and hydrogen sulfide also form hydrates and are of particular interest. When hydrates form, water crystallizes to create a lattice of molecular-sized cages that *trap* guest molecules without chemical bonding between the *host* water and the *guest* molecules (Fig. 2.2).

The hydrate crystal structure largely depends on the guest molecule housed in the lattice. Unlike hydrated salts, gas hydrates are non-stoichiometric, meaning that the ratio of guest-to-water molecules can vary based on formation conditions. As an example, if all cages of a Type-I (sI) hydrate were filled with methane, the ratio would be 5.75 H_2O:CH_4. However, in reality, the filling varies around 6 H_2O:CH_4.

Gas hydrates often act to concentrate gases (and thereby increase energy density in the case of hydrocarbons). For methane, one volume of hydrate contains more than 160 volumes of gas at standard pressure and temperature conditions, STP (Fig. 2.3). Considering that a cubic meter of natural gas at STP has an energy density of around 0.04×10^6 kJ, a cubic meter of methane hydrate contains about 6.20×10^6 kJ. Table 2.1 shows a comparison of the energy density for a number of common fuels.

C. Giavarini and K. Hester, *Gas Hydrates*, Green Energy and Technology,
DOI: 10.1007/978-0-85729-956-7_2, © Springer-Verlag London Limited 2011

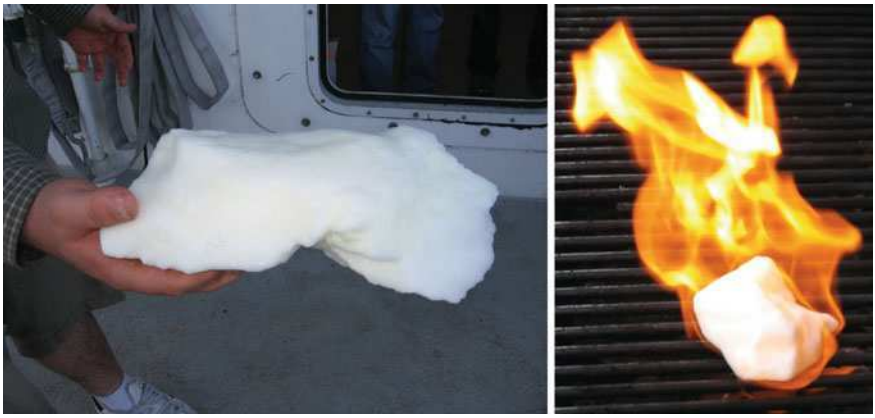

Fig. 2.1 The appearance of methane hydrate is similar to that of ice. Unlike ice, it is possible to burn the methane inside the hydrate and support a flame (Photo credit: Peter Walz, MBARI)

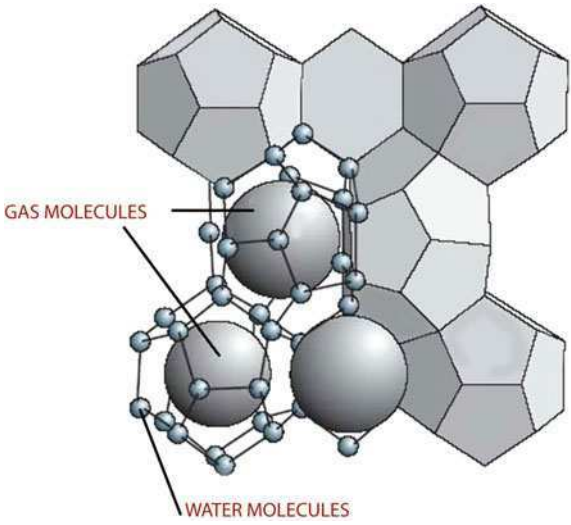

Fig. 2.2 The inclusion or *trapping* of gas molecules in the gas hydrate lattice. The molecular-sized "cages" are composed of hydrogen-bonded water molecules (Reproduced from SETARAM)

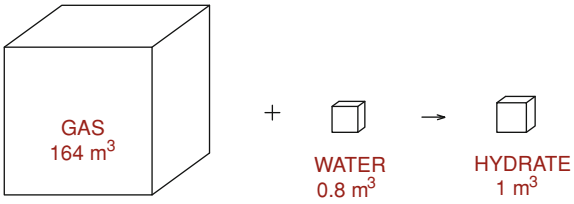

Fig. 2.3 Volumetric proportions between water and gas in a methane hydrate

Table 2.1 Comparison of the energy density of some fuels [7]

Combustible	Density (g/ml)	Energy Density (BTU/ft^3)	Energy Density (kJ/m^3)
CH_4 (gas)	6.66×10^{-4}	1,012	37,706
CH_4 (LNG)	0.42	570,000	21.2×10^6
CH_4 (sI hydrate)	0.91	165,968	6.2×10^6
Liquid hydrogen	0.07	229,000	8.5×10^6
Gasoline	0.74	876,000	32.6×10^6
Jet fuel	0.78	910,000	33.9×10^6
Diesel	0.78	995,000	37.1×10^6

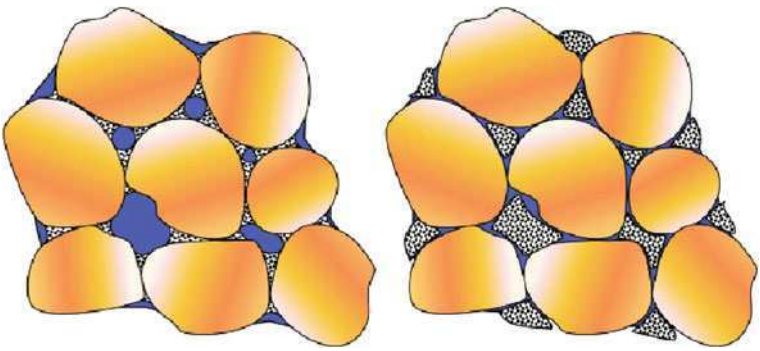

Fig. 2.4 Distribution of natural hydrates in the pore spaces of sediment (Image credit: Tim Kneafsey, Lawrence Berkeley National Laboratory)

The density of methane hydrate is similar to that of ice (around 0.91 g/cm^3 vs. 0.92 g/cm^3 of ice). There is some variation in the density based on pressure and temperature conditions and if other guests are present in the hydrate.

Suitable temperature and pressure conditions for hydrate formation can be found in on land permafrost regions as well as in vast stretches of underwater sediments, including ocean and lakes.

In terrestrial permafrost regions, given the low surface temperatures, hydrates are stable near the ground's surface. In marine settings, at over 400–500 m of water depth, the low temperatures and high pressures are able to stabilize hydrates in the sediment pore space (Fig. 2.4), up to a few 100 m below the seabed. The lower limit of hydrate stability is defined by the local geothermal gradient. Normally, temperature increases by 3–4°C every 100 m of depth for sediments on the continental slope. With increasing depth, a temperature is reached where hydrates are no longer stable.

The source of methane in naturally occurring hydrates is largely from biogenic origin, where methane is generated in situ by *methanogenesis* as bacteria break down organic matter. Methane can also migrate from deeper *thermogenic* sources.

Table 2.2 Major scientific research achievements in gas hydrates from 1810 to 1925

Year	Event
1778	Inference of SO_2 hydrate by Sir Joseph Priestly
1810	Discovery of chlorine hydrates by Sir Humphry Davy
1823	Definition of the hydrate formula (Cl_2-$10H_2O$) by Faraday
1828	Discovery of bromine hydrates by Löwig
1829	Verification of SO_2 hydrate existence ($SO_2 \cdot 7H_2O$)
1884	Le Chatelier defined the slope change for the P–T hydrate stability curve for chlorine hydrate at 273K
1882	Discovery of CO_2 hydrate
1877–1882	Discovery of mixed CO_2-PH_3 and H_2S-PH_3 hydrate
1888	Villard discovered hydrates containing methane, ethane, ethylene, acetylene, and nitrous oxide
1890	Villard discovered propane hydrates and found that the lower quadruple point temperature decreases with increasing molecular weight of the hydrate guest
1896	Villard suggested that N_2 and O_2 could also form gas hydrates
1902	de Forcrand was the first to report the use of the Clausius–Clapeyron equation to calculate gas hydrate heats of formation and compositons
1925	de Forcrand discovered hydrates of krypton and xenon

2.2 A Little Historical Information

The evolution of man's knowledge on gas hydrates has developed in three main phases [8]:

- The first phase began with the discovery that certain gases can form solid compounds with water (1810) and continued as a scientific curiosity as researchers prepared and experimented with new compounds in the laboratory.
- The second phase began in the 1930s when it was observed that blockages in oil and natural gas pipelines could be caused by gas hydrates. The high pressures used for hydrocarbon pipeline transportation, when combined with cold temperatures, created an ideal setting for hydrate formation and led to serious problems.
- The third phase, starting the 1960s, began with the discovery that huge quantities of gas hydrates existed in permafrost and oceanic sediments. The presence of hydrates, many millions of years old, was later confirmed in other parts of the universe, including planets and moons.

Working in an age before modern refrigeration, Sir Joseph Priestly used the cold winter nights (around −8°C) in 1778 to study the freezing of water in the presence of different gases. He found *ice* formed from the mixture of SO_2 and water. It is now known that SO_2 forms a gas hydrate below 8°C. Another important observation he made was that, as the *ice* melted, it sunk to the bottom of the liquid water. Unlike ice, which floats on water, SO_2 hydrate is denser and will sink. This was likely the first recorded observation of a gas hydrate. However, Priestly did not recognize this discovery and it would not be until 1810 that gas hydrates would

be officially discovered. Sir Humphry Davy reported the discovery of gas hydrates formed from chlorine during his Bakerian Lecture to the Royal Society of London [3].

Subsequent initial research was largely focused on identifying other compounds that were capable of forming hydrates, as shown in Table 2.2. It was not until 1888 that hydrates were shown to form with light hydrocarbon gases, i.e., methane, ethane, and propane [10].

Practical interest in gas hydrates really began in 1930s when it was discovered that they caused blockages in pipelines, even above ice formation temperatures. The importance of understanding gas hydrates was recognized by industry and gave rise to the modern beginnings of hydrate research. Focus was given on finding the conditions in which hydrate crystals grow, predicting when they would form thermodynamically, and ways to prevent them. This included using inhibitors such as methanol.

In 1967, the Russians were the first to discover a large deposit on methane hydrates in the Siberian permafrost [4]. In the following years, part of the five billion cubic meters of gas produced from the Messoyakha gas field was from the decomposition of gas hydrates.

In the following decade, hydrates were found in the West beginning in Alaska and the Mackenzie Delta in Canada. This was followed by the realization that hydrates also existed in deep sea sediments. Efforts to better understand naturally occurring hydrates included deep-sea drilling with systematic investigations to characterize hydrate deposits, with samples extracted from areas such as the east coast of the US, the Gulf of Mexico, Guatemala, and South America.

International projects in recent years, including countries such as Japan, India, Canada, and US, have been implemented to explore the viability of gas hydrates, both on land and at sea, as a future source of methane. Experimental gas production tests of permafrost hydrates have been conducted in Canada in 2002 and 2008 (Fig. 2.5), with Japan planning for a marine test in the upcoming years (see Chap. 8).

2.3 Research Efforts and the Potential of Gas Hydrates

Some countries, such as Japan, Canada, and the US, have invested heavily into scientific and technical research on gas hydrates. The first government program by the US Department of Energy dates back to 1982. Since the early 1990s, a tri-annual (International Conference on Gas Hydrates, or ICGH) is hosted dealing exclusively with gas hydrates, along with gas hydrate research appearing in numerous other international conferences yearly.

The energy potential of natural hydrates is now the main driver for research in many countries. However, for a long time, the focus of hydrate research was mainly driven by energy companies and related to the area of *flow assurance*, i.e. maintaining the flow of oil in pipelines and wells. Hydrate formation in pipelines

Fig. 2.5 Flare from a methane hydrate production test in Canada (Photo credit: Tim Collett)

can and has led to loss of production, imparting a significant economic toll. In addition, accidents involving gas hydrates have led to property damage and loss of life. Problems associated with the formation of gas hydrates have become especially topical with the 2010 Deep Water Horizon rig explosion and subsequent attempts to stop the flow of oil into the Gulf of Mexico.

Much of the gas hydrate research related to flow assurance deals with hydrate inhibitors. Historically, industry attempted to avoid hydrates by adding thermodynamic inhibitors, such as methanol and ethylene glycol, to shift conditions out of the hydrate stable zone, similar to adding salt to melt ice on a driveway. However, because of economic and environmental reasons (see Chap. 7), the current paradigm has shifted to managing hydrate formation. This has led to so-called *kinetic* hydrate inhibitors. These chemicals, typically polymers, can be used in much lower concentrations. They act to slow down the onset and/or growth of hydrates to keep the oil and gas flowing. Anti-agglomerants are also being studied to keep hydrates from sticking together, preventing formation of a hydrate *plug*. To study hydrate growth and plugging, as well as inhibitor effectiveness, industry often uses large flow loops to simulate pipeline flow (Fig. 2.6).

Much basic research still continues in the laboratory to determine thermal and mechanical properties of hydrate systems. Very sophisticated research is also

Fig. 2.6 The "Lyre loop" multiphase flowloop for the study of hydrates in pipelines at IFP (French Petroleum Institute) near Lyon, France

being conducted on nucleation, i.e., when the first crystal of hydrate forms. One of the challenges with hydrate studies is the formation of well-defined and consistent samples of high hydrate concentrations. Studying gas hydrates in sediments is even more complex and the challenge remains of creating well-characterized reproducible hydrate samples.

Besides natural hydrates representing an immense source of energy, a number of other hydrate applications exist. One of the newest and most interesting is based on new systems for the transportation and storage of gases using gas hydrates. It has been shown that methane hydrates have an anomalous meta-stability range between −40 and 0°C. In particular, between −8 and 0°C, the rate of hydrate decomposition is considerably slowed down, even under atmospheric pressure [9]. This provides an opportunity to transport methane gas in the form of hydrate under much milder conditions than other alternatives, such as LNG. One could envision this as a possible way for *stranded* natural gas to be produced, converted to hydrate, and transported to market for sale.

Gas hydrates could also be applied to upcoming challenges faced with capture, transportation, and storage of carbon dioxide. CO_2 is selectively concentrated in hydrates over nitrogen (N_2), the other main component of flue gases. CO_2 could also be injected and disposed of in permafrost and marine sediments in the form of gas hydrate. One technology being explored is the exchange of CO_2 with methane in natural hydrates. When contacted with methane hydrate, CO_2 has been shown to replace the methane in the hydrate cages. This would allow for the simultaneous recovery of energy and sequestration of carbon in a natural hydrate reservoir. Gas hydrates have even been studied as a hydrogen storage material. Once thought to

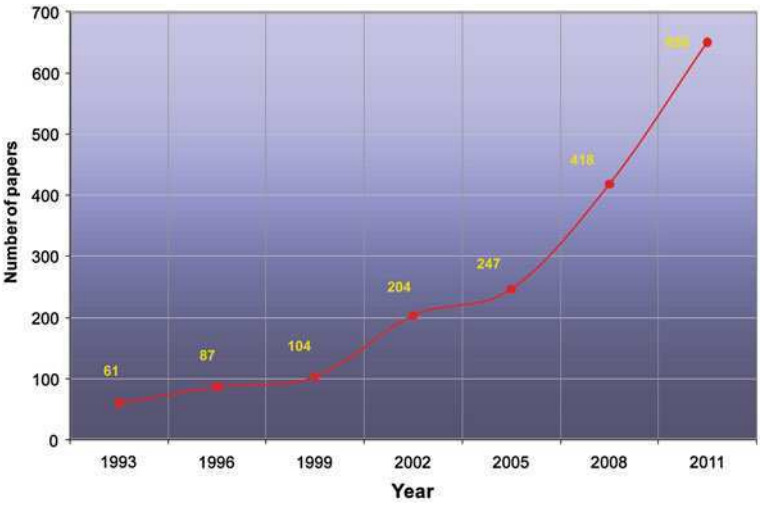

Fig. 2.7 Number of papers presented at the International Conferences on Gas Hydrates, held every three years in different countries

be a *non-former*, H_2 will occupy the cages of gas hydrates under high pressure conditions.

A number of discussions among the scientific community are focusing on the potential hazards associated with gas hydrates, especially submarine slope-stability issues, both natural (earthquakes, increasing sea temperature) or human induced. One of the major conclusions related to gas hydrate from the AAPG Conference (Vancouver 2004) was the acknowledgment that more effort is needed to document the problems induced by hydrates during oil and gas drilling and completion processes [2].

The extent of the hydrate literature has significantly grown in recent years. The field of gas hydrates covers many applications and a variety of disciplines from geology and chemistry to physics, oceanography, cosmology, and engineering. Around 40 publications were written in the first hundred years after their discovery. From the period between 1965 and 2010, the number of publications exceeded 4,000. The curve in Fig. 2.7 shows the trend of the papers presented at the first seven ICGHs, from 1993 (New Paltz, NY) to 2011 (Edinburgh, UK). The 61 presentations of 1993 have now become more than 650 in 2011 ICGH edition.

There are many excellent texts on hydrates, with varying areas of focus and level of detail. These books include [1, 5, 6, 7] and [8].

References

1. Carroll J (2009) Natural gas hydrates. A guide for engineers, 2nd edn. Gulf-Elsevier, Oxford
2. Collett T, Johnson A, Knapp G, Boswell R (2009) Natural gas hydrates: energy resource potential and associated geological hazards. AAPG Memoir 89, Tulsa

3. Davy H (1811) On some of the combinations of oxymuriatic acid and oxygen, and on the chemical reactions to these principles to inflammable bodies. Philos Trans R Soc Lond 101:1
4. Makogon YF (1974) Hydrates of natural gases (in Russian). Nedra, Moscow
5. Makogon YF (1997) Hydrates of hydrocarbons. PennWell Books, Tulsa
6. Max MD (2003) Natural gas hydrate in oceanic and permafrost environments. Kluwer, London
7. Max MD, Johnson AH, Dillon WP (2006) Economical geology of natural gas hydrates. Springer, Dordrecht
8. Sloan ED, Koh CA (2008) Clathrate hydrates of natural gases, 3rd edn. CRC Press, Boca Raton
9. Stern L, Circone S, Kirby S, Durham W (2001) Anomalous preservation of pure methane hydrate at 1 atm. J Phys Chem B 105:1756–1761
10. Villard P (1888) Sur quelques nouveaux hydrates de gaz. Compt Rend 106:1602–1603

Chapter 3
The Structure and Formation of Gas Hydrates

3.1 A Strange Mixture: Water

Formation of crystals of gas hydrates is possible given the particular way water molecules interact. Formed from the union of two atoms of hydrogen and one oxygen atom, water has an apparently anomalous boiling point of 100°C. Based on its size, it should be around −80°C! This property and others that make water so fascinating to study comes from water's ability to form hydrogen bonds. Water is a polar molecule where a partial positive charge can exit on the hydrogen atoms with the oxygen being slightly negative. A hydrogen atom from one water molecule can form a *secondary* hydrogen bond between the oxygen on another water molecule (Fig. 3.1). This bond is around a tenth of the strength of the primary covalent bonds holding the water molecule together. Nonetheless, this gives rise to a number of the peculiar properties of water.

Water is also different from most other liquids in that it has a density maximum that is not at its freezing point. At 1 bar (atmospheric pressure), water has a maximum density around 4°C. When water solidifies, it actually increases in volume. That is the reason ice floats on water. As water forms into solid ice, the water molecules are arranged in an orderly fashion, forming hexagonal crystals (Fig. 3.2) which occupy more space than when they are in the more disordered liquid state. This occurs in part due to the presence of hydrogen bonding between the water molecules.

Another important feature of water is its ability to dissolve many substances, such as salts. Seawater typically contains around 3.5% by weight of sodium chloride and other salts. Gases such as carbon dioxide (CO_2) and hydrogen sulfide (H_2S) also are relatively soluble with water. However, hydrocarbons such as methane and natural gas are considered insoluble and only very small amounts of them will dissolve in water. Hydrocarbon solubility in water, while quite low, increases with pressure and decreases with temperature. Salinity also affects solubility, where a saline solution will contain less gas than pure water under the same pressure and temperature conditions.

C. Giavarini and K. Hester, *Gas Hydrates*, Green Energy and Technology,
DOI: 10.1007/978-0-85729-956-7_3, © Springer-Verlag London Limited 2011

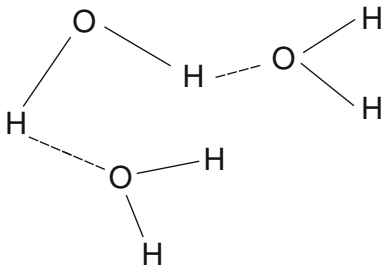

Fig. 3.1 Hydrogen bonding creates a continuous structure between the water molecules

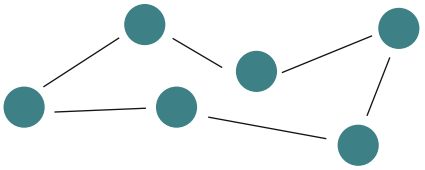

Fig. 3.2 The three-dimensional hexagonal arrangement of water molecules in ice crystals

Just as a gas is dissolved into water, water can also be dissolved or *dispersed* into a gas. Water saturation in a gas is a function of pressure and temperature (Fig. 3.3, referring to water in natural gas).

3.2 The Formation of Gas Hydrates

Water by itself forms ice at 0°C. The presence of other molecular species under the appropriate conditions can cause the hydrogen-bonded H_2O molecules to orientate around these molecules and form a solid crystal. The water acts as the host structure, composed of cages that trap and greatly concentrate *guest* molecules (Fig. 3.4). The stabilization of the solid hydrate is not due to direct bonding of the guest molecule with the host water molecules. The guest molecules are free to rotate in the molecular water cages. Instead, the hydrate is stabilized by an attractive van der Waals type force between the guest molecules and the water. In order for a hydrate form, you need three conditions to be satisfied:

- the presence of a sufficient quantity of water,
- the presence of a hydrate *guest*, such as methane, ethane, CO_2, etc.,
- the right P,T conditions for the guest present (typically high pressure and low temperature).

Ice and hydrate have many similarities and some marked differences. Table 3.1 shows a comparison of ice and methane hydrate.

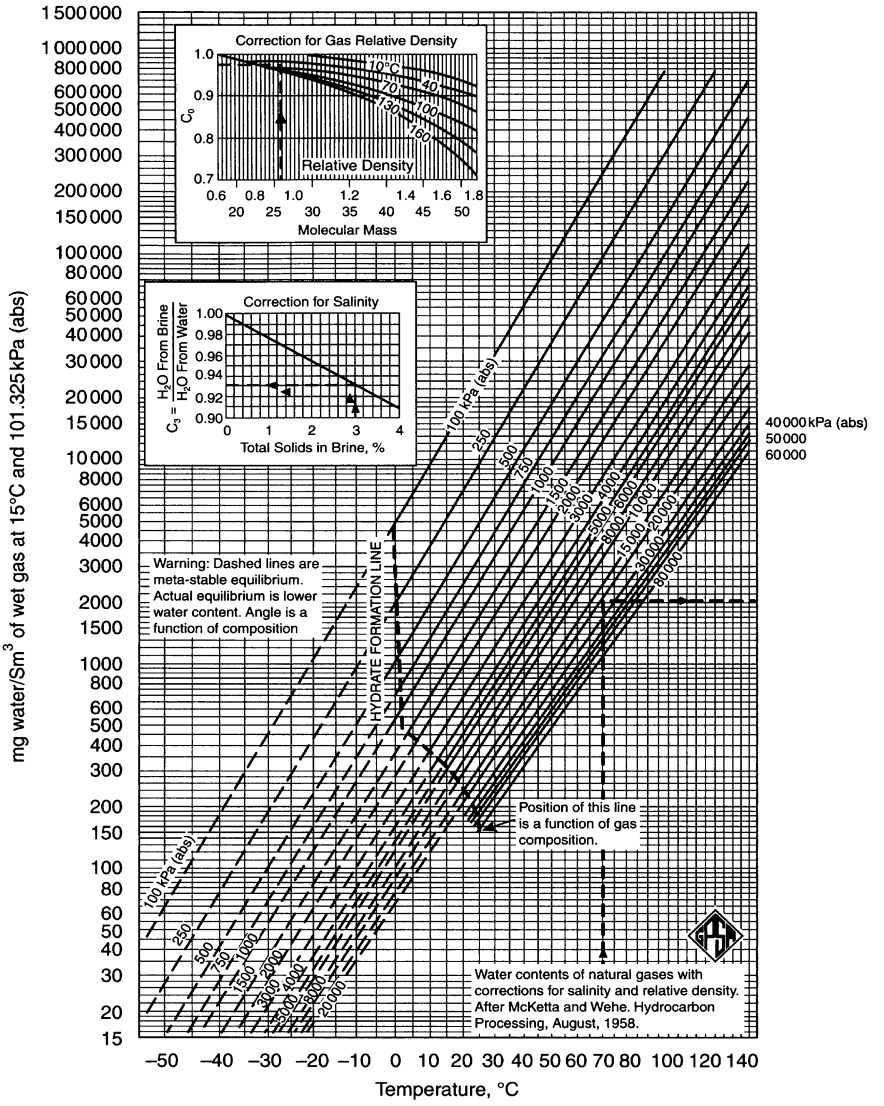

Fig. 3.3 Water content of natural gas as a function of pressure and temperature (Mc Ketta-Wehe chart, GPSA Eng. Data Book, 1997)

3.3 The Crystal Structures of Gas Hydrates

Hydrates are solid compounds with well-defined crystal structures, formed from water molecules hydrogen-bonded and arranged as *molecular cages*. These cages trap hydrate guest molecules, which stabilize the crystal lattice. Generally speaking, each hydrate cage contains up to one guest molecule. Multiple cage

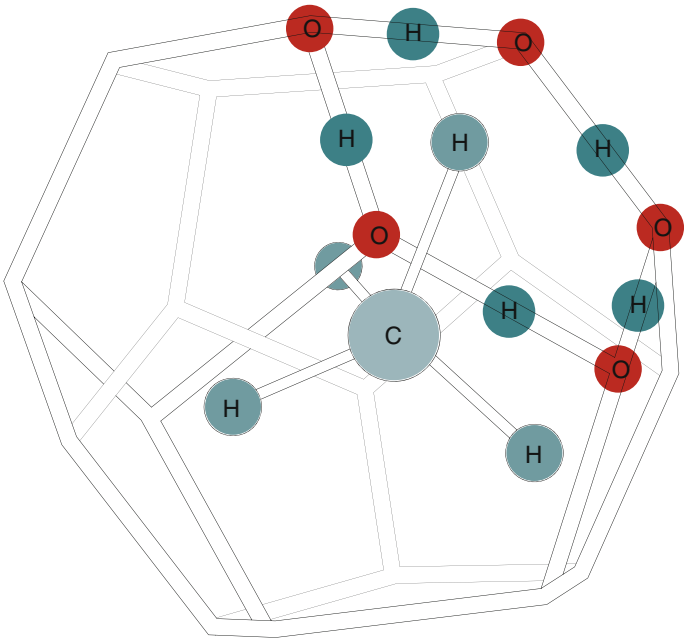

Fig. 3.4 Gas molecules enclosed in the water cavities of the hydrate

Table 3.1 Comparison of key properties between ice and methane hydrate [11]

Property	Ice	CH_4 hydrate
Density (g/mL)	0.916	0.912
Heat of fusion (kJ/mol H_2O)	6	9
Thermal conductivity at 263 K (W/(m K))	2.25	0.49
Dielectric constant at 273 K	94	~58
Young's modulus at 273 K (10^9 Pa)	9.5	~8.4
Longitudinal sound velocity (km/s)	3.8	80
Compressibility at 273 K (10^{-11} Pa)	12	14
Index of refraction	1.3082	1.3485

occupancy can occur but typically very high pressures are required. The ratio of water-to-guest molecules is referred to as the *hydration number*.

The most common structures for hydrocarbon mixtures and other common gases are Structure I (sI) and Structure II (sII). These structures were identified using X-ray diffraction near the middle of the twentieth century through painstaking work by von Stackelberg and colleagues [21]. Table 3.2 compares some of the main properties of sI and sII hydrates, while Fig. 3.5 shows the polyhedral cages that stack in space to create the structures.

The sI unit cell (smallest repeating crystal unit) is a body-centered cubic lattice composed of 46 water molecules which form 6 *large* cages and 2 *small* cages. As

Table 3.2 Comparison between sI and sII hydrates [2]

	sI	sII
Water molecules per unit cell	46	136
Cages per unit cell:		
Small	2 (5^{12})	16 (5^{12})
Large	6 (5^{12} 6^2)	8 (5^{12} 6^4)
Theoretical formula*:		
All cages filled	X * 5¾ H_2O	X * 5⅔ H_2O
Mole fraction of gas in hydrate	0.1481	0.1500
Only large cages filled	X * 7⅔ H_2O	X * 17 H_2O
Mole fraction of gas in hydrate	0.1154	0.0556
Cage diameter (Å):		
Small	7.9	7.8
Large	8.6	9.5
Unit cell volume (m^3)	1.728×10^{-27}	5.178×10^{-27}
Typical guest	CH_4, C_2H_6, H_2S, CO_2	C_3H_8, i–C_4H_{10}, N_2

X is the hydrate guest

shown in Fig. 3.5, the small cage in the sI hydrate is a pentagonal dodecahedron, with 12 pentangonal faces. The common notation for the sI small cage in hydrate literature is 5^{12}, which indicates that the cage has twelve 5-sided faces. The sI large cage is a 14-sided tetrakaidecahedron and referred to as the $5^{12}6^2$ cage due to its twelve 5-sided faces and two 6-sided faces.

With one molecule per cage, the theoretical sI hydrate number (n) for a fully occupied lattice is 5.75 (46/8). However, in gas hydrates, there are almost always some cages which remain empty resulting in a higher hydration number.

Gases that form sI hydrates include methane, ethane, CO_2, and H_2S. The small sI formers such as methane and H_2S stabilize the small cages while still being large enough to also provide stability to the sI large cages. Larger sI formers like ethane have little to no occupancy of the small cages and reside almost exclusively in the large cages. Hydrates are non-stoichiometric and hydration numbers vary widely based on the hydrate former and conditions. Methane occupies almost all of the cages (around 95% of the large cages and 85% of the small cages) with $n = \sim 6$ [3]. Carbon dioxide does not fit as well into the 5^{12} cages and only occupies around 50% of them ($n = \sim 6.6$). Ethane has practically no occupancy of the 5^{12} cages as it is too large ($n = \sim 7.9$). However, occupancies of around 5% of the 5^{12} cages have been observed experimentally at higher pressures [19].

The sII unit cell is a face-centered cubic lattice composed of 136 water molecules which contain eight *large* cages and sixteen *small* cages. The sII small cage is the same as that in sI. The sII large cage is a hexakaidecahedron and called the $5^{12}6^4$ cage due to its twelve 5-sided faces and four 6-sided faces. The sII $5^{12}6^4$ cage is larger than the sI large cage. The hydrate number for this structure with full occupancy is 5.67 (136/24).

Common sII formers include large guests such as propane and *i*–butane. These guests are too large to fit in the small cages and result in a hydration number

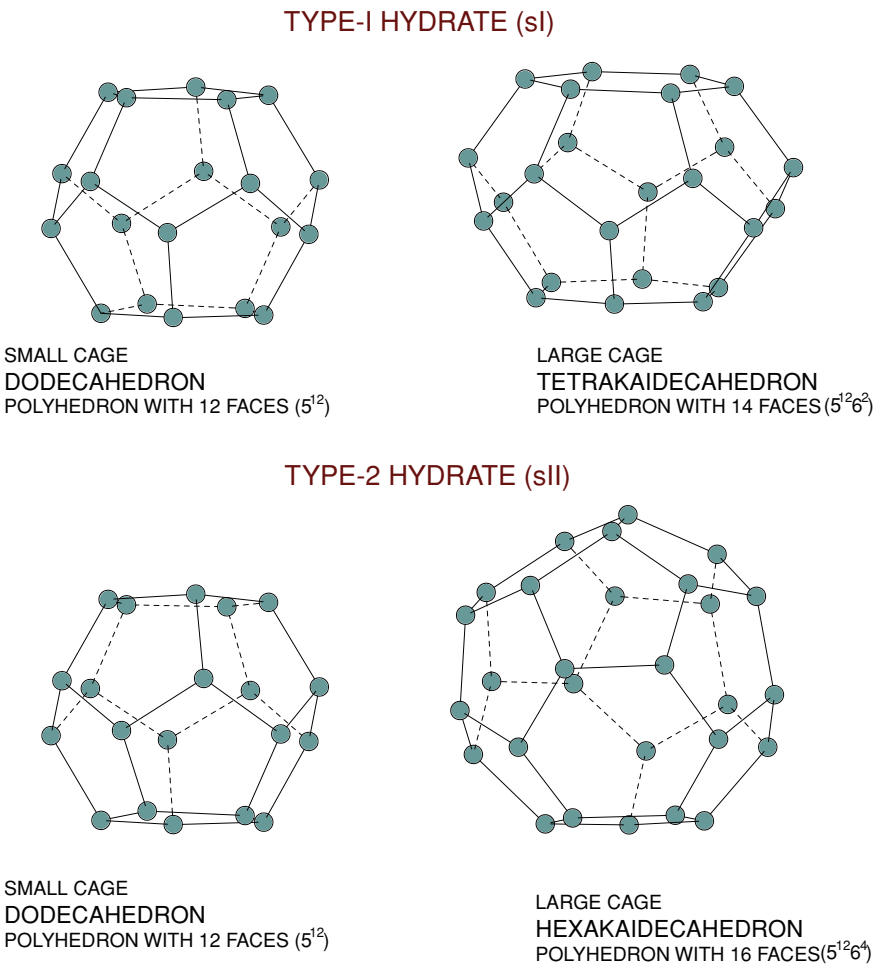

Fig. 3.5 Polyhedral structures of the sI and sII hydrates

around 17. In addition to these larger guests, the smallest of hydrate formers also form a sII hydrate such as hydrogen, helium, and nitrogen.

Beginning with von Stackelberg [21], the realization occurred that guest size was a dominate factor in determining the stable hydrate crystal structure. Figure 3.6 shows the relationship between stable hydrate structure and guest size [14]. For molecules less than around 3.8 Å, sII is the stable structure. This is likely due to the large/small cage ratio of 0.5 in the sII unit cell. These small guests offer little stability to the large cages and prefer to form the structure with the highest density of small cages.

While once thought to not form hydrates at all, the smallest formers such as H_2 and He do form gas hydrates but can require enormous pressures. Near the size

Table 3.3 Molecular size and diameter ratio between molecules and hydrate cages [16]

Molecule		Molecular diameter / Cage Diameter			
	Cage type	sI		sII	
	Molecule diameter (Å)	5^{12}	$5^{12}\,6^{2}$	5^{12}	$5^{12}\,6^{4}$
He	2.28	0.447	0.389	0.454	0.342
H_2	2.72	0.533	0.464	0.542	0.408
N_2	4.1	0.804	0.700	0.817	0.616
O_2	4.2	0.824	0.717	0.837	0.631
CH_4	4.36	0.855	0.744	0.868	0.655
H_2S	4.58	0.898	0.782	0.912	0.687
CO_2	5.12	1.00	0.834	1.02	0.769
C_2H_6	5.5	1.08	0.939	1.10	0.826
C_3H_8	6.28	1.23	1.07	1.25	0.943
i–C_4H_{10}	6.5	1.27	1.11	1.29	0.976
n–C_4H_{10}	7.1	1.39	1.21	1.41	1.07

limit of the sI large cage, some interesting behavior can occur. Molecules such as trimethylene oxide and cyclopropane can form either sI or sII depending on the conditions (e.g., concentration and pressure). When you reach molecules such as propane and *i*–butane, they can no longer fit in the sI $5^{12}6^{2}$ cage and sII again becomes the stable hydrate structure. The largest sII formers such as n–butane and cyclohexane actually require a small *help* guest molecule which fits in the 5^{12} cages to form a hydrate.

Table 3.3 shows the molecular size of some gases and the ratio between their diameter and various hydrate cages. When this ratio falls below $\sim$0.76, the guest is thought to no longer contribute significantly to stabilizing the cage. When the value is greater than unity, the guest can no longer fit in the cage.

There is one more common hydrate structure which forms from even larger guest molecules. It is less frequently observed but still important. The structure H (sH) hydrate has a hexagonal lattice containing 34 water molecules and three cage types: three small 5^{12} cages, two medium $4^{3}5^{6}6^{3}$ cages, and one large $5^{12}6^{8}$ cage (Fig. 3.7). The sH hydrate forms with molecules such as methylcyclohexane. However, like the largest sII formers, sH only forms when a second help-gas (e.g., CH_4) is present to stabilize the 5^{12} and $4^{3}5^{6}6^{3}$ cages.

Along with the three most common hydrate structures, numerous other hydrate crystal structures have been discovered. They normally occur only for a few guest molecules, including dimethyl ether and bromine, and the reason for not following the size versus structure relationship in Fig. 3.6 is not fully understood. High pressures can also induce changes in the stable hydrate structure. This could be practically useful for the study of hydrates in the field of cosmology. Hydrates have been hypothesized to exist in numerous places outside of Earth. Pressures in some of these places, such as Titan (moon of Jupiter), can lead to the occurrence of these high pressure phase transitions.

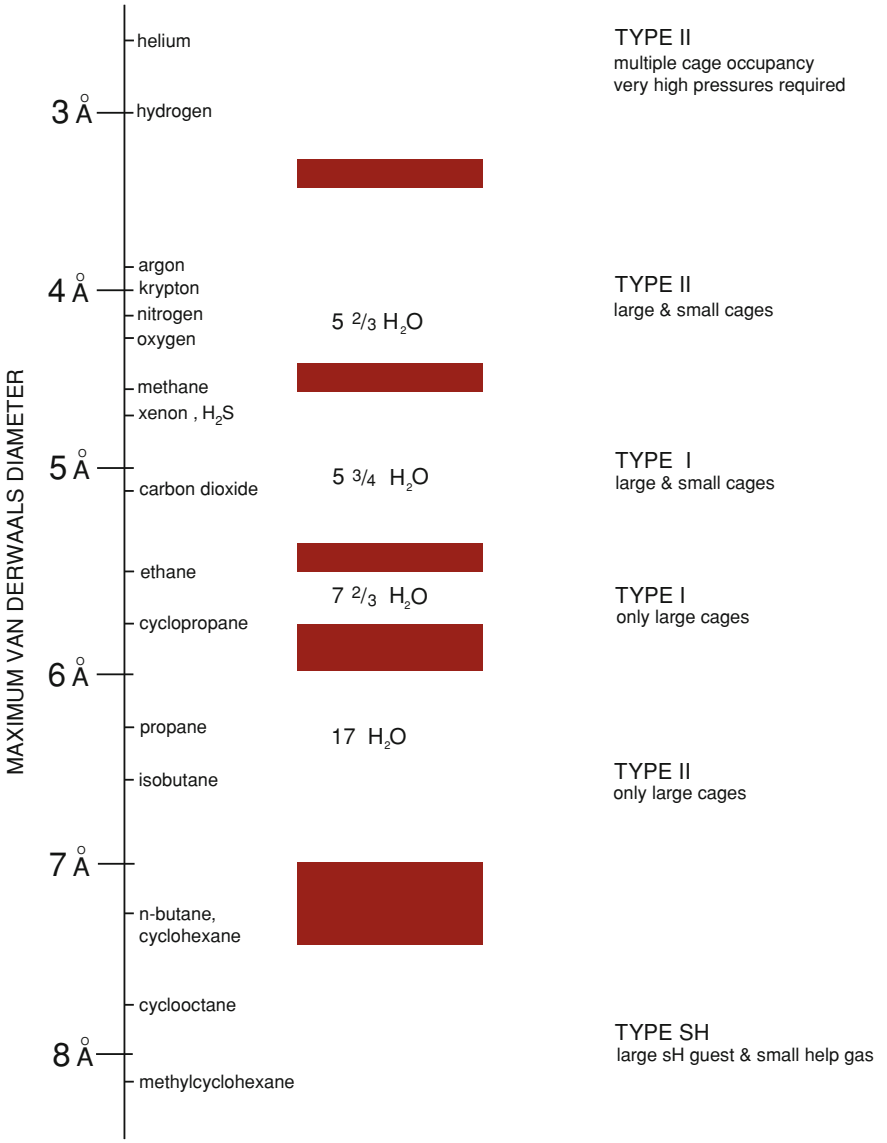

Fig. 3.6 Relationship between size and type of molecule that can form gas hydrate

3.4 Other Possibilities and Curiosities

The world of gas hydrates is extremely diverse and complex. This book aims to focus on natural gas hydrates. However, we feel it is important to highlight for the reader some of the more interesting hydrates formed from other gases and liquids. While we often call them gas hydrates, hydrate can form from liquids as well as gases.

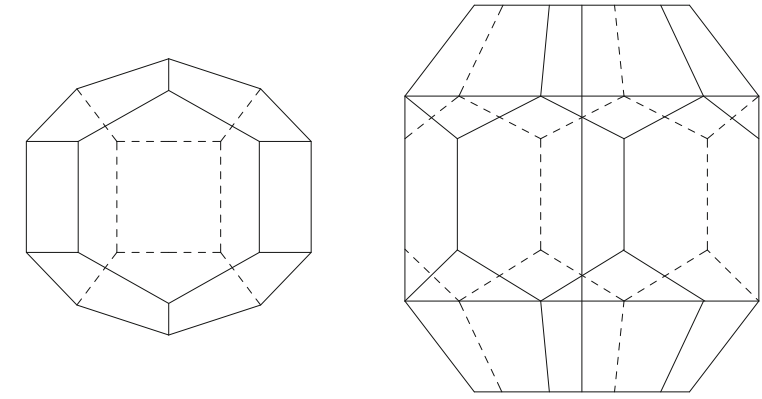

Fig. 3.7 The irregular dodecahedral and icosadeltahedral cages, that together with the dodecahadedra, form the sH hydrate

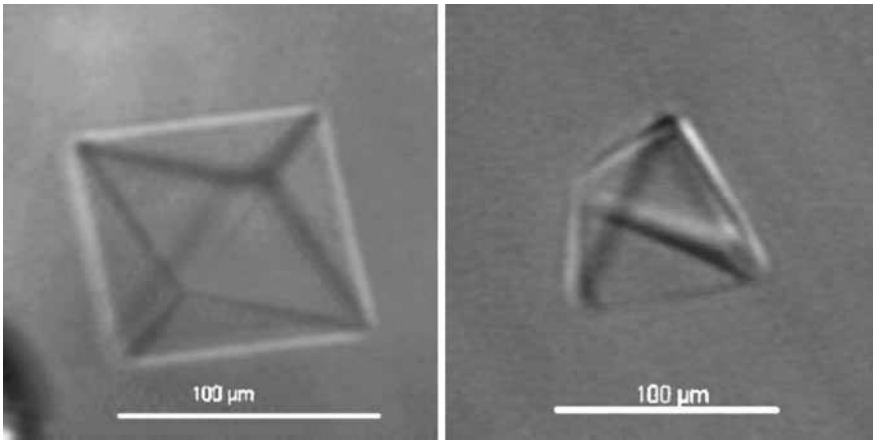

Fig. 3.8 Single crystal air hydrates found in the ice cores from central Greenland at 1271 m and 1378 m depth [12]

It was not that long ago that most thought gases such as hydrogen, helium, and nitrogen did not form hydrates. It is now known that they do indeed form hydrates but require much higher pressures than their natural gas counterparts. As an example at around 273 K, hydrogen hydrates require around 400 MPa of pressure to be stable. Compare this to the 2.6 MPa needed for methane hydrates.

Hydrates can also form from air. However, due to the high pressures required, air hydrates are not found on the Earth's surface. They are, in fact, present in polar ice sheets (Fig. 3.8). Pressure increases with depth in these ice sheets and combined with the cold temperatures, air hydrates are stable [12]. The air in the polar

ice (as bubbles and hydrate) was trapped and buried. Ice depth can be correlated with time and this air is the most direct record of past atmospheric conditions. Understanding these air hydrates is critical to properly interpret the ice-core records.

While we typically say that hydrates require high pressures, many hydrate guests form under one atmosphere of pressure (1 bar) here on Earth. This was the case for the first hydrate guests discovered, i.e., SO_2 and Cl_2. Others include cyclic ethers such as ethylene oxide (C_2H_4O, EO), trimethylene oxide (C_3H_6O, TMO), and tetrahydrofuran (C_4H_8O, THF). EO forms sI and THF forms sII. TMO is quite interesting as it will form either sI or sII depending on its concentration in the aqueous phase. One compound that is perhaps the closest analog for studying natural gas hydrates under atmospheric pressure conditions is cyclopentane. It forms a sII hydrate at around 7°C.

Because of its miscibility with water and ability to form under atmospheric pressure, THF has been studied extensively as an analog to hydrates found in nature. THF has also been used as a hydrate promoter. It can dramatically reduce hydrate stability conditions and increase formation kinetics [6, 15, 16]. This was especially true for hydrogen hydrates. The discovery of hydrates formed from hydrogen created excitement about the possibility of a hydrogen storage medium where the only byproduct was water [10]. However, the extremely high pressures needed made them impractical. By forming hydrogen hydrates with THF, the formation conditions were dramatically reduced [7]. The drawback to this approach is that THF occupies the large cages of the sII hydrate, reducing the overall hydrogen storage capacity. Recent work has shown a metastable form of the THF + H_2 hydrate can allow for 3.4 wt% H_2 in the hydrate under milder pressure conditions than pure H_2 hydrate [17].

3.5 The Conditions for Hydrate Formation

3.5.1 Pressure–Temperature Phase Diagrams

For both theoretical and practical reasons, a very important aspect of gas hydrate studies is knowing under what conditions they are stable (and what other phases are co-existing with the hydrate). This information is often presented visually in the form of a Pressure–Temperature (P–T) phase diagram. Figure 3.9 shows an example of a P–T diagram for a typical hydrate-forming hydrocarbon and water. The hydrate stability curve ($2–2^1–2^{11}$) defines the point at which hydrate is stable. The hydrate stability region is to the left of this line, towards lower temperatures and higher pressures.

The first change in slope at Q_1 is the lower quadruple point, where four phases exist simultaneously: liquid water (L_w), ice (I), hydrate (H), and hydrocarbon vapor (V). Below Q_1, hydrates form from ice instead of liquid water.

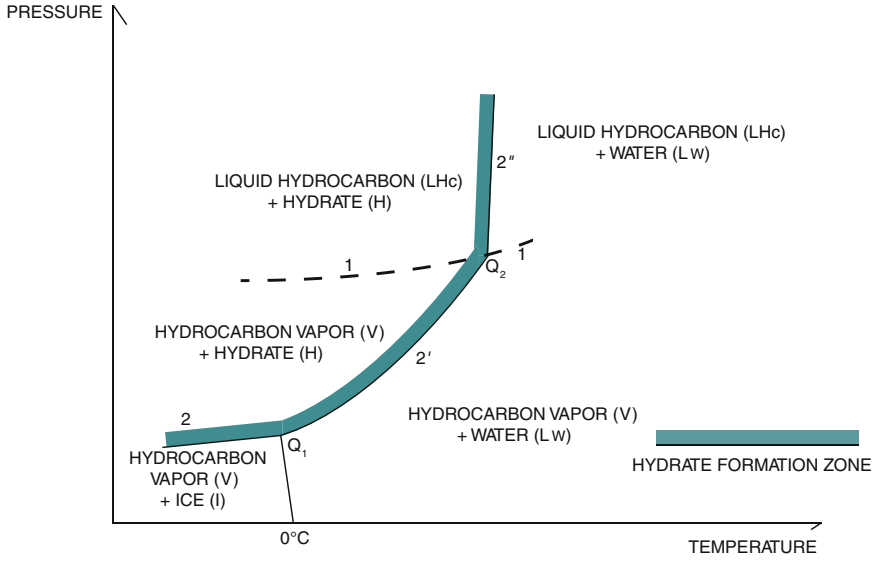

Fig. 3.9 A typical P–T diagram for a pure hydrocarbon (larger than methane)

The second change in slope occurs at Q_2 (or the upper quadruple point). At Q_2, liquid water (L_w), hydrate (H), hydrocarbon vapor (V), and liquid hydrocarbon (L_{HC}) coexist. The dashed curve (1) represents the vapor pressure curve for the mixture (where the hydrocarbon transitions from the vapor to the liquid phase occurs). After Q_2, the hydrate formation curve becomes very steep, effectively giving an upper temperature limit for hydrate formation.

Quadruple points are typical in hydrate-forming systems and each of them occurs at one specific pressure–temperature condition. The hydrate stability curve ($2 - 2^1 - 2^{11}$) connects the quadruple points and is a line where 3-phases are in co-existence. For example, $L_W + H + V$ are all present on line 2^1 and $I + H + V$ exist on line 2. It is often referred to as the 3-phase line. On either side of the 3-phase line, there are two-phase regions.

Figure 3.10 shows the P–T diagrams from methane, ethane, propane, and *i*–butane. These diagrams are frequently reported in the literature on a semi-logarithmic scale of pressure (lnP versus 1/T), which yields almost straight lines for hydrate stability. The numerical values for hydrate formation of methane, ethane, propane, CO_2, and H_2S are given in Tables 3.4, 3.5, 3.6, 3.7, 3.8, taken from Carroll [2].

As shown in Fig. 3.10, the hydrate formation curve becomes very steep when the second quadruple point is reached. This effective upper temperature limit for hydrate formation decreases with the number of carbon atoms in each molecule. For example, while pure ethane can exist up to around 14°C, pure propane hydrate cannot exist above $\sim$ 6°C. For gases such as methane and nitrogen, an upper quadruple point does not exist because the gases are already above their critical

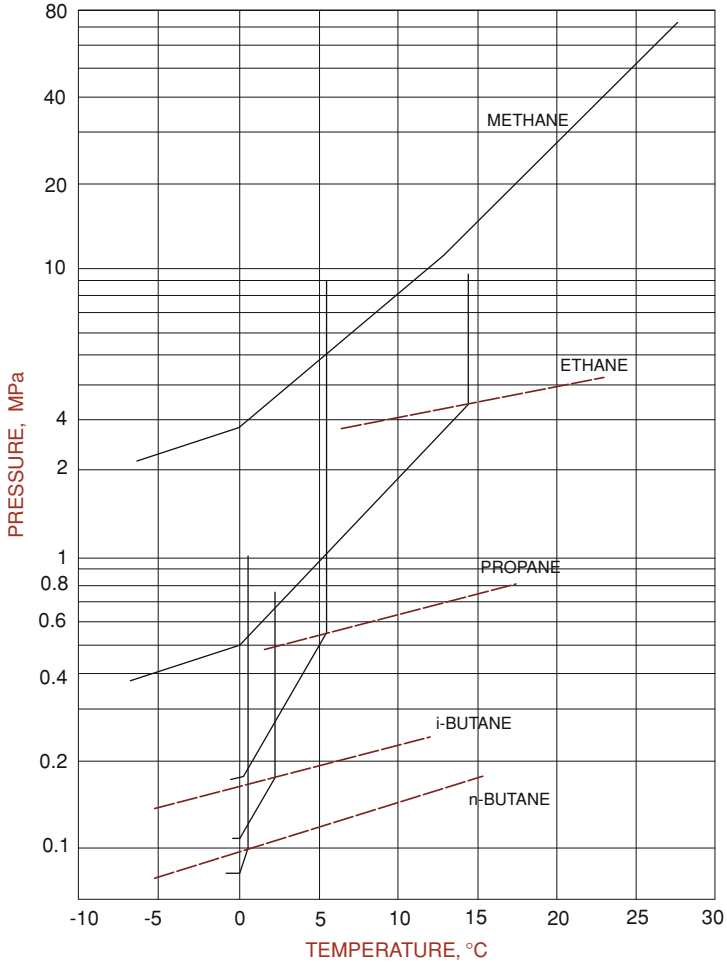

Fig. 3.10 P–T diagram for hydrocarbons from methane to butane [8]

point. As a result, hydrates from these gases can exist over a much larger temperature range.

Most natural gases are primarily methane with some heavier hydrocarbons and can contain other components (e.g., CO_2, H_2S, N_2) as well. The phase behavior of these mixtures will be qualitatively similar to the P–T diagram for pure methane. However, the hydrate stability curve will be shifted based on the composition of the gas.

If there are sufficient amounts of the heavy hydrocarbons to create a liquid hydrocarbon phase, the phase behavior becomes more complicated. Figure 3.11 shows an amended P–T diagram for the case when liquid hydrocarbon is present (Sloan and Koh [16]. The 3-phase line (2^{11} in Fig. 3.9) widens to become a

Table 3.4 Formation conditions of methane hydrate [2]

Temperature (°C)	Pressure (MPa)	Phases	Composition (mol%)		
			aqueous	vapor	hydrate
0	2.6	L_A–H–V	0.1	0.027	14.1
2.5	3.31	L_A–H–V	0.12	0.026	14.2
5	4.26	L_A–H–V	0.14	0.026	14.3
7.5	5.53	L_A–H–V	0.16	0.025	14.4
10	7.25	L_A–H–V	0.18	0.024	14.4
12.5	9.59	L_A–H–V	0.21	0.024	14.5
15	12.79	L_A–H–V	0.24	0.025	14.5
17.5	17.22	L_A–H–V	0.27	0.025	14.5
20	23.4	L_A–H–V	0.3	0.027	14.6
22.5	32	L_A–H–V	0.34	0.028	14.6
25	44.1	L_A–H–V	0.37	0.029	14.7
27.5	61.3	L_A–H–V	0.41	0.029	14.7
30	85.9	L_A–H–V	0.45	0.029	14.7

Note: The compositions of the aqueous phase (L_A) and the hydrate phase (H) are mole percent of the "guest" (CH_4). For the vapor phase (V), the composition is the mole percent of water

Table 3.5 Formation conditions of ethane hydrate [2]

Temperature (°C)	Pressure (MPa)	Phases	Composition (mol%)		
			aqueous		
0	0.53	L_A–H–V	0.037	0.126	11.5
2	0.61	L_A–H–V	0.041	0.117	11.5
4	0.77	L_A–H–V	0.047	0.107	11.5
6	0.99	L_A–H–V	0.054	0.096	11.5
8	1.28	L_A–H–V	0.062	0.086	11.5
10	1.68	L_A–H–V	0.072	0.075	11.5
12	2.23	L_A–H–V	0.083	0.065	11.5
14	3.1	L_A–H–V	0.096	0.052	11.5
14.6	3.39	L_A–L_H–V–H	0.098	0.049-V 0.025-L_H	11.5
15	4.35	L_A–L_H–H	0.098	0.025	11.5
16	10.7	L_A–L_H–H	0.103	0.023	11.5
16.7	15	L_A–L_H–H	0.105	0.022	11.5
17.5	20	L_A–L_H–H	0.106	0.022	11.5

Note: The compositions of the aqueous phase (L_A) and the hydrate phase (H) are mole percent of the "guest" (C_2H_6). For the vapor phase (V), the composition is the mole percent of water. L_H indicated a liquid rich in C_2H_6

3-phase region (C–F–K–C in Fig. 3.11). This is caused by the various vapor pressures of the different compounds in the mixture. The upper quadruple point (Q_2) becomes a 4-phase line in this region (K–C).

Unlike the practically insoluble natural gas hydrocarbons, compounds such as CO_2 have a greater water solubility ($CO_2 + H_2O \rightarrow CO_2(aq) + HCO_3^- + H^+$).

Table 3.6 Formation conditions of propane hydrate [2]

Temperature (°C)	Pressure (MPa)	Phases	Composition (mol%)		
			aqueous		
0	0.17	L_A–H–V	0.012	0.36	5.55
1	0.21	L_A–H–V	0.014	0.31	5.55
2	0.26	L_A–H–V	0.017	0.27	5.55
3	0.32	L_A–H–V	0.019	0.23	5.55
4	0.41	L_A–H–V	0.023	0.19	5.55
5	0.51	L_A–H–V	0.027	0.17	5.55
5.6	0.55	L_A–L_H–V–H	0.028	0.158-V 0.0094-L_H	5.55
5.6	1	L_A–L_H–H	0.028	0.0093	5.55
5.6	5	L_A–L_H–H	0.028	0.0088	5.55
5.7	10	L_A–L_H–H	0.028	0.0083	5.55
5.7	15	L_A–L_H–H	0.028	0.0079	5.55
5.7	20	L_A–L_H–H	0.028	0.0074	5.55

Note: The compositions of the aqueous phase (L_A) and the hydrate phase (H) are mole percent of the "guest" (C_3H_8). For the vapor phase (V), the composition is the mole percent of water. L_H indicated a liquid rich in C_3H_8

Table 3.7 Formation conditions of CO_2 hydrate [2]

Temperature (°C)	Pressure (MPa)	Phases	Composition (mol%)		
			aqueous		
0	1.27	L_A–H–V	1.46	0.058	13.8
2	1.52	L_A–H–V	1.67	0.056	13.9
4	1.94	L_A–H–V	1.92	0.053	13.9
6	2.51	L_A–H–V	2.21	0.051	14.1
8	3.3	L_A–H–V	2.54	0.049	14.2
9.8	4.5	L_A–L_C–V–H	2.93	0.051-V 0.21-L_C	14.2
10	7.5	L_A–L_C–H	2.97	0.22	14.5
10.3	10	L_A–L_C–H	3	0.24	14.7
10.8	15	L_A–L_C–H	3.1	0.25	14.7
11.3	20	L_A–L_C–H	3.1	0.27	14.7

Note: The compositions of the aqueous phase (L_A) and the hydrate phase (H) are mole percent of the "guest" (CO_2). For the vapor phase (V), the composition is the mole percent of water. L_C indicated a liquid rich in CO_2

There have been suggestions of direct disposal of CO_2 in the deep ocean in liquid or hydrate form. However, liquid CO_2 as well as CO_2 hydrate will dissolve in under-saturated seawater [1, 4, 13, 18].

The P–T diagram for a binary CO_2–H_2O system is shown in Fig. 3.12. There are two quadruple points: Q_1 at −1°C and 10.42 bar and Q_2 at 10°C and 47.13 bar. Above Q_2, where liquid CO_2 is present, the hydrate stability line rises sharply limiting the temperature where hydrate is stable.

Table 3.8 Formation conditions of H_2S hydrate [2]

Temperature (°C)	Pressure (MPa)	Phases	Composition (mol%)		
			aqueous		
0	0.1	L_A–H–V	0.37	0.62	14.2
5	0.17	L_A–H–V	0.52	0.54	14.3
10	0.28	L_A–H–V	0.74	0.46	14.4
15	0.47	L_A–H–V	1.08	0.38	14.5
20	0.8	L_A–H–V	1.58	0.32	14.6
25	1.33	L_A–H–V	2.28	0.28	14.6
27.5	1.79	L_A–H–V	2.84	0.25	14.7
29.4	2.24	L_A–L_S–V–H	3.35	0.24-V 1.62-L_S	14.7
30	8.41	L_A–L_S–H	3.48	1.69	14.7
31	19.49	L_A–L_S–H	3.46	1.77	14.7
32	30.57	L_A–L_S–H	3.41	1.83	14.7
33	41.65	L_A–L_S–H	3.36	1.88	14.7

Note: The compositions of the aqueous phase (L_A) and the hydrate phase (H) are mole percent of the "guest" (H_2S). For the vapor phase (V), the composition is the mole percent of water. L_S indicated a liquid rich in H_2S

3.5.2 Compositional Phase Diagrams

For a two-component system (hydrate guest + water), the phase diagram has a third dimension related to composition. While the P–T diagram allows one to know under what conditions hydrates are stable and what phases are present, they do not give information on the composition of those phases. For compositional information, one can take slices at constant temperature to create pressure-composition (P-x) diagrams or, at constant pressure, to create temperature-composition (T-x) diagrams. An example of this is shown in Fig. 3.13 for methane hydrate, where a T-x diagram was constructed at a constant pressure of 4.8 MPa [16]. For ease of reading, the diagram is not to scale.

In the T-x diagram of methane + water, there are three single phase regions: a vapor region above, a liquid water region to the left, and a hydrate region. Note that there are slight changes in hydrate composition as we change temperature. This is due to hydrates being non-stoichiometric and the hydrate number can vary based on experimental conditions.

If we started with a mixture of hot steam and 50 mol% methane at 4.8 MPa and cooled the system, condensation would begin at Point 1. This is the dew point of our mixture. The condensation would be liquid water containing a small amount of methane (composition found at Point a). While the methane content appears significant in the figure, remember that it is not to scale and the actual methane content in the water is less than 0.1%. If we continued to cool the system, we next reach the 3-phase hydrate stability line at Point 2 (phase compositions can be found at Point *c* (L_w), Point *b* (H), and Point *d* (V)). If we continue to cool further,

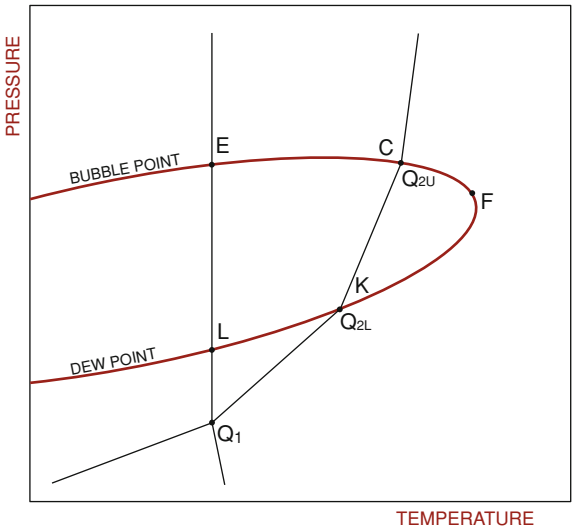

Fig. 3.11 P–T diagram for a natural gas containing a liquid hydrocarbon phase [16]

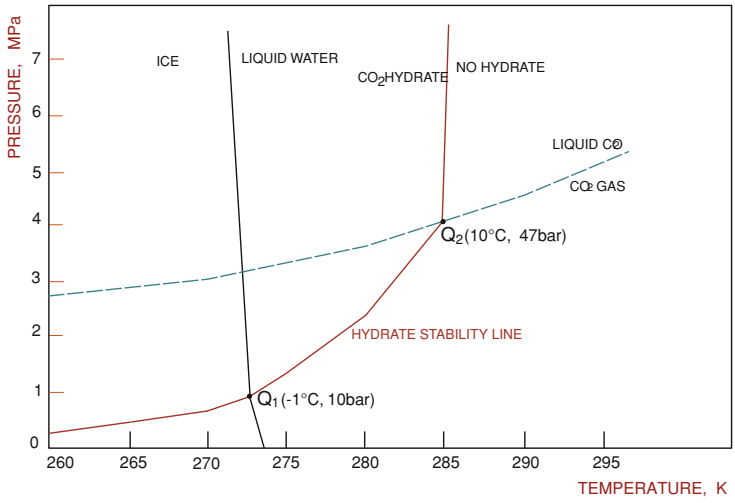

Fig. 3.12 P–T diagram from a binary system of CO_2 and water

the system will remain at the 3-phase temperature until all of the liquid water is consumed. At this point, we enter a 2-phase region containing hydrate and vapor. This is because the system had an excess of gas compared to water. If we started with a methane content in the feed between Points *b* and *c*, the vapor phase would be limiting and we would be in the 2-phase L_w-H region. Referring back to Fig. 3.10, the P–T diagram shows that there is a two-phase region to the left of the 3-phase line but it is either H–V or L_w–H based on the initial feed composition. To determine this, a compositional phase diagram is required.

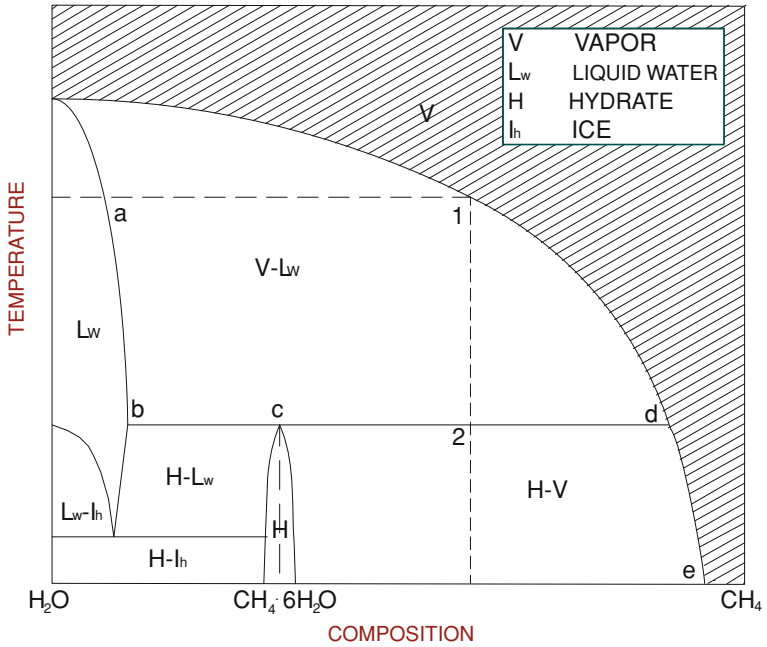

Fig. 3.13 T-x diagram from methane and water at 4.8 MPa (modified from [16])

Between Point *d* and *e*, this diagram confirms that hydrate formation can occur directly from the vapor phase, in the absence of a liquid water phase. Hydrate formation from water vapor could be very important in the transportation of natural gas and allows one to know the level of dehydration needed to fully eliminate the chance of hydrate formation.

3.6 Hydrate Formation Kinetics

To better understand gas hydrates, one should see how they can be prepared in the laboratory. The study of these *synthetic* laboratory hydrates is important to further our understanding of their characteristics and basic properties. This includes formation and dissociation kinetics under various conditions, with and without additives.

Hydrate can be formed from water or ice in the presence of a hydrate-forming gas (e.g., CH_4, CO_2) under pressure. This can be accomplished using a pressure vessel (or reactor) similar to that shown in Fig. 3.14. Such a reactor is able to withstand several tens of bar of pressure and is equipped with a cooling jacket, which allows circulating coolant to control the reactor temperature.

When forming from liquid water, an agitator (such as a mixing rod) is useful in reducing formation time due to metastability and mass transfer limitations as the

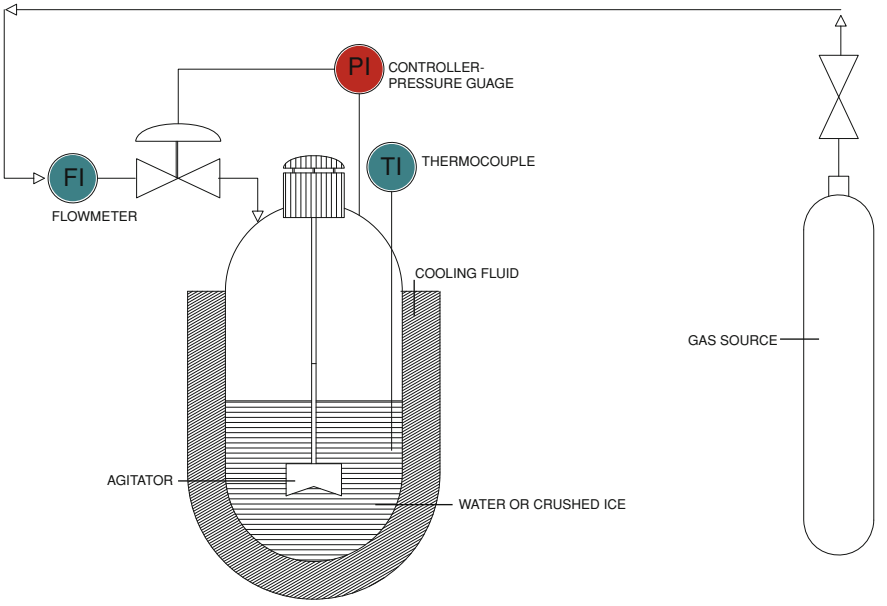

Fig. 3.14 Schematic of typical experimental equipment for hydrate studies

hydrate forms and reduces the contact between the water and hydrate-forming gas. Alternatively, other designs such as rocking cells which tilt the reactor have been used as well.

When forming from ice, the ice should be added as a fine powder to increase the surface area allowing more contact with the hydrate former. It is also possible to visually observe the formation and dissociation by adding sight glasses to the reactor or installing a fiber optic camera. Visual observation is not necessary required, however, as pressure and temperature measurements provide sufficient data to determine the rate and extent of hydrate formation. Because hydrates tend to concentrate gases, a large pressure drop is often observed with hydrate formation. In addition, the formation process is exothermic which cause the temperature in the reactor to rise.

A typical experiment begins with loading the reactor with water and pressuring the purged or evacuated head space with the desired hydrate-forming gas. The temperature is then lowered below the hydrate stability temperature. In practice, some subcooling (on the order of 4–6°C) along with agitation is needed to start nucleation and the initial growth of hydrate crystals.

Figure 3.15 shows a typical pressure and temperature response during methane hydrate formation. Starting at 5 MPa, the temperature is lowered to around 2°C. At this pressure, this represents a subcooling of around 5°C. The initial drop in pressure to around 4.2 MPa is due to the gas cooling from 25°C and some of the methane dissolving into the water phase to reach saturation. Hydrate nucleation and formation is observed starting at 2.5 h with a rapid decrease in pressure and an

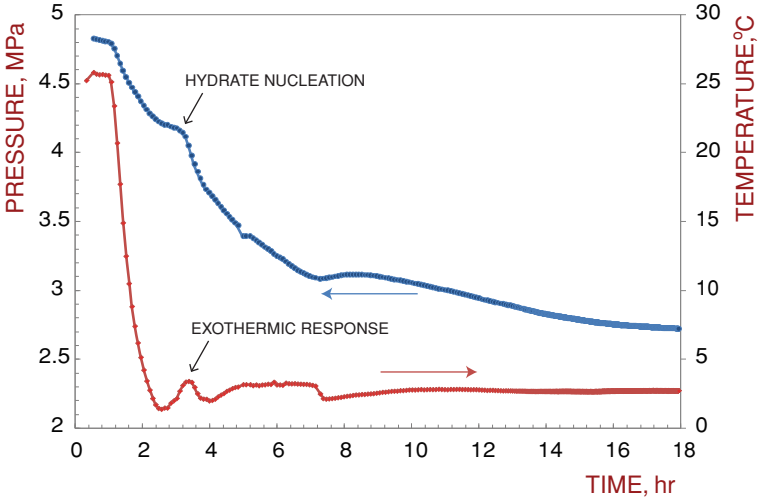

Fig. 3.15 Typically experimental readings during methane hydrate formation (RC-1 reactor, Hydrate Laboratory, University of Rome)

increase in temperature, due to the exothermic hydrate formation reaction. For the next 15 h, the pressure continues to drop to around 2.5 MPa. The overall pressure drop (around 1.7 MPa) is directly related to the amount of methane being concentrated into the hydrate phase and is used to calculate the total amount of hydrate formed. Based on the initial amount of water added, a conversion percentage to hydrate can be determined. The temperature is maintained above 0°C to prevent ice formation.

Figure 3.16 shows the same type of experiment using propane. One should note the relatively long induction time of 18 h before hydrate nucleation. While propane forms hydrate at relatively low pressure compared to methane (as shown in Fig. 3.10), the temperature window between the ice point and the second quadruple point is small. This limits the amount of subcooling that can be applied and makes hydrate formation from propane experimentally more difficult [5]. Due to mass transfer limitations, formation from liquid water in such a reactor often leads to only limited conversion (30–70%) of the total water-to hydrate. There are experimental methods that have been developed to increase the overall conversion. One way to increase the contact surface area with the water and hydrate-forming gas is to use a spray nozzle to introduce the water into the reactor under pressure as small micro droplets. Hydrates formed using a spray nozzle results in very high percentage conversion and generally forms a soft and granular hydrate (Fig. 3.17) versus the more compact hydrate obtained in the stirred reactor.

More contact area is also accomplished using fine grained ice particles. The formation rate and yield have been shown to be directly related to the size of the ice particles. As the ice particles decrease in size, the surface to volume ratio increases and results in more rapid and complete conversion. Formation rates for

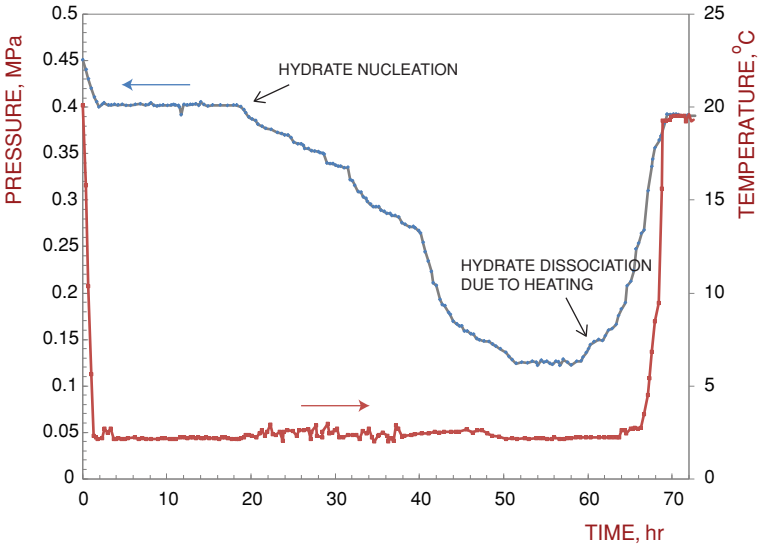

Fig. 3.16 Graph of propane hydrate formation (RC-1 reactor, Hydrate Laboratory, University of Rome)

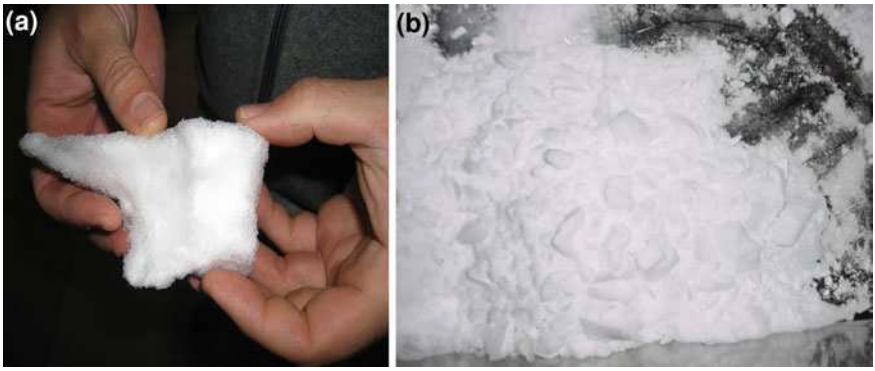

Fig. 3.17 **a** Compact methane hydrate (Photo credit: X. Zhang), and b) granular hydrate formed using a spray nozzle (Hydrate Laboratory, University of Rome)

various ice particle sizes were found for methane and CO_2 hydrates at 271–272 K [9]. Forming below the ice point allows for higher subcoolings and, in the case of propane, hydrate formation can begin almost instantaneously [5]. Another technique to obtain high conversion from liquid water is to introduce a small amount of surfactant into the water.

The stirred reactor experiments described above were *isochoric*, or constant volume, experiments. It is also possible perform these experiments as *isobaric*, or

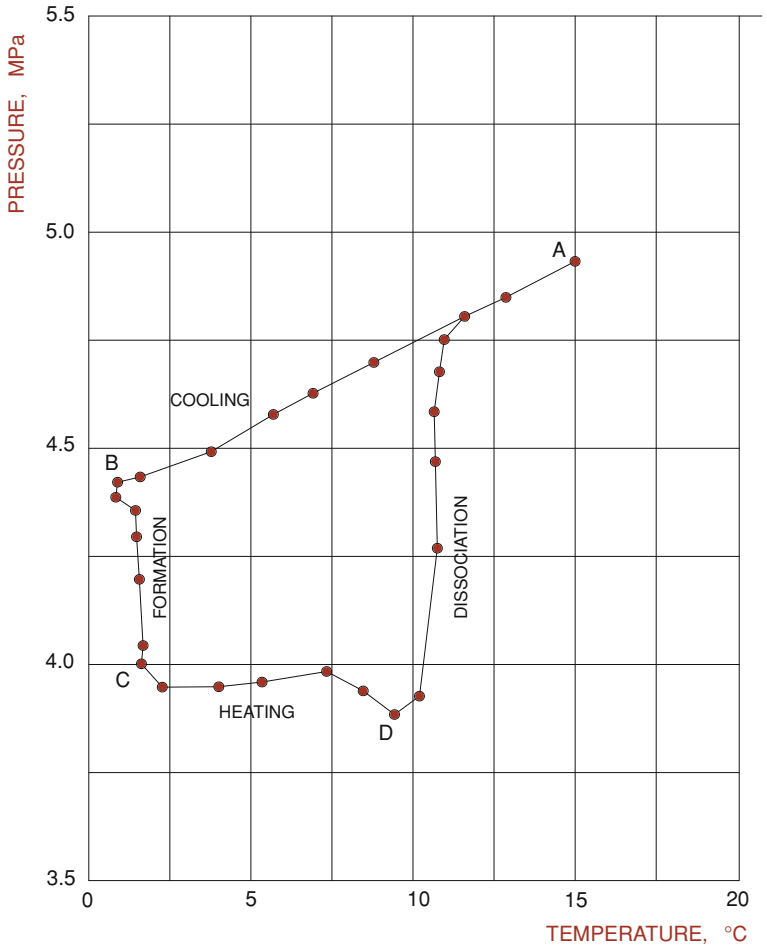

Fig. 3.18 Determining the actual hydrate stability conditions through isochoric cooling and slow heating

constant pressure. In this type of experiment, the rate and overall gas consumption, instead of pressure drop, is used to calculate formation rate and conversion.

Because of metastability, it is not generally possible to accurately measure the hydrate formation curve by the hydrate formation experiments described above. The hydrate formation curve is experimentally determined using the procedure shown in Fig. 3.18, called a hysteresis loop. Starting from Point A, the isochoric system (in this case, methane + water) is cooled until Point B, where hydrate formation is observed. Following the end of hydrate formation (Point C), the system is slowly heated in a step-wise manner until hydrate dissociation is observed at Point D. As hydrate dissociates, the gas is released, increasing the pressure, until it returns to the original curve at Point E. This point of intersection

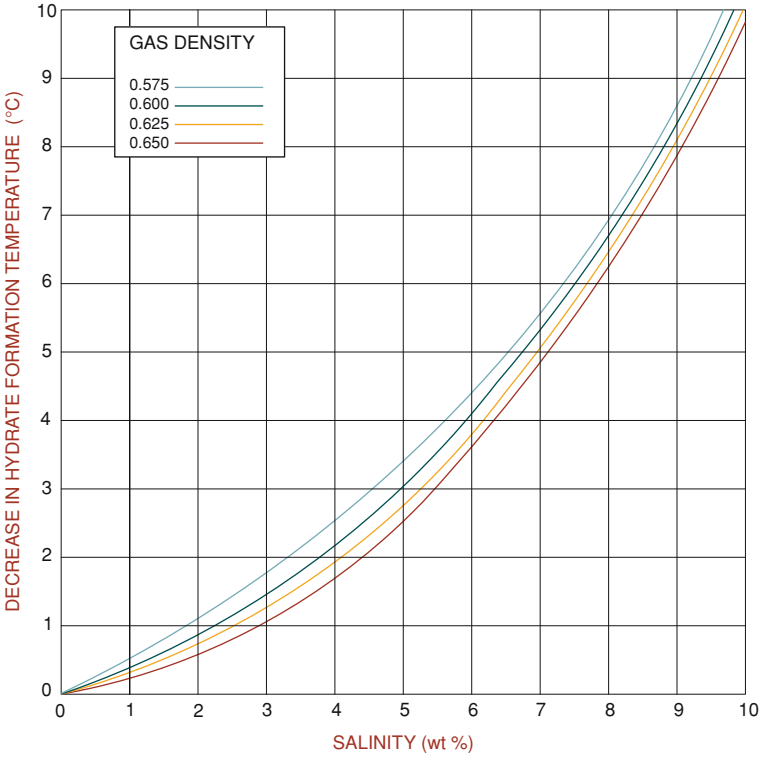

Fig. 3.19 Inhibiting influence of sea water on hydrate formation. As salt concentration increases, the hydrate stability temperature decreases for a given pressure [2]

is one point of the 3-phase hydrate stability line on the P–T diagram. Extreme care must be taken when performing such experiments as heating too quickly can lead to artificially high hydrate stability temperatures.

3.7 Influence of Inhibitors and Multiple Hydrate Components

Hydrates are found in large quantities in marine sediments. Unlike most laboratory studies, the water around these marine hydrates contains salts, primarily sodium chloride. Salts act as thermodynamic hydrate inhibitors and reduce the stable hydrate temperature for a given pressure. This effect is similar to putting salt on ice in the winter. The salt lowers the temperature at which ice is stable in a manner similar to hydrate. This change must be accounted for to accurately predict hydrate formation conditions. The influence of salinity is shown in Fig. 3.19. A similar effect occurs when compounds such as methanol and ethylene glycol are added to the water phase. These two compounds are the most widely used by industry to

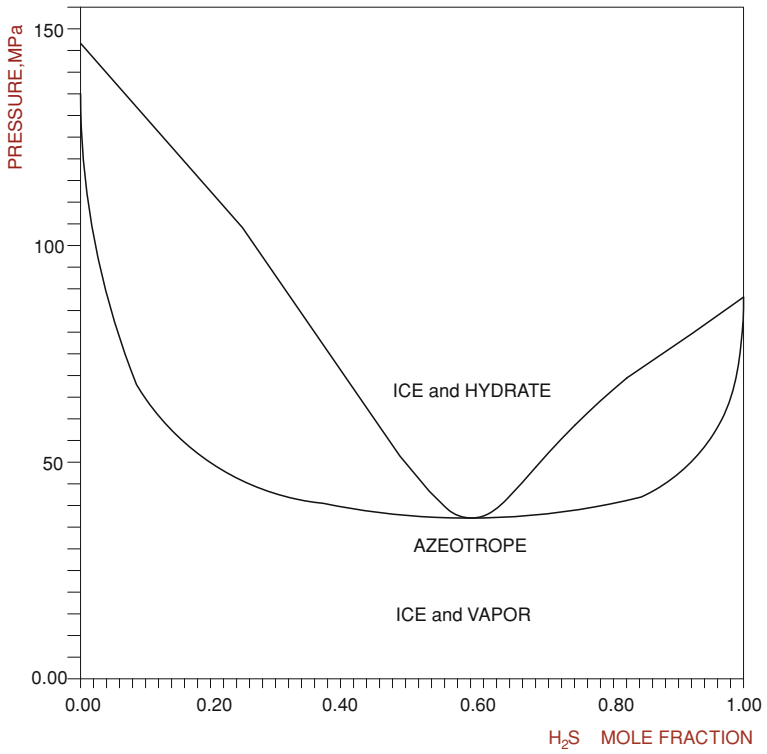

Fig. 3.20 Presence of an azeotrope at 270 K for a mixture of H_2S and propane

avoid hydrates by shifting the hydrate stability curve away from operating conditions.

As mentioned above, the presence of more than one hydrate former in a gas mixture complicates the prediction of the hydrate stability region and the stable crystal structure (e.g., sI, sII). For natural gas, sII is the predominant structure due to the presence of heavier hydrocarbons, such as ethane, propane, and butanes. These molecules are very stabilizing for the large cage of sII and even small amounts will result in sII hydrate formation. To get an example of how significant a second hydrate former can be, we will look at a system of methane and propane. At 15°C, pure methane hydrate forms a sI hydrate at 12.8 MPa (∼ 1,856 psi). When 1% propane is added, sII is the stable structure and the stability pressure drops dramatically by almost 40% to 7.7 MPa (∼ 1,117 psi). Another unexpected observation was the formation of sII with mixtures of methane and ethane. While both form sI are pure components, certain mixtures of the two gases will result in a sII hydrate. Interestingly, this type of behavior was predicted in the original paper by van der Waals and Platteeuw [20].

Azeotropes can also be found in certain mixtures, including binary systems of propane–hydrogen sulfide, methane–ethylene, methane–ethane, methane–propane,

and other. In such azeotropic mixtures, there is a point where the hydrate and vapor phases have the same composition (Fig. 3.20). In these mixtures of guests, the resulting hydrate phase can be more stable than either of the pure compounds. This synergistic increase of hydrate stability is related to how the guests occupy the hydrate cages. By mixing hydrogen sulfide and propane, the hydrate formation pressure is lowered to 0.64 bar compared with 1.45 and 3.18 bar for pure compounds, respectively. In this case, propane can only occupy the sII large cages while H_2S favors the small cages, resulting in an overall increase in hydrate stability.

References

1. Brewer PG, Friederich G, Peltzer ET, Orr FM Jr (1999) Direct experiments on the ocean disposal of fossil fuel CO_2. Science 284(5416):943–945
2. Carroll J (2009) Natural gas hydrates. A guide for engineers, 2nd edn. Gulf-Elsevier, Oxford
3. Circone S, Kirby SH, Stern LA (2005) Direct measurement of methane hydrate composition along the hydrate equilibrium boundary. J Phys Chem B 109(19):9468–9475
4. Gabitto J, Tsouris C (2006) Dissolution mechanisms of CO_2 hydrate droplets in deep seawaters. Energy Conv Manag 47(5):494–508
5. Giavarini C, Maccioni F, Santarelli ML (2003) Formation kinetics of propane hydrates. Ind Eng Chem 42(7):1517–1521
6. Giavarini C, Maccioni F, Santarelli ML (2007) Dissociation rate of THF-methane hydrates. Petrol Sci Tech 26(18):2147–2158
7. Hester KC, Koh CA, Miller KT et al (2005) Molecular storage of hydrogen in binary THF/H_2 clathrate hydrate. In: Proceedings of the international conference on gas hydrates 5, Trondheim, 13–16 June, paper 1374
8. Katz DL, Lee RL (1990) Natural gas engineering: production and storage. McGraw-Hill Publ Co, New York
9. Komai T, Kawamura T, Kang SP et al (2002) Formation kinetics of gas hydrates from fine ice crystals. In: Proceedings of the international conference on gas hydrates 4, Yokohama, 19–23 May, 474–477
10. Mao WL, Mao H, Goncharov AF et al (2002) Hydrogen clusters in clathrate hydrate. Science 297:2247–2249
11. Max MD (2003) Natural gas hydrate in oceanic and permafrost environments. Kluwer Academic Publishers, London
12. Pauer F, Kipfstuhl J, Kuhs WF, Shoji H (1996) Classification of air clathrates found in polar ice sheets. Z Polarforsch 66:31–38
13. Rehder G, Kirby SH, Durham WB et al (2004) Dissolution rates of pure methane hydrate and carbon-dioxide hydrate in undersaturated seawater at 1000-m depth. Geochem Cosmochem Acta 68(2):285–292
14. Ripmeester JA (2000) Hydrate research-from correlations to a knowledge-based discipline: the importance of structure. In: Holder GD, Bishnoi PR (eds) Gas hydrates. Annals of the New York Academy of Sciences, vol 912. New York, pp 1–16
15. Seo YT, Kang SP, Lee H (2001) Experimental determination and thermodynamic modeling of methane and nitrogen hydrates in the presence of THF, propylene oxide, 1–4 dioxane and acetone. Fluid Phase Eq 189(1–2):99–110
16. Sloan ED, Koh CA (2008) Clathrate hydrates of natural gases, 3rd edn. CRC Press, Boca Raton

17. Sugahara T, Haag JC, Pinnelli S et al (2009) Increasing hydrogen storage capacity using tetrahydrofuran. J Am Chem Soc 131(41):14616–14617
18. Teng H, Yamasaki A, Chun MK, Lee H (1997) Why does CO_2 hydrate disposed of in the ocean in the hydrate-formation region dissolve in seawater? Energy 22(12):1111–1117
19. Udachin KA, Ratcliffe CI, Ripmeester JA (2002) Single crystal diffraction studies of structure I, II and H hydrates: structure, cage occupancy and composition. J Supramol Chem 2(4–5):405–408
20. van der Waals JH, Platteeuw JC (1959) Clathrate solutions. Adv Chem Phys. doi:10.1002/9780470143483.ch1
21. von Stackelberg M (1949) Feste gas hydrate. Naturwissenschaften 36(11):327–359

Chapter 4
Methods to Predict Hydrate Formation Conditions and Formation Rate

4.1 Methods to Predict Hydrate Formation Conditions

Being able to predict hydrate formation conditions (pressure and temperature for a particular gas mixture) is crucial for the oil and gas industry, largely due to the risk of hydrate blockages in pipelines during oil and gas transportation and storage. In addition, any attempt to develop exploitation methods of the natural gas resources in hydrates must start with understanding under what conditions hydrates are stable.

Predicting hydrate stability conditions have developed over the years. We will begin with a review of relatively quick and simple hand calculations, followed by graphical and nomogram approaches, and finish with the state-of-the-art computer-based calculations using rigorous thermodynamic models.

4.1.1 Hand Calculation Methods

Hand calculation methods for hydrate stability were largely developed in the 1940s by Katz and colleagues. These relatively simple and eloquent methods, before the days of computers, were powerful in allowing one to predict hydrate stability for the first time, often quite accurately [22].

The two most popular and widely used hand calculations methods are the gas gravity method and the *k*-value method. The gas gravity method is based solely on the density of a natural gas. Plotted on a P–T diagram similar to those shown in Chap. 3, several curves are shown representing natural gases of different densities (Fig. 4.1). Density is in the form of specific gravity relative to air. It can be measured experimentally or calculated by dividing the average molecular weight of the gas of interest (e.g., 16.04 g/mol for CH_4) by that of air (28.966 g/mol).

The second method is based on the calculation of a *k*-value. The *k*-value is defined for each component as the mole fraction ratio between the vapor and

C. Giavarini and K. Hester, *Gas Hydrates*, Green Energy and Technology,
DOI: 10.1007/978-0-85729-956-7_4, © Springer-Verlag London Limited 2011

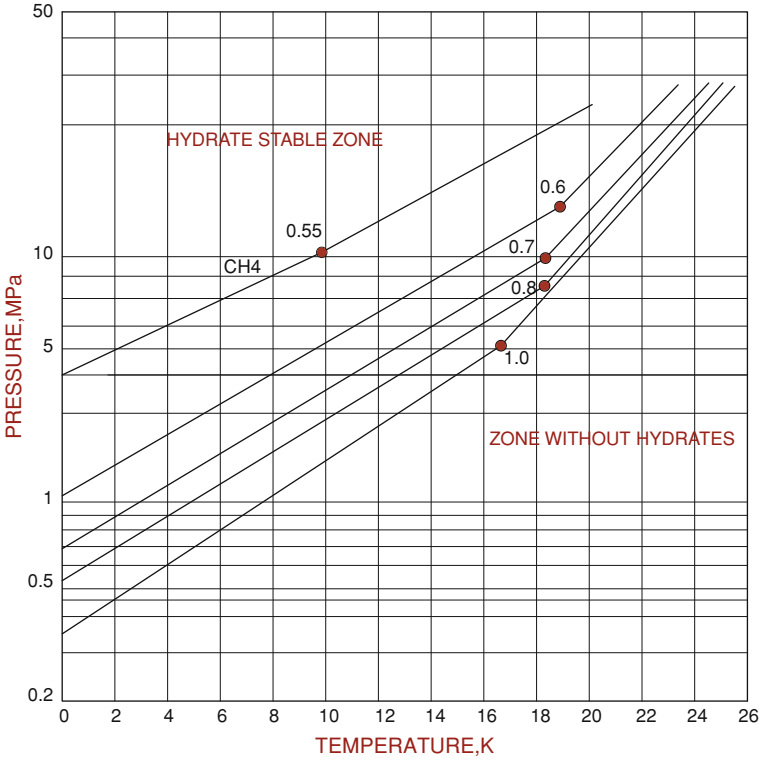

Fig. 4.1 Formation conditions for gas hydrates formed from *sweet* natural gas (not containing sulfur compounds) as a function of density (gravity relative to air). The *upper curve* is relative to natural gas with a density of 0.55 (16/29); the other curves are relative to other gas densities [4]

hydrate phase. If the *k*-value is unity, the component does not preferentially concentrate in either phase. If the value is <1, the component concentrates preferentially in the hydrate phase versus the vapor phase. The reverse is true if $k > 1$. A more detailed explanation of the *k*-value method is given by others including Carroll [4] and Sloan and Koh [18], along with various *k*-value graphs.

Ballie and Wichert [2] developed a more complex method using a nomogram valid for gas densities between 0.6 and 1.0. The method allows for the presence of hydrogen sulfide in addition to propane. This was an advantage to this approach since hydrogen sulfide was not valid in the previously discussed methods. Using a nomogram (Fig. 4.2) is not immediately intuitive. For this reason, we will present the steps needed to use the nomogram to calculate the temperature of hydrate formation for a particular gas mixture.

1. Find the gas mixture density in the chart as well as the desired pressure.
2. From the selected pressure, move to the right until the curve with the mixture's hydrogen sulfide concentration is intersected (interpolate if needed).
3. Move vertically down until one of the density lines is reached.

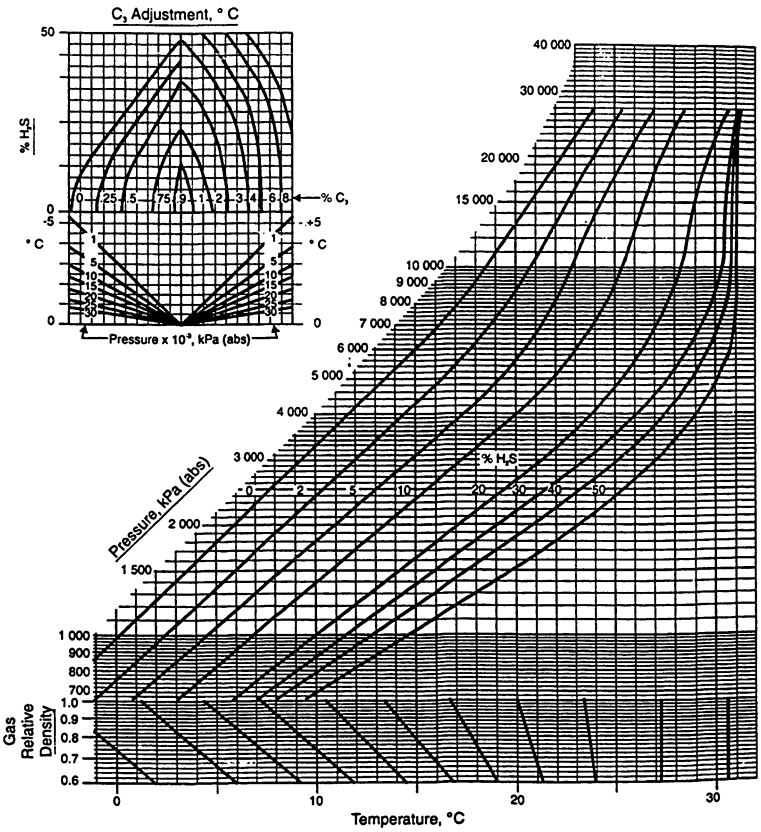

Fig. 4.2 Nomogram from Baillie and Wichert used to estimate hydrate formation conditions [4]

4. Move in this line until you reach the gas mixture density.
5. Move vertically down to determine the *base* temperature for the given density and pressure.
6. Next, using the small diagram of the left, find the mixture's H_2S concentration on the upper graph and move horizontally until you reach the mixture's propane concentration.
7. Move vertically down to the lower graph until you intersect the line for the desired pressure. If you are on the left hand side of the lower graph, go to step 8a. If you are on the right hand side of the lower graph, go to step 8b.

8a. Read the temperature correction on the left axis and subtract it from the base temperature recorded in Step 5.

8b. Read the temperature correction on the left axis and add it from the base temperature recorded in Step 5.

A similar procedure can be applied to determine the pressure for a given temperature, as long as the gas density is known. All of the above methods do not

explicitly take into account the hydrate crystal structure (e.g., sI, sII). In fact, under the range of conditions, transitions between sI and sII may be occurring. Despite this, they are relatively accurate (to around 15–20%) especially for sweet natural gas mixtures (those containing no H_2S). These hand calculation methods were based on specific types of gas mixtures and extrapolating to other gas mixtures can lead to large variations in accuracy.

4.1.2 Computer-Based Thermodynamic Models

Hand-calculation methods are still sometimes used at least to give a first approximation. However, today, there are several software packages which are relatively simple to use and provide phase equilibrium calculations based on rigorous thermodynamic models. The basis for these calculations is normally the chemical potential and the minimization of the Gibbs free energy. A minimum in the Gibbs free energy will determine which phases are stable, including hydrates. This approach also allows for the determination of which particular hydrate structure (e.g., sI, sII, sH) will form. It is even possible to have co-existence of multiple hydrate structures.

Thermodynamically, the chemical potential of the hydrate phase can be calculated in two steps. The first step is the formation of a hypothetical *empty* hydrate lattice (or crystal) made from pure water. Then, in the second step, the cages are filled with guest molecules.

$$\text{Pure water } (\alpha) \rightarrow \text{ Empty lattice}(\beta) \rightarrow \text{ Filled lattice } (\text{H})$$

The change in chemical potential is calculated as:

$$\mu^{\text{H}} - \mu^{\alpha} = \left(\mu^{\beta} - \mu^{\alpha}\right) + \left(\mu^{\text{H}} - \mu^{\beta}\right) \tag{4.1}$$

From Eq. 4.1, the first term on the right relates to the free energy contribution from the host water molecules. It represents a phase change of water from liquid (or ice) to a hypothetical empty lattice. This change can be calculated using traditional thermodynamics [13, 18]. The second term represents the free energy contribution and lattice stabilization by the guest molecules. In 1959, van der Waals and Platteeuw proposed the first model to calculate the $\mu^{\text{H}} - \mu^{\beta}$ term based on statistical thermodynamics. This model was a key step in predicting hydrates and still used today in largely the same form. The approach by van der Waals and Platteeuw [20] was to treat hydrate guests in the water cages as gas molecules adsorbed onto a surface, forming an ideal solid solution.

The major assumptions in the formulation by van der Waals and Platteeuw are that each cage contains only one guest. Moreover, guests do not interact with each other and guest molecules do not distort the cages. Based on those assumptions, the $\mu^{\text{H}} - \mu^{\beta}$ term in Eq. 4.1 can be expressed as:

$$\mu^H - \mu^\beta = RT \Sigma \nu_i \ln(1 - X_i) \tag{4.2}$$

where ν_i is the number of cages in a unit cell and X_i is a probability function related to a guest molecule occupying a cage of type i. X_i is a function of the cage type, the guest molecule, pressure, and indirectly the temperature. The term X_i can be expressed as:

$$X_i = (c_i P)/(1 + c_i P) \tag{4.3}$$

where c_i (also called a Langmuir constant) is a function of the guest molecule and the cage type. The larger the Langmuir constant, the more affinity a guest has for a particular cage type.

The Langmuir constant has traditionally been treated as empirical and regressed from experimental data. Recently, researchers have shown that it can be calculated without the need for experimental measurements, using quantum mechanical methods [1, 9].

This fundamental model of van der Waals and Platteeuw opened up the possibility to predict and understand gas hydrate phase equilibria behavior for a wide range of gases and their mixtures, without having to measure every possible system experimentally. Many different interesting and exciting behaviors were first predicted using this model and later verified experimentally, such as azeotropes (see Chap. 3) and unexpected hydrate structures (sII formation from a mixture of two sI guest molecules).

This model was adopted and used for practical engineering calculations in oil companies who needed accurate predictions for a wide variety of gas mixtures. Parrish and Prausnitz [12] first extended the model to multi-component mixtures. This was accomplished by changing the X_i expression in Eq. 4.2 to a summation over all the components:

$$\mu^H - \mu^\beta = RT \Sigma_i \nu_i \ln(1 - \Sigma_k X_{ki}) \tag{4.4}$$

In addition, the pressure term in Eq. 4.3 was replaced by the fugacity for each component:

$$X_{ki} = c_i f_k/(1 + \Sigma_j c_{ij} f_j) \tag{4.5}$$

where f_i is the fugacity of each component in the desired gas mixture. Fugacity can be solved for using any equation of state, such as Peng and Robison [14] or Soave–Redlich–Kwong [19]. By assumping the hydrate structure, an iterative procedure allows for the free energy to by minimized where $\mu^H - \mu^\alpha = 0$.

Over time, other additions and modifications were made. In 1977, Ng and Robinson [11] modified Eq. 4.1 to allow for hydrate predictions in the presence of a liquid hydrocarbon (e.g., oil). Most recently, hydrate predictions have been performed using a Gibbs Energy Minimization technique. In this approach, no assumptions are made about the stable hydrate structure.

4.1.3 Software Packages for Hydrate Prediction

Today, there are several software packages available for hydrate phase equilibria prediction. The most commonly used programs in industry are MultiFlash (Infochem) and PVTSim (Calsep). CSMGem, which was developed at the Colorado School of Mines, is available with purchase of the book by Sloan and Koh [18]. Other programs include HydraFlash (Heriot-Watt U.), EQUI-Hydrate (DB Robinson Schlumberger), and Prosim (Bryan Research and Engineering). This is by no means a complete list of available programs which predict hydrates. Carroll [4] presents a comparison between many of the most popular programs.

4.2 Hydrate Formation Kinetics

The hydrate formation process can be divided into two steps: nucleation followed by growth. Stable hydrate nuclei generated from a supersaturated solution lead to the growth of hydrate crystals. The time interval between supersaturation and the formation of the first clusters is called the *nucleation* or induction time.

Skovborg et al. [17] defined a *driving force* for hydrate nucleation in terms of the chemical potential difference between water in the liquid and hydrate phase. Nucleation times are stochastic and difficult to predict. One interesting observation has been the *memory effect*. This effect occurs when hydrate is dissociated by decreasing the pressure or raising the temperature. If the system is again brought into the hydrate stable zone (cooling or re-pressurizing), hydrates form with little to no nucleation time. This is likely due to microscopic crystallites remaining in solution as the memory effect goes away if the system is sufficiently heated (around 40°C) or enough time is given [18].

The driving force has also been defined on the basis of the fugacity difference for the guest molecule [10] and as the degree of subcooling, which is the hydrate formation temperature minus the system temperature [21]. These three definitions correspond to particular cases of a more general concept expressed by the variation of the Gibbs free energy of the system [18]. Therefore, the rigorous definition of the driving force for the formation of a new phase is the chemical potential difference between the old phase and the new one, and the difference is called *supersaturation* [8].

Once the critical radius has been reached, the further growth of the nucleus is related to a decrease in the Gibbs free energy and is spontaneous. If energy is not removed, temperature will rise as far as the hydrate stability temperature due to the exothermic nature of hydrate formation. Heat transfer becomes important for further hydrate formation. This effect could be used in a beneficial way for preventing plugging in pipelines. If sufficiently insulated, temperatures in the pipeline could reach the hydrate stability temperature slowing or stopping further hydrate formation.

4.2.1 Modeling of Hydrate Formation Kinetics

A critical review of the literature on gas hydrates kinetics is provided by Ribeiro and Lage [15] who analyzed 14 models. In fact, contrary to hydrate thermodynamics, hydrate kinetics are not so well understood. Prof. Bishnoi's group at the University of Calgary (Canada) largely began this research over three decades ago and has provided an important contribution to this area. We mention briefly some of these models.

4.2.1.1 Model of Eglezos, Kalogerakis, Dholabhai, Bishnoi

The so-called *Englezos model* [5] is probably the most widely known and applied hydrate kinetic model. According to it, hydrate formation is composed of three steps:

1. diffusion of the guest molecule from the gas/liquid interface to the liquid bulk
2. diffusion of the guest molecule from the liquid bulk to the hydrate/solution interface
3. reaction of water and guest molecule at the hydrate/solution interface.

The driving force for hydrate formation is defined as the difference between the fugacity f of the dissolved gas and the fugacity f_{ex} at the experimental conditions.

The growth rate of a hydrate nucleus with an interfacial area A is:

$$dn/dt = K\ A\ (f\ -\ f_{ex}) \tag{4.6}$$

where K is the kinetic constant associated with steps 1 and 2.

4.2.1.2 Model of Skovborg and Rasmussen

Starting from the Englezos model, Skovborg and Rasmussen [16] proposed its simplification assuming that all resistance to mass transfer during hydrate formation is due to the diffusion of the gas from the gas/liquid interface to the liquid bulk and removing the population balance equation introduced by Englezos. Their approach is as follows:

$$dn/dt\ =\ k\ A_{g/l}C_w\left(x_{eq}\ -\ x_b\right) \tag{4.7}$$

where k is the mass transfer coefficient at the gas/liquid interface; x_{eq} is the gas mole fraction in the liquid in equilibrium with the gas at the interface; x_b is the gas mole fraction in the liquid bulk in equilibrium with the hydrate phase; C_w is the initial water concentration. The model can also be applied to multicomponent systems.

4.2.1.3 Model of Herri, Pic, Gruy, and Cournil

When the Englezos model was developed, there were no instrumental techniques for measuring particle size distribution (e.g., light scattering). This is important as the particle size related to the surface area is a key input to the various models. Herri et al. [6] proposed a new model by modifying the model of Jones et al. [7] for the crystallization of calcium carbonate: the dynamic behavior is described by two differential equations. The Herri model is the only one which considers both nucleation and growth in the same step.

Following the Ribeiro and Lage conclusions [15], further research is necessary before a predictive, reliable model emerges for reactor design purpose. On the other hand, the thermodynamic equilibrium condition for hydrate formation can be predicted with deviations lower than 10% or better [3].

References

1. Anderson BJ, Bazant MZ, Tester JW, Trout BL (2005) Application of the cell potential method to predict phase equilibria of multi-component gas hydrate systems. J Phys Chem B 109(16):8153–8163
2. Baillie C, Wichert E (1987) Chart gives hydrate formation temperature for natural gas. Oil Gas J 85(4):37–39
3. Ballard AL, Sloan ED (2002) The next generation of hydrate prediction: an overview. J Supramol Chem 2(4–5):385–392
4. Carroll J (2009) Natural gas hydrates, 2nd edn. Gulf Professional Publishing-Elsevier, Amsterdam
5. Englezos P, Kalogerakis NE, Dholabhai PD, Bishnoi PR (1987) Kinetics of formation of methane and ethane gas hydrates. Chem Eng Sci 42:2647–2658
6. Herri JM, Gruy F, Pic JS et al (1999) Interest of in situ turbidimetry for the characterization of methane hydrate crystallization: application to the study of kinetic inhibitors. Chem Eng Sci 54(12):1849–1858
7. Jones AG, Hostomasky J, Zhou L (1992) On the effect of liquid mixing rate on primary crystal size during the gas-liquid precipitation of calcium carbonate. Chem Eng Sci 47(13–14):3817–3824
8. Kashchiev D, Firoozabadi A (2002) Nucleation of gas hydrates. J Cryst Growth 243(3–4):476–489
9. Klauda JB, Sandler SI (2002) Ab initio intermolecular potentials for gas hydrates and their predictions. J Phys Chem B 106:5722–5732
10. Natarajan V, Bishnoi PR, Kalogerakis K (1994) Induction phenomena in gas hydrate nucleation. Chem Eng Sci 49(13):2075–2087
11. Ng H-J, Robinson DB (1977) The prediction of hydrate formation in condensed systems. AIChE J. doi:10.1002/aic.690230411
12. Parrish WR, Prausnitz JM (1972) Dissociation pressure of gas hydrates formed by gas mixtures. Ind Eng Chem Process Dev 11(1):26–35
13. Pedersen KS, Fredenslung A, Thomassen P (1989) Properties of oils and natural gases. Gulf Publishing Co, Houston
14. Peng DY, Robinson DB (1976) A new two-constant equation of state. Ind Eng Chem Fundam 15(1):59–64

15. Ribeiro CP Jr, Lage PC (2008) Modelling of hydrate formation kinetics: state of the art and future directions. Chem Eng Sci 63(8):2007–2034
16. Skovborg P, Rasmussen P (1994) A mass transport limited model for the growth of methane and hydrates. Chem Eng Sci 49:1131–1143
17. Skovborg P, Ng H-J, Rasmussen P, Mohn U (1993) Measurements of induction times for the formation of methane and ethane gas hydrates. Chem Eng Sci 48(3):445–453
18. Sloan ED, Koh CA (2008) Clathrate hydrates of natural gases, 3rd edn. CRC Press, Boca Raton
19. Soave G (1992) Equilibrium constants from a modified Reidlich-Kwong equation of state. Chem Eng Sci 27(6):1197–1203
20. van der Waals JH, Platteeuw JC (1959) Clathrate solutions. Adv Chem Phys. doi:10.1002/9780470143483.ch1
21. Vysniauscas A, Bishnoi PR (1983) Kinetic study of methane hydrate formation. Chem Eng Sci 38(7):1061–1072
22. Wilcox WI, Carson DB, Katz DL (1941) Natural gas hydrates. Ind Eng Chem 33:662–672

Chapter 5
Physical Properties of Hydrates

5.1 Introduction

Hydrates can form from hundreds of different guest molecules. Interestingly, most of these guests crystallize as sI or sII hydrates. The properties of these hydrate crystals share many similarities with ice, yet there are some noted differences. Here we will give an overview of a selection of analytical techniques used to study gas hydrates followed by some of the main physical properties of hydrates.

5.2 Hydrate Formation in the Laboratory

In the laboratory, reactors capable of high pressure and low temperature operation are often used to form hydrates. These reactors vary in shape and size and operate in either continuous or batch modes, depending on the property of interest.

For studying dynamic fluid flow phenomena, such as hydrate formation during oil and gas transport in pipelines, flow loops can be used. As shown in Figs. 5.1, 5.2, these flow loops vary in shape and size. They allow for numerous tests, such as the effectiveness of additives to prevent hydrate formation, in realistic flow regimes. More discussions about flow loop studies can be found in Chap. 7.

When studying formation/dissociation kinetics or thermodynamic properties (such as heats of formation), batch reactors are commonly used. These autoclave-type reactors are placed in a temperature bath, or are jacketed with cooling fluid circulated to maintain the low temperatures needed for hydrate formation. A number of measurements are possible, from temperature to hydrate particle size during hydrate formation. Some examples are shown in Figs. 5.3–5.5. These examples show the variation in size from large liter scale stainless steel reactors (e.g., Fig. 5.3) to small micro-scale reactors (on the order of milliliters in volume, Fig. 5.4). This small cell has a sapphire window, which allows for visual observations of the hydrate growth and interrogation with techniques to learn more about

C. Giavarini and K. Hester, *Gas Hydrates*, Green Energy and Technology,
DOI: 10.1007/978-0-85729-956-7_5, © Springer-Verlag London Limited 2011

Fig. 5.1 An example of a wheel-shaped flowloop (Sintef, Norway)

Fig. 5.2 A large-scale flowloop over 140 m long (Lyre Loop, IFP, Lyon, France)

the hydrate structure and composition (e.g., Raman spectroscopy which will be discussed in the following sections). Figure 5.5 shows a medium volume calorimeter. This special type of cell is capable of sensitive and accurate measurements in small changes of heat; it is, therefore, ideal for measuring thermal properties or following reactions and their rates. Depending on the desired measurement, a wide range of possibilities exists for cell design and instrumentation to make that possible.

5.3 Techniques Used to Investigate Hydrates

5.3.1 X-ray Diffraction

The first technique used to study the crystal structure of hydrates was X-ray diffraction. It was used to identify the main structural types (sI and sII) and determine how the crystals were spatially ordered. When X-rays (or neutrons) are directed into a crystalline sample, constructive interference leads to sharp Bragg

Fig. 5.3 A high pressure reactor vessel used for hydrate formation in the laboratory [11]

Fig. 5.4 A bronze high pressure microreactor with a sapphire sight glass

peaks. As an example, Fig. 5.6 shows a series of X-ray diffraction patterns during the growth of CO_2 hydrate from ice [23]. The characteristic peaks present determine the crystal structure of the hydrate and ice. Over time, the increasing intensities of the hydrate peaks (and decreasing ice peak intensities) are directly related to the amount of hydrate present.

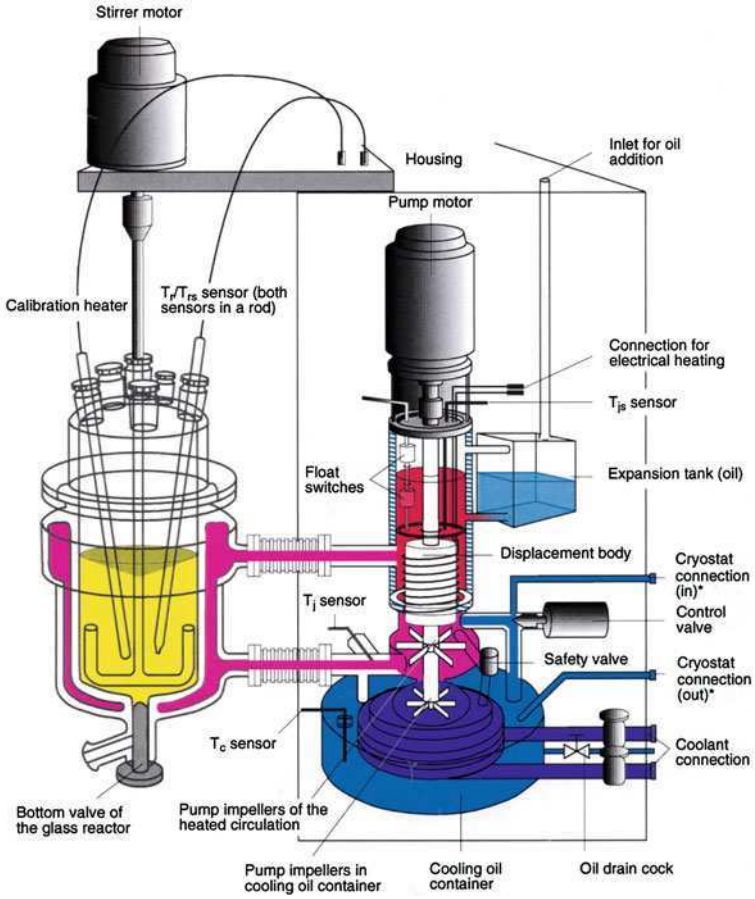

Fig. 5.5 A two liter high-pressure reaction calorimeter capable of measuring various thermophysical properties during hydrate formation and decomposition (Hydrate Laboratory, University of Rome La Sapienza)

5.3.2 Nuclear Magnetic Resonance Spectroscopy

Nuclear magnetic resonance (NMR) spectroscopy is one of the most powerful tools for studying chemical and physical properties of gas hydrates. When placed in a static magnetic field, certain nuclei have a property known as nuclear spin and absorb electromagnetic radiation (on the wavelength of radio waves). The frequency of the absorbed radiation (often referred to as ppm) gives information about the environment around nuclei. As shown in Fig. 5.7, the ^{13}C NMR spectra of methane during hydrate dissociation shows an increase in gas phase methane while the hydrate peaks decrease. Because methane in the sI large cage gives a

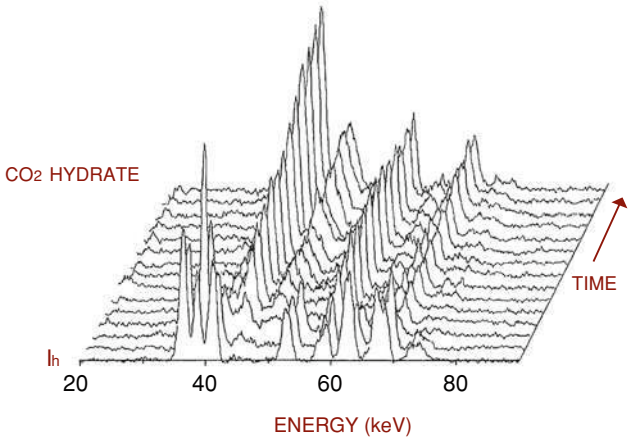

Fig. 5.6 X-ray diffraction patterns showing the growth of CO_2 hydrate from ice [23]

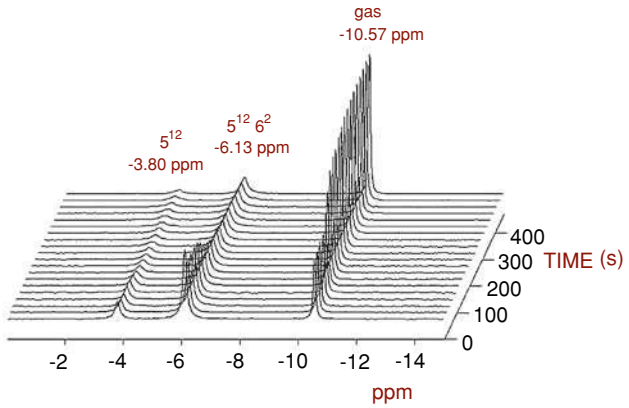

Fig. 5.7 Time-resolved ^{13}C NMR spectra during hydrate dissociation [9]

different peak than methane in the sI small cages, one can determine the relative filling of the two cages [9].

5.3.3 Raman Spectroscopy

Raman spectroscopy is another analytical technique which probes the molecular environment. It is non-destructive technique and can be used to measure hydrates under high pressure, such as through a sapphire window in a high-pressure cell (Fig. 5.4). This technique uses a laser which is focused on a sample. The laser photons mainly scatter elastically (at the same energy as the laser). However, a small number of photons are scattered inelastically (slightly different energy than

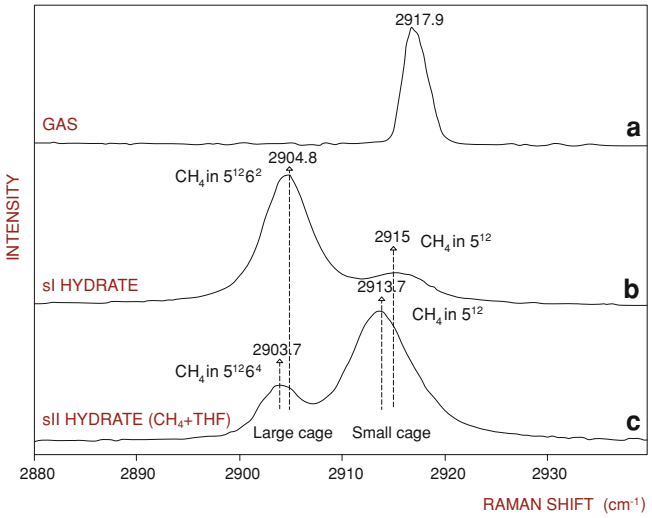

Fig. 5.8 Raman spectra showing methane in **a** the gas phase, **b** in the sI hydrate phase, and **c** in the sII hydrate (mixed methane + THF hydrate) [22]

the laser beam). This change is due to absorption by molecular vibrations of molecules. As shown in Fig. 5.8 for a stretching vibration of methane, the energy (Raman shift) for a given vibrational absorption is further affected by the environment around the molecule. Changes in both energy and peak width occur for methane in the gas phase and in the hydrate cages. The peak areas for methane in the different hydrate cages are also used to determine relative cage filling.

5.3.4 Differential Scanning Calorimetry

Differential scanning calorimetry (DSC) is a thermal analysis technique that measures variations in enthalpy (ΔH) as a function of temperature during heating and cooling cycles. Changes in ΔH as a function of time can also be monitoring using a constant temperature mode of operation. It is a rapid and versatile technique that only requires small amounts of sample (micro to milligrams) and can be run under pressure. This technique has been used to study hydrates since 1980 [2, 10, 15].

A recent more advanced version of this technique called modulated DSC (MDSC) allows for the separation of two curves: one for reversible thermodynamic phenomena and the other for irreversible kinetic phenomena. For hydrates, the curve related to reversible thermodynamic phenomena is particularly useful as these effects would not be visible in the traditional approach [5–7]. As shown in Fig. 5.9 for a sample of ethane hydrate, the MSDC technique allows for the presence of ice to be identified and quantified.

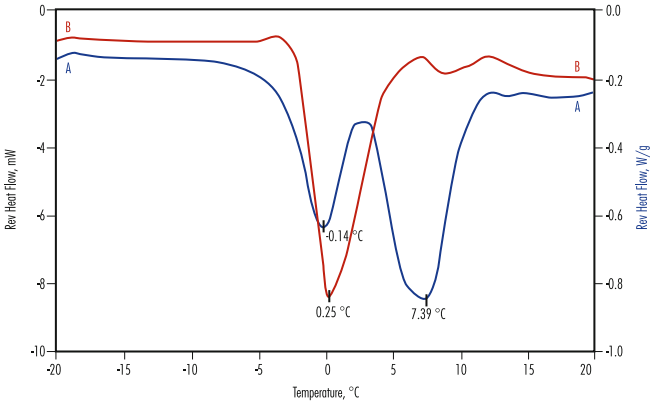

Fig. 5.9 Reversible MDSC curves for an ethane hydrate with different amounts of ice present. **a** 35% hydrate and 65% ice. **b** 15% hydrate and 85% ice. The ice melting peak is at about 0°C while the hydrate melting peak is at about 7°C (Hydrate Laboratory, University of Rome La Sapienza)

5.4 Some Key Hydrate Physical Properties

5.4.1 Hydrate Density

Hydrate density (or specific gravity) is one of the most basic and useful properties. Density is often determined by weighing a known volume of a substance. However, it is not readily possible to do this with hydrates as they must be under pressure to remain stable.

Density is the mass of a substance for a given volume. As hydrates are crystal structures, it is possible to determine the density based on the lattice size of the crystal and the concentration of guests filling the cages. The easiest volume to use is that of one unit cell. The volume of one unit cell of hydrate can be calculated using the unit cell lattice parameter. The lattice parameter is measured typically by X-ray or neutron diffraction and varies with pressure, temperature, and guest filling [20]. Values of 12 Å for sI and 17 Å for sII can be used for a good first approximation. One angstrom (Å) is equal to 10^{-10} m. As sI and sII hydrates have cubic lattices, the volume is obtained by cubing the lattice parameter.

Using this volume, the density is calculated as:

$$\rho_{\text{hydrate}}\left(\text{kg/m}^3\right) = 10^{27}\left[\left(\text{MW}_{\text{water}}\text{N}_{\text{W}} + \text{MW}_{\text{guest}}\text{N}_{\text{guest}}\right)/\left(\text{V}_{\text{hydrate}}\text{N}_{\text{A}}\right)\right] \quad (5.1)$$

where

MW_{water} is the molecular weight of water (18.02 gm/mol),
N_{w} is the number of water molecules per unit cell (46 for sI, 136 for sII), MW_{guest} is the molecular weight of the guest (in gm/mol),
N_{guest} is the number of guest molecules per unit cell,

Table 5.1 Densities for hydrates with various guests

Guest molecule	Structure	Mol. Wt. (g/mol)	Density (kg/m^3)	Density (lb/ft^3)	Density (mol/L)
Methane	sI	17.74	911	56.9	51.4
Ethane	sI	19.37	951	59.4	49.1
Propane	sII	19.46	902	56.3	46.4
Iso-butane	sII	20.24	925	57.7	45.7
Carbon dioxide	sI	21.38	1086	67.8	50.8
Hydrogen Sulfide	sI	20.24	1040	64.9	51.4
Ice	Ih	–	917	57.2	50.9

$V_{hydrate}$ is the volume of one unit cell (12 $Å^3$ for sI and 17 $Å^3$ for sII),
N_a is Avogadro's number (6.022×10^{23} mol^{-1}).

This can easily be extended to multi-component hydrates by adding more guest terms to the numerator. The molecular weight of the hydrate is simply defined as the numerator divided by Avogadro's number. Table 5.1 shows densities for many hydrates of interest.

5.4.2 Thermal Properties of Hydrates

5.4.2.1 Heat Capacity

Heat capacity, or specific heat, is a thermal property that is of practical importance in areas such as energy production from hydrates. Heat capacity of a material is defined as the amount of heat required to change a body's temperature by a given amount. Heat capacities, as with heats of dissociation, are most often measured on calorimeters, instruments specially designed to measure changes in heat.

Limited studies have reported heat capacity data on hydrates [20]. Hydrate heat capacity increases with temperature and, therefore, it should be measured under expected process conditions. Methane hydrate heat capacity has been shown to linearly increase from 0.87 to 2.08 J/gm hydrate/K between 85 and 270 K [10]. These values for heat capacity are similar to ice.

Above the ice point from ~279 to 285 K, the heat capacity of methane hydrate increases from 2.08 to 2.28 J/gm hydrate/K [8]. These values are about half of the heat capacity of liquid water.

5.4.2.2 Thermal Conductivity

Thermal conductivity is the rate at which heat is transferred through a material. While many hydrate properties are analogous to ice, hydrate thermal conductivity is anomalously low, about a fifth of that of ice. The thermal conductivity values for

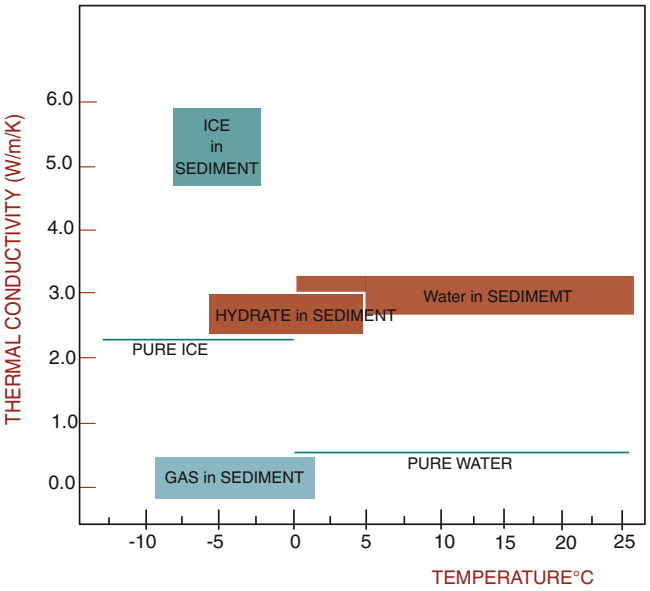

Fig. 5.10 Typical thermal conductivity values for components in the bulk phase and in sediment [20]

hydrates are more like a glass than a well-defined crystal structure [24]. The reason for this difference is that the guest molecules in the cages effectively disrupt and slow the flow of heat through the hydrate.

Pure methane hydrate thermal conductivity is similar to liquid water, around 0.5–0.6 W/(m K) [8, 13, 25]. Much of the interest in hydrate thermal conductivity is related to producing energy from gas hydrates. Therefore, thermal conductivity measurements are often performed on hydrates in sediment. This results in a composite thermal conductivity which is a *mixture* of each component's thermal conductivity. Figure 5.10 shows typical thermal conductivity values for components in the bulk phase and in sediment.

5.4.2.3 Thermal Expansivity

Most materials tend to expand when heated. A measurement of this change is thermal expansivity. This is another property where hydrates and ice differ (Fig. 5.11). This difference between hydrate and ice can again be attributed to the guest molecules. Tse and White [24] proposed that the guest molecules were exerting a small internal pressure on the cage walls, slightly weakening the hydrogen bonding of the host waters.

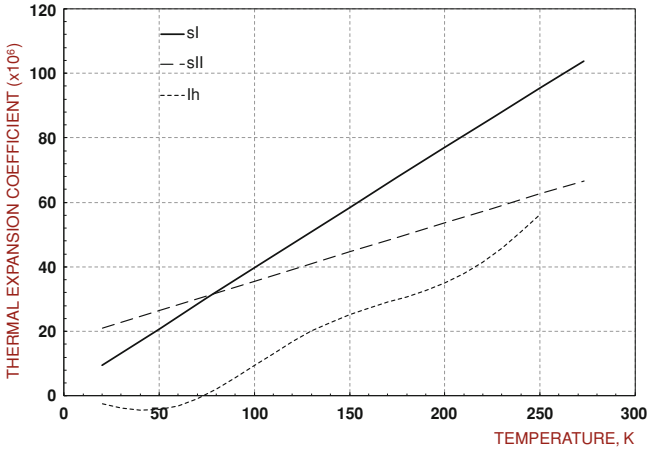

Fig. 5.11 Thermal expansion coefficient for sI & sII hydrate, as well as ice [12]

The size of the hydrate lattice is a function of crystal structure and the hydrate guests. The guest affects the absolute size of the hydrate lattice, where larger guests result in a large lattice. However, the thermal expansivity (or the rate of change in volume with temperature) is largely only a function of the crystal structure [12].

5.4.2.4 Heat of Dissociation

The heat (or enthalpy) of dissociation for hydrates is a fundamentally important property to characterize for a number of reasons. It represents the energy change when water and gas is converted to hydrate. Hydrates formation, like ice, is an exothermic process, meaning heat is released. Conversely, hydrate dissociation is endothermic and energy is required to keep the process going.

The amount of heat released (or consumed) has practical implications both for flow assurance (preventing hydrate blockages in pipelines) and production of methane from natural hydrates. When producing hydrates, the endothermic process will remove heat and lower the surrounding temperature even below the ice point. Ice formation could have dramatic implications on the rate of gas production.

Hydrate heat of dissociation data in the literature is typically reported on an energy per mole (or gram) of gas basis. Another potentially useful way to report heats of dissociation would be on the basis of moles of water. The filling fraction of hydrate guests varies with guest type and conditions. However, the number of water molecules per unit cell remains constant. Reporting on a water basis allows for a more direct comparison of the effect of the hydrate guest on the heat of dissociation. Table 5.2 shows the heats for dissociation for various guests.

Table 5.2 Heats of dissociation for various hydrate guests [10]

Guest molecule	Structure	Hydration number (n)	ΔH_d (kJ/mol gas)	ΔH_d (kJ/mol water)
Methane	sI	6.00	54.2	9.03
Ethane	sI	7.67	71.8	9.36
Propane	sII	17	129.2	7.60
Iso-butane	sII	17	133.2	7.84
Ice	Ih	–	–	6.01

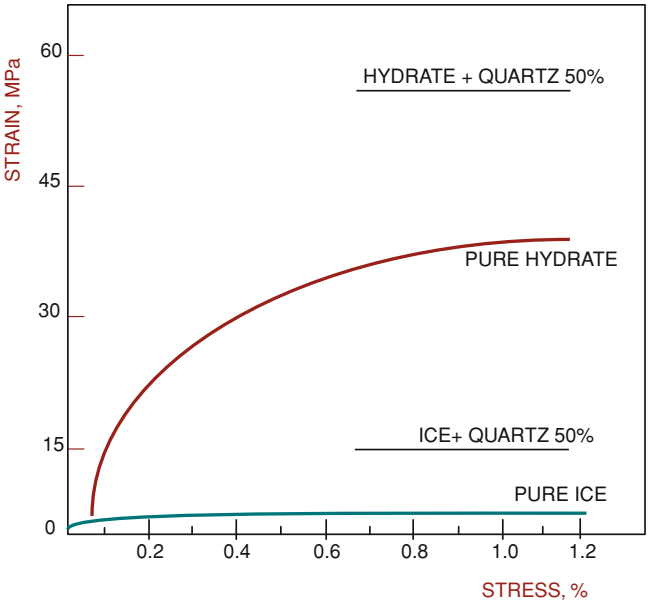

Fig. 5.12 Stress versus strain curves for samples of hydrate and ice [4]

For a good engineering approximation, one can use the Clausius-Clapeyron equation to predict the hydrate heat of dissociation in the following form [19]:

$$d(\ln P)/d(1/T) = -\Delta H_d/(z\,R) \tag{5.2}$$

where ΔH_d is the heat of dissociation, z is the gas compressibility factor, and R is the ideal gas constant. The left-hand side term can be easily determined with phase equilibria data.

This approximation has been shown to work well under low pressure conditions. However, the Clausius-Clapeyron equation has increasing prediction error for the methane hydrate heat of dissociation at higher pressures (around 25% over-prediction at 20 MPa). For better accuracy the more rigorous Clapeyron equation should be used. Recent experimental work has verified the prediction using the Clapeyron equation for the methane heat of dissociation, which remains almost constant up to 20 MPa [1, 8].

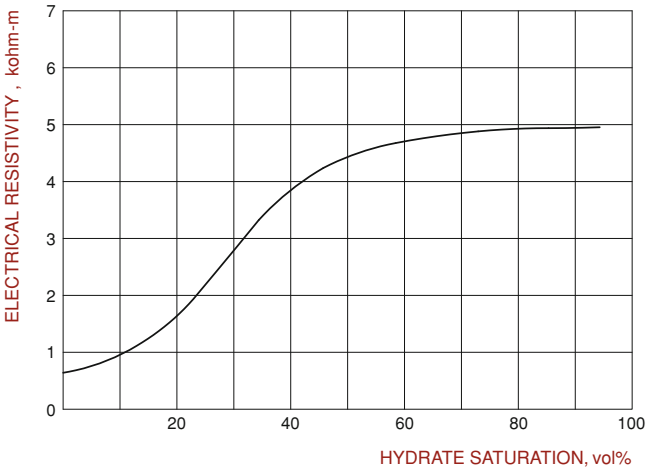

Fig. 5.13 Changes in electrical resistivity as a function of hydrate saturation in a water-filled sediment sample [16]

5.4.3 Mechanical Properties of Hydrates

Pure hydrates are twenty times stronger than ice. In compressional deformation experiments, ice (Ih) was found to deform significantly faster than pure methane hydrate [3]. Figure 5.12 shows the resistance to plastic deformation for methane hydrate and ice, both as bulk phases and in quartz sand [4]. The hydrate samples were consistently stronger than the ones with ice and significantly increased the cohesion strength of the sediments. This could be an important property when considering production of methane from hydrate reservoirs. Experiments on hydrates in sand cores have shown that increased hydrate saturation led to increased mechanical strength in the cores [14, 18]. Depending on where hydrate forms in the pore space, it could provide significant stability to the sediment matrix. Understanding how hydrate forms in the pore space and the strength it provides to the sediment is critical when evaluating the effect of hydrate dissociation, both due to energy production (Chap. 8) or natural environmental changes (Chap. 10). Currently work is being conducted to evaluate geomechanical stability in response to hydrate dissociation using numerical studies by a reservoir simulator coupled with geomechanical strength calculations [17]. More on how the hydrate forms in the pore space will be discussed in Chap. 6.

5.4.4 Electrical Properties of Hydrates

Similar to ice, gas hydrates are electrical insulators. This is an important property as it is one way to estimate hydrate saturations in natural hydrate reservoirs. As

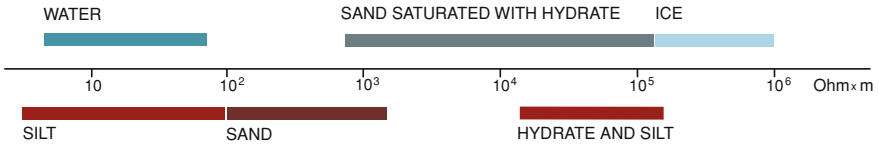

Fig. 5.14 Electrical resistivity for methane hydrates, in sand and shale [16]

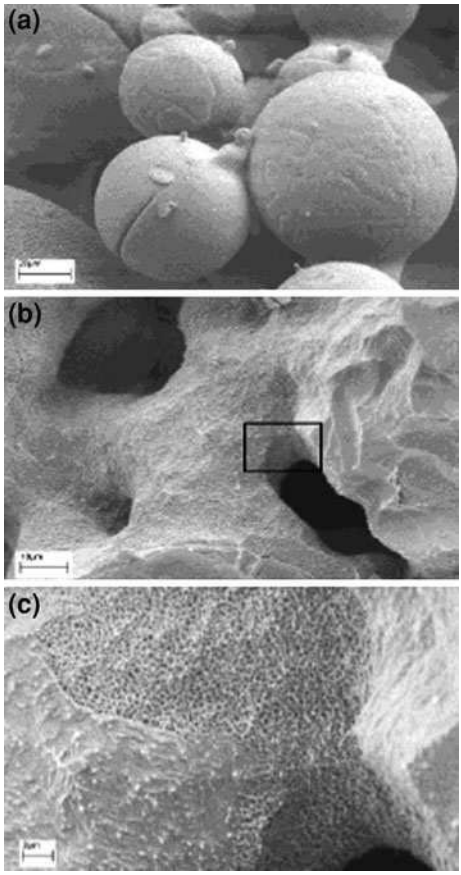

Fig. 5.15 Field emission scanning electron images of **a** ice before hydrate formation, **b** hydrates completely covering the ice grains now sintered together after 55 h of hydrate formation, **c** magnification of the box in image b showing the porous nature of the hydrate [21]

shown in Fig. 5.13, as hydrate forms in a sample filled with sediment and water, the electrical resistivity increases. Resistivity measurements performed during and after drilling allow for hydrate zones (areas of high resistivity) to be discovered and evaluated. Figure 5.14 shows typically electrical resistivity values for the various phases on water and sediment.

Fig. 5.16 Flame produced from combustion of methane gas released from dissociating hydrate (Photo courtesy of MBARI)

5.4.5 Hydrate Morphologies

Hydrate morphology and texture can be viewed on the microscopic and mesoscopic level using techniques such as scanning electron microscopy (SEM). Images of the hydrate surface can give valuable information about how the hydrate is formed, its strength (presence of defects in the crystal structure), and how gas and water could be transported through it (porosity of the hydrate). An example of this is given in Fig. 5.15 where methane hydrate was formed form powdered ice. The images show micro-pores covering the surface of the methane hydrate. These tiny pores could allow for gas to be transported deeper into the ice grain, which would react to form further hydrate.

5.4.6 Safety-Related Properties

The appearance of hydrates is similar to that of ice. When under stable conditions, the gas inside the hydrate is trapped and poses minimal risk. As hydrate dissociates, the released gas can be treated using standard safety procedures for the particular gas. In the case of methane, dissociating hydrate exposed to an ignition source will not cause an immediate explosion but produces a flame as the methane burns (Fig. 5.16).

In fact, a project presented by the US Navy at the Third International Conference on Gas Hydrates in Salt Lake City, Utah, USA in 1999, hypothesized about the ability to build cruisers capable of storing and transporting methane hydrates in the walls of the hull. The slowly dissociating methane hydrate could provide a source of much cleaner fuel than normal marine fuel.

Special care must be taken with hydrates in a confined pressure vessel. The formation of hydrate tends to concentrate gas. When the hydrate dissociates, this released gas can rapidly increase the internal pressure and cause the vessel to fail and rupture.

References

1. Anderson GK (2004) Enthalpy of dissociation and hydration number of methane hydrate from the Clapeyron equation. J Chem Thermodyn 36:1119–1127
2. Dalmazzone C, Dalmazzone D, Herzaft B (2000) DSC: a new technique to characterize hydrate formation in drilling muds. Proceedings SPE Annual Tech Conference, Dallas, 1–4 Oct, 62962
3. Durham WB, Kirby SH, Stern LA (2003) The strength and rheology of methane clathrate hydrates. J Geophys Res 108(B4):2182–2186
4. Durham WB, Stern LA, Kirby SH, Circone S (2005) Rheology and structural imaging of sI and sII end-member gas hydrates and hydrate sediment aggregates. In: Proceedings of the international conference on gas hydrates 5, Trondheim, 13–16 June, Paper 2030
5. Giavarini C, Maccioni E, Santarelli ML (2003) Formation kinetics of propane hydrates. Ind Eng Chem Res 42:1517–1521
6. Giavarini C, Maccioni F, Santarelli ML (2006) Modulated DSC for gas hydrates analysis. J Therm Anal Calorim 84(2):419–423
7. Giavarini C, Santarelli, Maccioni ML (2008) Dissociation rate of THF-methane hydrates. Petrol Sci Tech 26(18):2147–2158
8. Gupta A, Kneafsey TJ, Moridis GJ et al (2006) Composite thermal conductivity in a large heterogeneous porous methane hydrate sample. J Phys Chem B 110(33):16384–16392
9. Gupta A, Dec SF, Koh CA, Sloan ED (2007) NMR investigation of methane hydrate dissociation. J Phys Chem C 111:2341–2346
10. Handa YP (1986) Compositions, enthalpies of dissociation, and heat capacities for clathrate hydrates of methane, ethane, and propane, and enthalpy of dissociation of isobutene hydrate, as determined by a heat-flow calorimeter. J Chem Thermodyn 18:915–921
11. Haneda H, Sakamoto Y, Kawamura T et al (2005) Experimental study of the dissociation behavior of methane hydrate by air. In: Proceedings of the international conference on gas hydrates 5, Trondheim, 13–16 June, Paper 1025
12. Hester KC, Huo Z, Ballard A et al (2007) Thermal expansivity of sI and sII clathrate hydrates. J Phys Chem B 111:8830–8835
13. Huang D, Fan S (2004) Thermal conductivity of methane hydrate formed from sodium dodecyl solution. J Chem Eng Data 49:1479–1482
14. Hyodo M, Nakata Y, Yoshimoto N, Ebinuma T (2005) Basic research on the mechanical behavior of methane hydrate-sediments mixture. J Jpn Geotech Soc Soils Found 45(1):75–85
15. Levik OI, Gudmundsson JS (2000) Calorimetry to study metastability of natural gas hydrate at atmospheric pressure below 0°C. In: Holder GD, Bishnoi PR (eds) Gas hydrates. Annals of the New York Academy of Sciences, vol 912, pp 602–613
16. Makogon YF (1997) Hydrates of hydrocarbons. PennWell Books, Tulsa

17. Rutqvist J, Moridis GJ (2007) Numerical studies on the geomechanical stability of hydrate-bearing sediments. Offshore Technical Conference, 30 April–3 May, Houston, doi:10.4043/18860-MS
18. Santamarina JC, Ruppel C (2008) The impact of hydrate saturation on the mechanical, electrical, and thermal properties of hydrate-bearing sand, silts, and clay. In: Proceedings of the international conference on gas hydrates 6, Vancouver, 6–10 July, Paper 5817
19. Sloan ED, Fleyfel F (1992) Hydrate dissociation enthalpy and guest size. Fluid Phase Eq 76:123–140
20. Sloan ED, Koh CA (2008) Clathrate hydrates of natural gases, 3rd edn. CRC Press, Boca Raton
21. Staykova DK, Kuhs WF, Salamatin AN, Hansen T (2003) Formation of porous gas hydrates from ice powers: diffraction experiments and multistage model. J Phys Chem B 107:10299–10311
22. Subramanian S, Kini RA, Dec SF, Sloan ED (2000) Structural transition studies in methane + ethane hydrate using Raman and NMR. In: Holder GD, Bishnoi PR (eds) Gas hydrates. Annals of the New York Academy of Sciences, vol 912. pp 873–886
23. Takeya S, Takeo H, Uchida T (2000) In situ observations of CO_2 hydrate by X-ray diffraction. In: Holder GD, Bishnoi PR (eds) Gas hydrates. Annals of the New York Academy of Sciences, vol 912. pp 973–982
24. Tse JS, White MA (1988) Origin of glassy crystalline behavior in the thermal properties of clathrate hydrates: a thermal conductivity study of tetrahydrofuran hydrate. J Phys Chem 92(17):5006–5011
25. Waite WF, Gilbert LY, Winters WJ, Mason DH (2005) Thermal property measurements in tetrahydrofuran hydrate and hydrate-bearing sediment between −25 and 4°C, and their application to methane hydrate. In: Proceedings of the international conference on gas hydrates 5, Trondheim, 13–16 June, Paper 5042

Chapter 6
Hydrates in Nature

6.1 Introduction

Over thirty years after hydrates were found to form in oil and gas pipelines, it was discovered that naturally formed hydrates were present in large quantities in marine and permafrost sediment. Many of these natural hydrate deposits are thousands of years old. Scientists from the USSR are credited with the discovery of natural hydrates and led the early work in this field [22]. Soon after gas hydrates were discovered to exist in nature, scientists began to estimate how much of this new material was out there [36, 37].

The amount of methane estimated to be in natural hydrates is vast and could be as more than double conventional natural gas reserves [19]. Extensive research on natural hydrates including drilling programs with coring and geophysical logging has helped refine knowledge of the extent and distribution of natural hydrates.

In this chapter, we will show how research has helped shape our understanding of natural hydrates and present the current state-of-the-art on where hydrates form and how much hydrate is present in nature. In addition, we will present some of the interesting ecosystems that live around these crystals of water filled with methane.

6.2 Where Gas Hydrates are Found in Nature

As shown in Fig. 6.1, gas hydrates are found throughout the World on every continent. They are mainly present off the coasts on the continental margins and below the permafrost. Hydrates have even been found in inland seas (e.g., Black Sea, Caspian Sea) and fresh water lakes (e.g., Lake Baikal).

To better understand why we find natural hydrates where we do, we must look at the criteria that must be met for hydrate formation. Firstly, the pressure and temperature must be in the hydrate stability zone and, secondly, a sufficient

C. Giavarini and K. Hester, *Gas Hydrates*, Green Energy and Technology,
DOI: 10.1007/978-0-85729-956-7_6, © Springer-Verlag London Limited 2011

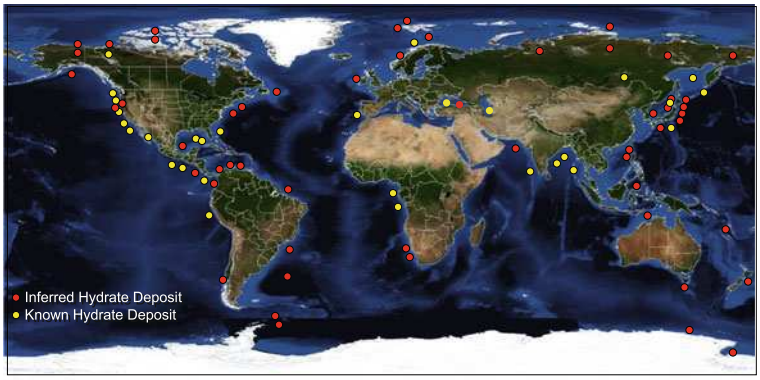

Fig. 6.1 Worldwide occurrences of gas hydrates

amount of hydrate-forming gas must be present. In areas where these two conditions are present, natural hydrates are likely to be found.

6.2.1 Where Gas Hydrates are Stable

The first step in determining where natural hydrates occur is to define the areas globally which are in the gas hydrate stability zone (GHSZ). This means having the high pressures and low temperatures needed to stabilize hydrates. Defining the global GHSZ gives an upper bound to possible natural hydrate occurrences.

Worldwide, it is estimated that over 99% of the gas in natural hydrates is methane [20]. Some hydrate deposits do contain other components such as heavier hydrocarbons, CO_2, and H_2S [26]. However, for defining the general global GHSZ, methane is considered to be the only hydrate-forming gas present.

Figure 6.2 shows a simple description of the GHSZ for marine and permafrost sediments. As shown in Fig. 6.2b for the marine setting, temperature (dashed line) near the sea surface rapidly decreases until the *thermocline* is reached, which separates the warm surface waters and the deeper cold water mass. At that point, the temperature slowly decreases and reaches around 3–4°C, which is common for most of the seafloor around the World. Hydrates become stable where the temperature crosses the hydrate stability line (solid line). This typically occurs below 300–600 m of water depth (based on local temperature profiles and salinity). However, the ocean water does not contain enough gas to stabilize hydrate and the top of the GHSZ is defined at the seafloor. Moving down into the sediment, the temperature begins to slowly warm again following the geothermal gradient (global average: 0.02°C/m). While the pressure continues to increase with depth, after 500–1,000 m deep, the temperature becomes too hot for hydrates to remain stable. This is commonly referred to as the base of the GHSZ.

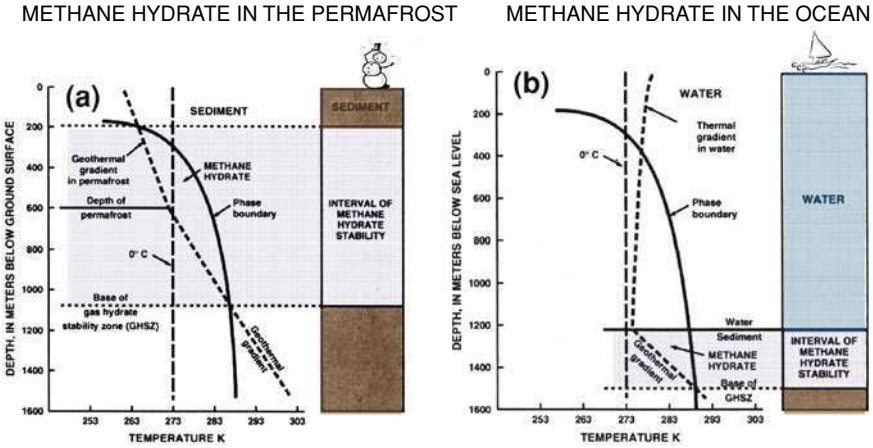

Fig. 6.2 Gas hydrate stability zone (GHSZ) for **a** permafrost and **b** marine settings. In the permafrost, the GHSZ typically begins at 100–300 m depth and can extent for hundreds of meters below the base of permafrost (which typically occurs at 150–600 m depth). In the marine setting, the GHSZ can begin below 300–600 m and extent for hundreds of meters below the sea floor

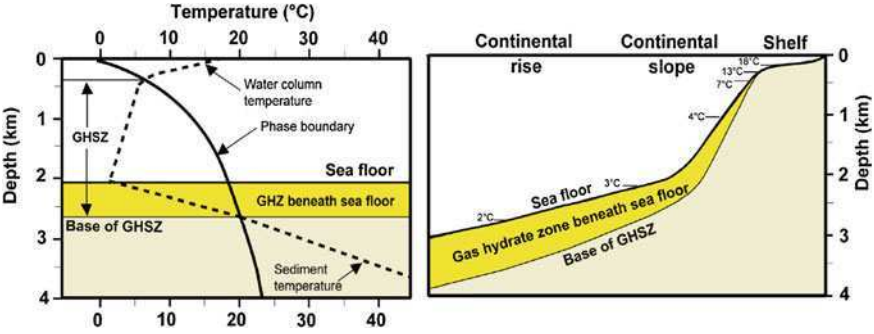

Fig. 6.3 Changes in the extent of the GHSZ with changing bottom water temperature and depth (Modified from [1])

The thickness of the GHSZ depends on bottom water temperature, salinity, geothermal gradient, and depth. From Fig. 6.2b, the hydrate stability line is crossed before reaching the seafloor, where hydrates can first be present. Figure 6.3 shows the effect of water depth on the depth of the GHSZ for a typical ocean temperature profile. As shown, the GHSZ is the thinnest where temperatures are relatively high and pressures are low. However, as we go to deeper water depths with the colder bottom water temperatures below the thermocline, the GHSZ reaches depths over 1,000 m.

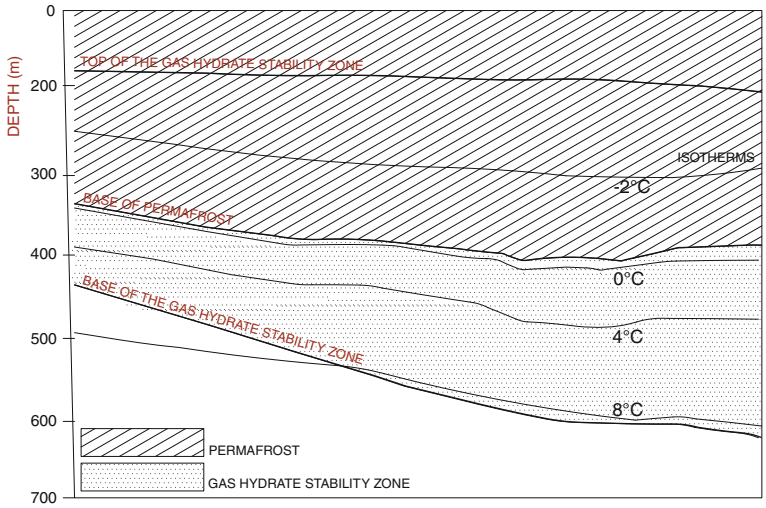

Fig. 6.4 The relationship between the zone of permafrost and the GHSZ for methane hydrate in Prudhoe Bay (North Slope, Alaska). From Collett and Dallimore [4]

The situation is similar in the permafrost (Fig. 6.2a). The temperature line crossing the hydrate stability line marks the top of the GHSZ, which typically begins at 100–300 m depth. The GHSZ can extend for hundreds of meters. Figure 6.4 shows the relationship between the GHSZ and the base of permafrost. The depth of the GHSZ is related to the base of permafrost, which is at 0°C. A deeper base of permafrost will increase the depth of the GHSZ.

Using the above criteria to define the GHSZ, one could survey the globe and determine where hydrate formation is possible. In fact, over 90% of the ocean seafloor and most of the permafrost are in the GHSZ. This was the approach taken for the earliest estimates of natural hydrates [36, 37]. However, in order to give a more accurate estimate for actual natural hydrate occurrences, it is necessary to determine areas where sufficient gas supplies exist within the GHSZ.

6.2.2 Where the Gas in Hydrates Comes From

While large areas exist where the stability conditions for hydrates are met, it turns out that much these areas do not contain hydrates. The reason hydrates are not found in most ocean and permafrost sediment is that there is not sufficient gas supply. Referring back to Fig. 6.1, it is obvious that hydrate accumulations are prevalent on the continental margins. However, discoveries of hydrates on the vast abyssal plains have been not reported. The observed global distribution of natural hydrates will become clearer by looking at the sources of hydrate-forming gas. The main sources for methane in hydrates are biogenic and thermogenic.

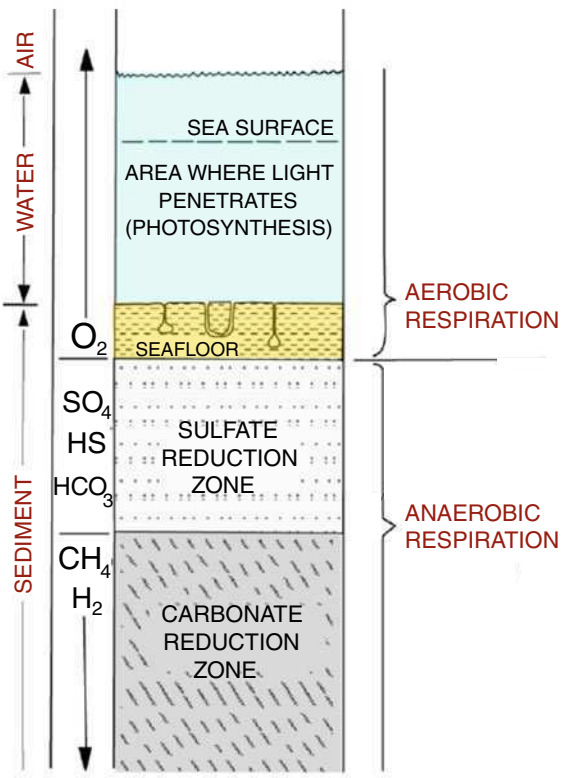

Fig. 6.5 Graphical representation of the diagenesis of organic matter in seafloor sediments (Modified from Bohrmann and Torres [1])

6.2.2.1 Biogenic Gas

Biogenic gas is the predominant gas source for forming natural hydrates and is mainly methane [10]. Non-living organic matter (also known as detritus) sinks in the ocean and accumulates on the seafloor. Over time, this organic matter is buried in the silty seafloor sediment. In the absence of light, energy for microbial life is obtained by breaking down this organic matter. Aerobic oxidation or respiration occurs in the presence of oxygen, producing CO_2. As aerobic oxidation quickly consumes the limited amount of oxygen available, the seafloor sediment turns anoxic leading to anaerobic fermentation. In this zone, ranging from a few centimeters to several meters deep into the seafloor, the bacteria reduce the sulfate ion present in the seawater producing H_2S. When depths are reached where most of the sulfate has been reduced, ancient single celled organisms known as *archea* dominate in breaking down the remaining organic matter into methane in a process called methanogenesis. The methanogenesis zone is extensive, often hundreds of meters deep, and continues until sediment temperatures reach 75–80°C. The processes undergone by the organic carbon after its initial deposition on the

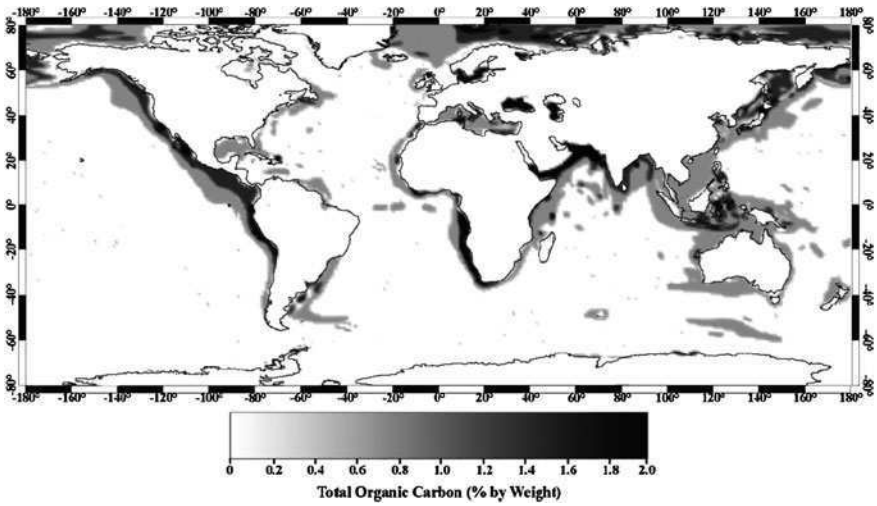

Fig. 6.6 Total organic carbon distribution on the seafloor (from [18])

seafloor, including sulfate reduction and methanogenesis, are collectively known as *organic diagenesis*. Figure 6.5 shows a graphical representation of these zones of microbial activity in seafloor sediments.

For hydrates to be stable, a sufficient amount of methane is needed in the pore water. This methane concentration must be higher than its solubility in water. For the methanogenic archea to produce enough methane, a continual supply of organic carbon needs to rain down from the upper ocean. Figure 6.6 shows the total organic carbon distribution on the seafloor. Areas around the continental margins have relatively high sedimentation rates and fluxes of organic carbon, while these rates are much less in other parts of the ocean. This availability of organic carbon largely controls the amount of biogenic methane produced and the subsequent observed locations of the vast majority of global hydrate deposits (Fig. 6.1). Even on the continental margins where hydrates are present, hydrates often do not extend all the way to the seafloor. Generally, the highest concentrations of gas are found near the base of the GHSZ. This is because both deeper migrating gas is focused to this area and methane solubility increases with depth. On an area known as Hydrate Ridge off the coast of Oregon, USA, the GHSZ is around 135 m but the uppermost 40 m does not contain hydrate [35]. The zone which contains hydrate (in the previous example, from 40 m depth to the base of the GHSZ) is known as the Gas Hydrate Occurrence Zone (GHOZ). Above the GHOZ to the seafloor, the biogenic methane generated in situ is not sufficient to maintain hydrates. We will see later that areas do exist with hydrates at or near the seafloor. However, this is due to local pathways which channel deeper gas upward.

6.2.2.2 Thermogenic Gas

Thermogenic gas is formed deep in the Earth in a process called *catagenesis*. This type of gas is common in conventional gas reservoirs. Catagenesis occurs at temperatures from 50–200°C and *cracks* larger molecules in deposits of organic material known as *kerogen,* a precursor to oil. Unlike the biogenesis process, which selectively produces methane, catagenesis also creates high concentrations of heavier hydrocarbons such as ethane, propane, and butanes. Thermogenic gas in hydrates is far less common than biogenic gas. Because thermogenic gas is produced in areas much deeper than the GHSZ, the presence of thermogenic gas indicates that migration pathways existed for the gas to move upward to zones where hydrates are stable. There have been numerous observations, such as in the permafrost, of natural hydrates being composed of a mixture of biogenic and thermogenic gas.

6.3 Field Techniques to Study Natural Hydrates

Almost all of our current knowledge of natural hydrate deposits is due to ocean and permafrost surveys and drilling projects. These studies have greatly advanced our understanding of natural hydrates and how they form in the sediment. Some of the larger drilling projects, typically involving international partners, will be discussed in Chap. 8. Here we will discuss some of the ways to detect and measure natural hydrates in the field.

6.3.1 Remote Sensing Techniques

Drilling is expensive and the ability to remotely find hydrates and in-place amounts is highly desirable. The main tools used to look in the subsurface are seismic techniques and this realm belongs to geophysicists. Important information, such as sediment structure, can be inferred by measuring the time it takes for a seismic signal, sent into the sediment, to return. At the base of the GHSZ, a free gas layer can be present. The seismic technique is highly sensitive to free gas. It was discovered in the 1950s that a bottom simulating reflector (BSR) may have been present in some hydrate-bearing sediments (Fig. 6.7). The reflector observed is due to the seismic signal reaching a zone with gas in the pore space. The presence of gas does not typically occur in the GHSZ, but can be present at the base of the GHSZ, where hydrate becomes unstable. The presence of a BSR gives information about the presence of hydrates and the thickness of the GHSZ. While this is the best available tool to remotely detect the presence of hydrates, it has significant limitations. Firstly, it gives little information about hydrate saturations in-place. A BSR could be observed when very little hydrate is present. Secondly,

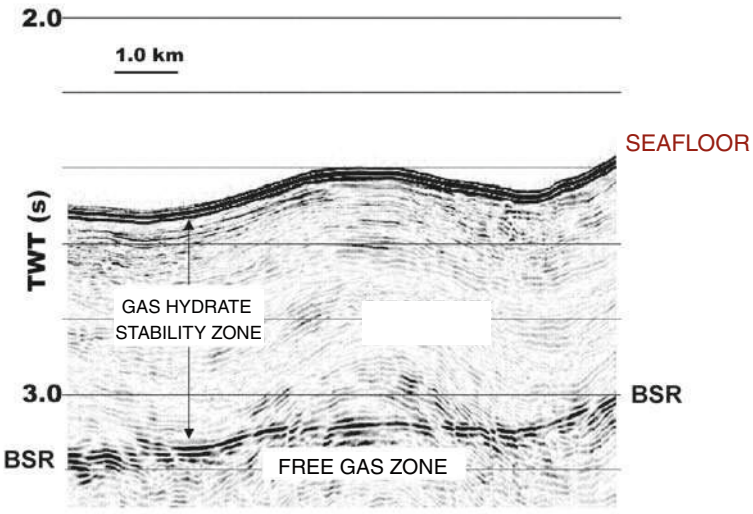

Fig. 6.7 Seismic image of the subsurface sediments with a BSR indicating the base of the GHSZ

a BSR is not always observed in hydrate-bearing sediments. Therefore, lack of a BSR does not rule out the presence of hydrate reservoirs. Because adequate tools do not yet exist for remotely detecting hydrates and their saturations in the pore space, drilling to this point is required to find and characterize hydrate-bearing zones.

6.3.2 Direct Sampling

The most direct way to learn about natural hydrates is to study them in the field. In this section we will discuss ways gas hydrates are studied on or near the seafloor (upper 10 m) and in deeper sediments. Most of the information learned about near-seafloor work is through direct sampling and performing laboratory analyses. Study of deeper hydrate deposits is accomplished by drilling wells and logging the wells with various tools, along with direct sampling.

6.3.2.1 Coring

Direct sampling through coring can be performed on the seafloor or during the drilling of a well. Coring allows for a direct observation and measurement of the natural hydrate and its interaction with the surrounding sediment (Fig. 6.8a). Gas

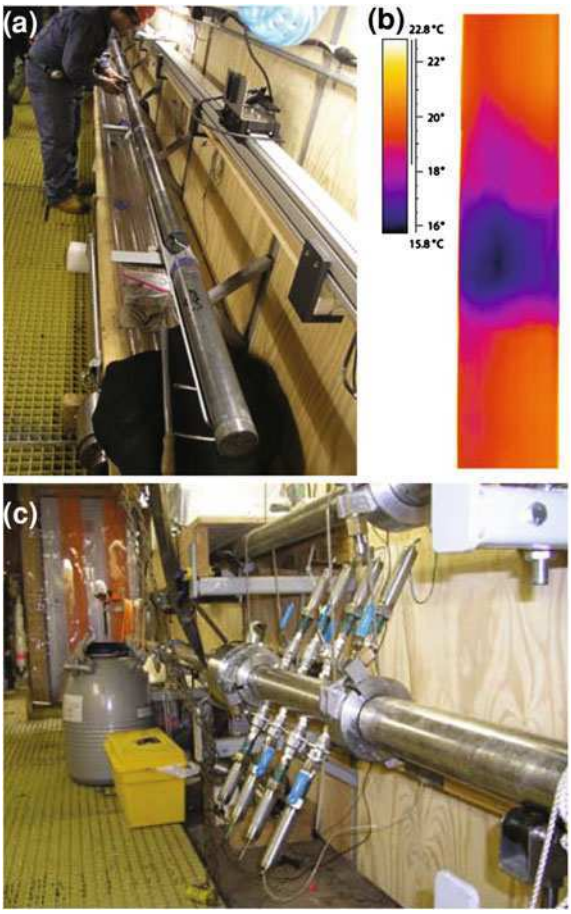

Fig. 6.8 Coring natural hydrates in the field. **a** Core processing lab aboard the drill ship during the DOE/JIP Gulf of Mexico Hydrate Research Cruise. **b** Thermal image of a hydrate-bearing core [7]. **c** Georgia Tech Mechanical Measurements tool used during the DOE/JIP Gulf of Mexico Hydrate Research Cruise (Photo credits: NETL Scientists, http://www.netl.doe.gov/technologies/oil–gas/futuresupply/methanehydrates/rd-program/gom_jip/Photo_day16/index.htm)

from recovered hydrates can be analyzed to determine composition, both chemical (hydrate structure) and isotopic (source of hydrate gas) [26]. Cores have allowed for a better understanding of how hydrate concentrates in different sediment types (e.g., fine silt versus coarse sand) and how it is distributed in the sediment [1]. Coring also serves as a way to ground-truth and calibrate well logging measurements (see next section).

Hydrate coring has always been challenging because hydrates become unstable as the pressure is lowered. Many times, recovered cores, which contained hydrates in situ, no longer did by the time they reached the deck of the ship. This is mainly true for hydrates present in low saturations in the sediment. Even for hydrate that does survive, significant dissociation and disturbance has occurred. These conventional cores are put in liquid N_2 as soon as possible, which preserves the hydrate. Thermal imaging is often used to rapidly identify sections of core containing hydrate. Figure 6.8b shows a thermal image of a core containing hydrate-bearing sediment.

Because hydrate dissociation is endothermic, hydrate-bearing sediment will show a lower temperature than the surroundings.

Even with dissociation, it is possible to estimate in situ hydrate saturation. This uses the fact that hydrates exclude salt when they form. During dissociation, the pore water is *freshened* as this pure water is released from the melting hydrate [35], [1]. By looking at the degree of freshening, hydrate saturation can be calculated.

Researchers are overcoming the problem of hydrate dissociation using pressurized coring devices. These pressure corers maintain the pressure on the sample during recovery and allow for hydrate-bearing sediment to be studied as close to the true in situ condition as possible. Progress is being made in this area. There are even newly developed ways to transfer recovered cores to secondary sampling vessels for interrogation with a number of techniques, always maintaining pressure. Figure 6.8c shows such a sample cell with probes to measure mechanical and electrical of a hydrate-bearing core. In the future, this could help resolve the question of how hydrate is present in the pore space: whether it is pore-filling (residing the middle of the pores) or cementing and coating the sediment grains.

6.3.2.2 Other Direct Sampling Methods

Because it is challenging to preserve hydrates during recovery and maintain them in their native state. Direct measurement techniques, without the need for recovery, are desirable. Such direct measurements have been performed on seafloor hydrates using a specially designed Raman spectrometer [16, 17]. While well-developed as a laboratory analytical tool for hydrate studies (see Chap. 5), this seagoing instrument is deployed using a Remotely-Operated Vehicle (ROV) (Fig. 6.9a). The probe head is connected with the spectrometer using fiber optics. As shown in Fig. 6.9b, the laser from the probe head can be focused on the hydrate outcrop allowing for a direct measurement of the hydrate structure and composition without disturbing the sample [15]. Recently, this deep-sea Raman technology was applied to in situ measurement of methane, sulfate, and sulfide in pore water near hydrate-bearing sediments. This approach provides a quantitative measure of dissolved methane and overcomes the problem in traditional cores of methane degassing during recovery [40].

6.3.3 Well Logging

Well logging provides important information about the subsurface. It can be performed while drilling (LWD: Logging while drilling) or later using tools lowered on a wire line. Well logging tools commonly used for hydrates measure a number of properties including density, electrical resistivity, sonic wave velocity, and NMR relaxation time. The presence of hydrates in the sediment will affect these measurements and allows for hydrate detection and characterization.

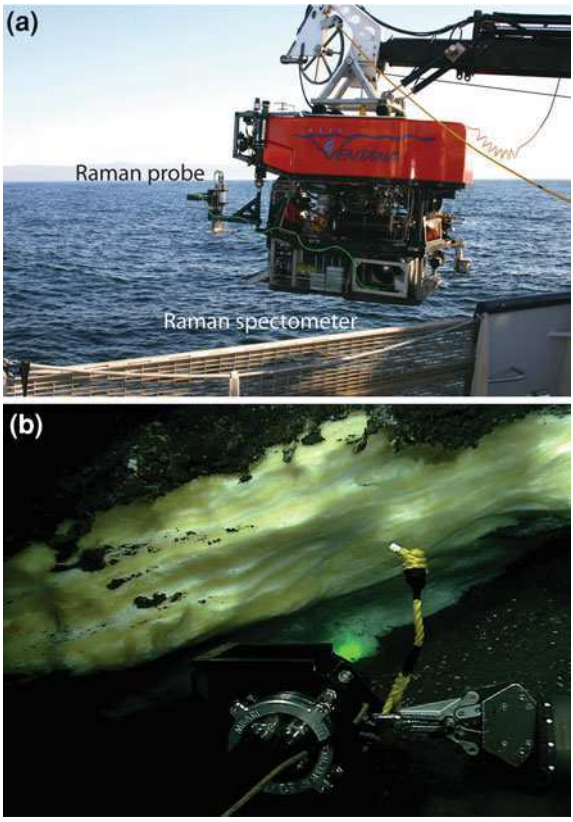

Fig. 6.9 Sea-going Raman spectrometer capable of measuring hydrate structure and composition. In **a** the spectrometer being deployed on the ROV Ventana; in **b** direct measurement of a hydrate outcrop at Barkley Canyon at 850 m water depth [16]

Combining these measurements can provide a clearer picture of the nature of the hydrate deposit. For example, hydrate saturation can be estimated when the density and NMR logs are combined [27].

6.4 How Gas Hydrates Occupy the Sediment Pore Space

From knowledge gained through field studies, we now know that both the depth (lithostatic pressure) and the container (sediment type) will affect how the hydrate occupies the pore space. Here we will look at hydrate deposits which occur near the seafloor and the deeper hydrates below.

6.4.1 Shallow Gas Hydrate Deposits

As discussed above, based on the rate of in situ generated methane, a GHOZ typically exists where hydrate is not found near the seafloor. However, in many

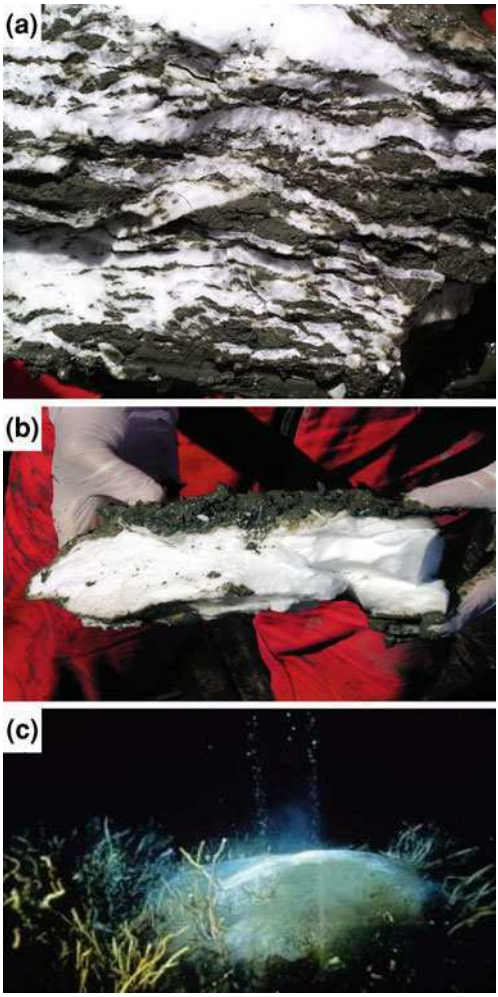

Fig. 6.10 Various types of natural Hydrate occurrences: **a** Layers of hydrates in clay sediments near the seafloor. Thickness of these layers range from millimeters to tens of centimeters, **b** massive hydrate deposit, **c** hydrate outcrop, or mound, on the seafloor (Photo courtesy of USGS)

areas, a migration pathway exists which allows for high gas fluxes to reach areas near the seafloor. In these venting sites, the gas is typically a mixture of biogenic and thermogenic gas. The vents are episodic and only supports seafloor hydrates while actively venting. Hydrates in seafloor locations where the gas stops venting will slowly dissolve over time.

The shallow seafloor is typically non-consolidated silts and clays. In these areas of high gas flux, a wide range of hydrate fabrics are found. Hydrate can exist in the pore space but also, in these shallow areas, the hydrates formed from high gas flux are able to overcome the lithostatic pressure and fracture the sediment, growing as massive chunks, lenses, and nodules. These hydrates appear bright-white in color with layers on the mm scale (Fig. 6.10a) to several centimeters thick (Fig. 6.10b).

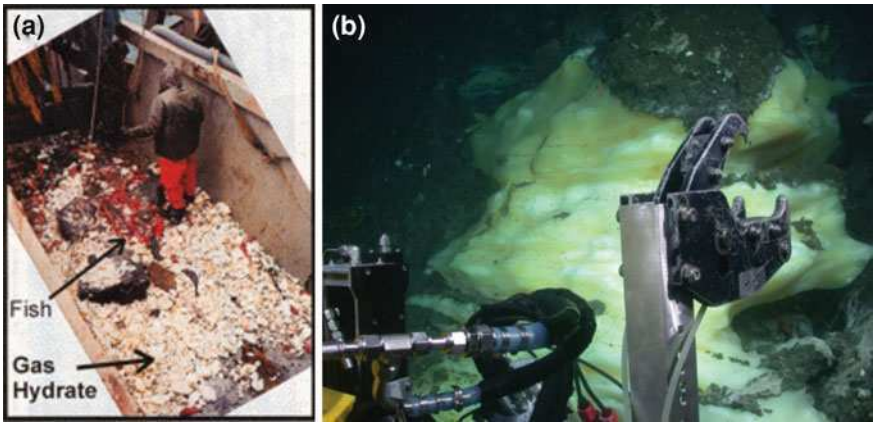

Fig. 6.11 In **a** fishing trawler *catches* tons of hydrates at Barkley Canyon [33]. In **b** hydrate mounds at 850 m depth on the seafloor at Barkley Canyon

They are generally orientated parallel to bedding planes and can be over 10 cm thick (Fig. 6.10c).

When a high flux of thermogenic gas exists to the seafloor, hydrate mounds can be formed. Thermogenic gas travels through local fractures from deep petroleum reservoirs. These accumulations focus an upward flow of fluids, often leading to gas venting and hydrate exposure on the sea floor. The gas is often accompanied with oil and condensate fluids. Unlike the almost pure methane hydrates we have discussed until this point, these local deposits are often enriched in significant quantities of heavier hydrocarbons. Because these mounds are a product of local fracture networks, it is difficult to predict where they occur. This could be one reason why there are relatively few known locations of these seafloor mounds. Our current detection ability of these accumulations is also quite limited. As an example, hydrate mounds at Barkley Canyon (off the coast of Vancouver, Canada) were discovered only when a fishing trawler unintentionally pulled up tons of hydrate, containing large amount of flammable gas, on deck (Fig. 6.11a, [33]). Hydrate mounds on the seafloor have been found in several places worldwide, including the Gulf of Mexico, the Caspian Sea, the Black Sea, and the Sea of Japan [9, 24, 29, 39]. Petroleum seepage is common in the Gulf of Mexico and thermogenic vent sites are often found at the rims of salt minibasins [31].

The only known thermogenic hydrate site on a convergent margin is in the Barkley Canyon. The proposed mechanism for this occurrence is that deep fluids are vertical migrating within the basin and these fluids are continually supported hydrate formation [28]. These hydrate mounds can extend several meters above the sea floor, partially veiled by a thin sediment cover (Fig. 6.11b). Bacterial mat and vesicomyid clams are observed around these hydrate mounds. In places such as the Gulf of Mexico, tube worms and other fascinating marine life have also been found [3, 30]. Marine ecosystems around seafloor hydrates will be discussed in more detail later in this chapter.

These exposed hydrates are dynamic systems that will respond to changes in currents, temperature, and venting rates. Some of these mounds are surprisingly stable. No major change in the shape or size of a mound was observed during a long-term time-lapse monitoring test (July 2001–July 2002) at Bush Hill Site GC-185 in the Gulf of Mexico [38].

The shallow deposits discussed in this section can contain areas with very high hydrate saturations. However, because they are formed from a local vent, their lateral extent is typically not large. Due to our limited knowledge of how much such shallow accumulations exist, deposits such as these are generally not included in global hydrate reserve estimates. Predicting these episodic deposits would require more understanding the local petroleum system at each location.

6.4.2 Deeper Gas Hydrate Deposits

Deeper in the sediment column, hydrate is not longer able to overcome the lithostatic pressure between the sediment grains and is therefore restricted to the pore space between the sediment or in fractures. Practical experience has shown that the host sediment is one of the dominant factors in controlling hydrate saturations. In clays and silts, low permeability and porosity results in low average hydrate saturations of less than 10 vol%. These are known as disseminated hydrates. These also represent the most prevalent known type of hydrate deposit (See Chap. 8). Observations from recovered hydrate cores show that most of the hydrate in clay-dominated sediment is present in a network of tiny fractures.

The situation is different for coarse grained sediments, such as sands. In layers of this type of sediment, hydrate can become highly saturated. Such hydrate reservoirs have been discovered around the World and represent the best chance for energy production from gas hydrates. These types of sandy layers are also the ones that were targeted for the on land production tests in the permafrost.

As more field studies are carried out, new hydrate deposits are being discovered in a wide variety of subsurface sediments. Recently, during the first leg of a drilling expedition by Indian National Gas Hydrate Program, a hydrate-filled volcanic ash layer 600 m below the seafloor was discovered off the Andaman Islands. This layer is one of the thickest and deepest gas hydrate deposit known to date.

6.5 How Much Methane is Trapped in Natural Hydrates

A thorough review of hydrate estimates and their methodologies is given by Milkov [26]. As more has been learned about hydrates, in large part through field drilling projects, estimates of total methane in hydrates has decreased as assumptions have become better constrained. Figure 6.12 shows estimates of in-place hydrates

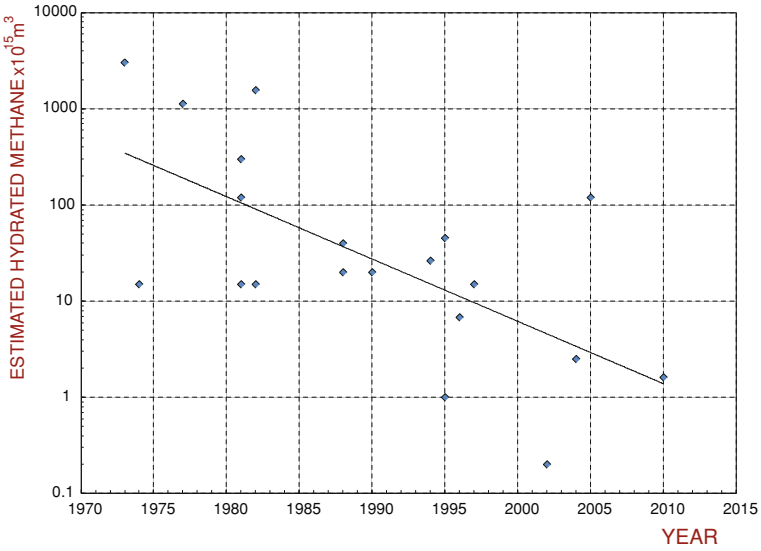

Fig. 6.12 Estimates of methane in natural hydrates over the last 30 years (from [32])

throughout the years. Early estimates considered the entire GHSZ to contain hydrates in high saturations. We have learned that hydrates are largely limited to the permafrost and around continental margins were sufficient organic carbon existed to produce methane. In addition, the sediment type plays a large role in local hydrate saturations. Most of the hydrate-bearing sediments are fine clays and silts and contain on average less the 2% hydrate by volume. There are zones of locally higher saturations, such as sandy layers, which will be targeted for energy production. Currently, the estimated amount of methane in natural hydrates is around $1–10 \times 10^{15}$ m^3. This number is still considerably larger than the estimated amount of conventional gas reserves and we will see in Chap. 8 the efforts by various countries to produce gas from hydrates.

6.6 The Ecology of Gas Hydrates: Ice Worms

Over the past 20 years, unprecedented technological advances have been made in the geological and biological exploration of the ocean floor. It is now possible to observe and sample with great detail these areas exceeding depths of 5,000 m, which represent most of the submerged surface of our planet. From early bathyscaphes, current exploration utilizes manned submersibles and remote-operated vehicles (ROVs) equipped with high-definition digital cameras, sensors, and sampling equipment capable of retrieving rocks and sediment to live animals.

Fig. 6.13 Bivalve mollusk community associated with a seafloor gas hydrate deposit at 2,150 m depth on the Blake Ridge off the US east coast (http://www.noaa.gov)

Oceanic exploration has led to the discovery of deep sea ecosystems associated with gas hydrates. The presence of hydrates in the seabed sediment creates a habitat that is exploited by dense communities of micro- and macro-organisms consisting primarily of bivalves (mussels, vesicomidi, and lucinidi) (Fig. 6.13), vestimentiferan tube worms (Fig. 6.14), polychaete worms, pogonophora, sponges, gastropods, and small crustaceans that survive by using the abundant chemosynthetic microorganisms prokaryotes (e.g., archaea and bacteria), both as a food source and as symbionts. These associations of species are very similar to another deep marine community found around hot hydrothermal and cold vent sites on the mid-ocean ridges [21].

At the dark depths needed for the existence of gas hydrates, the process underlying life is not photosynthesis (the process that uses light transmitted by the sun for the energy needs of organisms), but rather *chemosynthesis*. Chemosynthesis is a metabolic process by which autotrophic organisms (e.g., some bacteria) obtain both the energy necessary for transforming the carbon in organic substances and perform the biosynthesis necessary for processes of life through the oxidation of inorganic substances. These organisms behave as true primary producers, sustaining organisms at higher trophic levels on the food chain.

These amazing chemosynthetic communities living near gas hydrates are high in density and biomass. Ample availability of nutrients (methane trapped in the hydrate structure) promotes the proliferation of these organisms. They are real ecological oases in the deep sea environment, capable of supporting life. While not directly linked to the presence of gas hydrate, life in these oases take advantage of the abundance of available nutrients. Research from different geographical areas (Blake Ridge in the South Atlantic, Gulf of Mexico, continental margin of Cascadia off the coast of Oregon, Mediterranean Sea, and Barents Sea) have identified several species of fish, crinoids, sea cucumbers, nematodes, shrimps, and foraminifera in these oases.

Evidence for the existence of these ecosystems associated with deep sea gas hydrates has been found in fossiliferous outcrops. Some of the best examples of

Fig. 6.14 Vestimentiferan tube worms that live symbiotically with chemosynthetic bacteria in the presence of gas hydrates (From Chap. 6 of [13])

Fig. 6.15 Hesiocaeca methanicola, *ice worms*, on the surface of a deposit of hydrate in the Gulf of Mexico at 540 m depth (Photo: R. MacDonald, Texas A&M University-Corpus Christi, USA). The *yellow color* of the hydrate is due to oily condensate phase present in the hydrate deposit. These *ice worms* had dug tunnels that extended from the surface of the hydrate through to the underlying sediment (From Chap. 6 of [13])

these fossils are biological communities in the Tuscan-Emilian region (Italy) and were dated to more than six million years ago [5, 6, 34].

On July 12, 1997, the submersible research Johnson Sea-Link was diving in the Gulf of Mexico, at a gas hydrate outcrop at a depth of 550 m. Professor Charles Fisher of Pennsylvania State University and pilot Phil Santos from the Harbor Branch Oceanographic Institution observed strange movements on the surface of the hydrate deposit. Upon approaching the hydrate mound with the submersible, the observers noticed that the movements were caused by a dense colony of an unknown animal ([12], Fig. 6.15), who lived in a network of tunnels and caves that covered the entire surface of the hydrate. These animals survive in the absence of light and were dubbed *ice worms*.

Ice worms are polychaetes, animal organisms belonging to the phylum *Annelida*. They are pink in color, have a cylindrical body about 4 cm long, slightly flattened with bilateral symmetry. The most abundant species that proliferate in the

presence of gas hydrate is *Hesiocaea methanicola*. This species has no mouth or digestive tract and uses chemosynthetic bacteria living in its cellular tissues as its source of energy and nutrients.

The role hydrate ice worms play in the ecosystem is still unclear, but the most impressive feature is how they defend the cavities they occupy when they feel threatened. This occurs even when approached by simple external observers, like robot drones used by scientists to collect small samples or take photographs [2].

6.7 Natural Hydrates in Popular Culture

We have seen that marine geologists have known for the past 50 years about the presence of methane gas hydrates beneath the ocean floor. The gas entrapped by hydrates may be rapidly released if they are disturbed or there is a change in the internal temperature and pressure (See Chap. 10).

It has been speculated that the bubbles produced by these underwater ebullition events represent a danger to the ships. According to the well-known Archimedes' principle, an object will float on water when it receives an upward force equal to the magnitude of the water weight the object displaces. One proposed sinking mechanism attributes the vessels' loss of buoyancy to the gas bubbles released from underwater hydrates. These bubbles reduce the overall density of the water reducing its ability to float a vessel.

The *gasification* of seawater is a real phenomenon and has caused the collapse of oil platforms. It also poses a risk to ships and ferries in the Caspian Sea and coastal Siberia, where gas leakage occurs from the seafloor. The question being is whether gas hydrates are or have been responsible for such events.

Large releases of methane gas can also be hazardous for airplanes. If methane gas seeping from the seafloor makes it to the atmosphere before it is oxidized to CO_2, this methane-rich air could cause an engine explosion in low-flying aircrafts. To cause such an explosion, the methane concentration must be between 5–15% by volume. It seems unlikely that these concentration levels could be achieved at high altitudes, even for a large methane release.

Gas release from the seafloor can cause *pockmarks,* depressions of various size on the seafloor. Large quantities of these pockmark sites has been discovered on the ocean floor of the North Sea and in the region included in the triangle delimited by the Bahamas, Florida, and the Bermuda Islands (Fig. 6.16). A sunken vessel has been found in the center of one large pockmark site, known as the *Witches Hole* [23]. The flat resting position of the ship is quite unusual for a sunken vessel and seems to support the action of a sudden change in water density. In the last 60 years, various tenths of ships and airplanes have disappeared in the so called *Bermuda Triangle.*

Many articles and TV shows have investigated the Bermuda Triangle problem. According to some scientists and many in the media, the mystery of the vanished ships and airplanes could be due to gas ebullition from dissociating underwater

Fig. 6.16 The Bermuda Triangle

methane hydrates [14]. Experimental studies and simulations have been conducted on the effect that large bubbles and small gaseous bubbles produced by a gas release would have on floating bodies [8]. May and Monagham [25] argued that in the open sea, a rising plume of small bubbles could not exert enough upward drag force to float a vessel, even when its density is greater than that of the water. Because of this, they focused on the effect of a very large single bubble. They concluded that a large bubble could cause a vessel to sink.

While bubbles in water can theoretically cause a vessel to sink, no record of a recent methane release from seafloor hydrates has been observed. In a documentary in 1992 [11], no scientific evidence was found linking hydrates with these occurrences. Overall, while it is theoretically possible for hydrates to have caused vessels to sink, the responsibility of gas hydrates for such events has not been demonstrated at this time.

In the last years some novelists have used the methane hydrates to build fantastic adventures based on (quite) rigorous scientific knowledge. One of these is

Clive Cussler. He is the author of numerous action books and published *Fire in the Ice* in 2003. In this book, a Russian mobster is mining methane hydrates off the coast of the USA. Appearing to be a natural disaster, they plan to use the hydrates to cause huge submarine landslides, create tsunamis, and cause destruction to the western world.

More recently in 2004, the German writer Franz Schätzing published the science fiction novel *The Swarm* (Original German title: Der Schwarm). The main protagonists are ice worms, together with bacteria, which are destabilizing methane hydrates in order to generate large catastrophic landslides and resulting tsunamis. All of this is occurring as a form of rebellion to the sudden (on geological timescales) and clumsy invasion of the marine environment by man. There was a degree of scientific rigor brought by Schätzing in his novel. Some German researchers (e.g., Gerard Bohrmann of the University of Bremen), known internationally for the work on natural hydrates in the ocean, were not only scientific advisors to the author but also characters in the book itself.

> ….Bohrmann had no idea how deep the opening was. Outside, the shark was raging against the rocks, creating eddies of sediment and debris. The cloud also surrounds Dr. Bohrmann. Doctor Bohrmann? It was the voice of van Maasten, very weakly he said Bohrmann, for heaven's sake, please reply!

References

1. Bohrmann G, Torres ME (2006) Gas hydrates in marine sediments. In: Schultz HD, Zabel M (eds) Marine geochemistry. Springer, Heidelberg, pp 481–512
2. Camerlenghi A, Panieri G (2007) Diffusione in natura. In: Giavarini C (ed) Energia immensa e sfida ambientale. Gli idrati del metano. Editrice La Sapienza, ISBN 9788887242942 (in Italian)
3. Chapman R, Pohlman J, Coffin R et al (2004) Thermogenic gas hydrates in the northern Cascadia margin. EOS Trans 85(38):361
4. Collett TS, Dallimore SR (2000) Permafrost-associated gas hydrate. In: Max M (ed) Natural gas hydrate in oceanic and permaforst environments, vol 5. Kluwer Academic Publishers, Dordrecht, pp 43–60
5. Conti S, Fontana D (1999) Miocene chemotherms of the northern Apennines, Italy. Geology 27:927–930
6. Conti S, Gelmini R, Ponzana L (1993) Observazioni preliminaru sui calcari a Lucine dell'Appennino settentrionale (in Italian). Atti Soc Nat Mat Modena 124:35–56
7. D'Hondt SL, Jorgensen BB, Miller DJ et al (2003) The use of infrared thermal imaging to identify gas hydrate in sediment cores. In: Proceedings of ocean drilling program, initial reports 201
8. Denardo B, Pringle L, DeGrace C, McGuire M (2001) When do bubbles cause a floating body to sink? Am J Phys 69(10):1064
9. Diaconescu CC, Kieckhefer RM, Knapp JH (2001) Geophysical evidence for gas hydrates in the deep water of the South Caspian Basin, Azerbaijan. Mar Petrol Geol 18:209–221
10. Dillon WP, Max MD (2000) Natural gas hydrate in the oceanic and permafrost environments. Kluwer Academic Publishers, Dordrecht

11. Equinox Science Series (1992) The Bermuda triangle. Produced by Geofilms for Channel 4, UK
12. Fisher CR, MacDonald IR, Sassen R et al (2000) Methane ice worms: *Hesiocaeca methanicola* colonizing fossil fuel reserves. Naturwessenschaften 87:184–187
13. Giavarini C (2007) Energia immensa e sfida ambientale: Gli idrati del metano. Editrice La Sapienza, Roma (in Italian)
14. Gruy HJ (1998) Natural gas hydrates and the mystery of the Bermuda triangle. Petrol Eng Intl 71(3):71–79
15. Hester KC, Brewer PG (2009) Clathrate hydrates in nature. Ann Rev Mar Sci 1:303–327
16. Hester KC, Dunk RM, Walz PM et al (2007) Direct measurments of multi-component hydrates on the seafloor: pathways to growth. Fluid Phase Eq 261:396–406
17. Hester KC, Dunk RM, White SN et al (2007) Gas hydrate measurments at hydrate ridge using Raman spectroscopy. Geochem Cosmochim Acta 71:2947–2959
18. Klauda JB, Sandler SI (2005) Global distribution of methane hydrate in the ocean sediment. Energy Fuels 19:459–470
19. Kvenvolden KA (1999) Potential effects of gas hydrate on human welfare. Proc Natl Acad Sci U S A 96:3420–3426
20. Kvenvolden KA, Lorenson TD (2001) The global occurrence of natural gas hydrate. In: Paull, CK, Dillon WP (eds) Natural gas hydrates: occurrence, distribution, and detection. American Geophysical Union, Geophysical Monograph Series, vol 124, pp 3–18
21. Lonsdale P (1977) Clustering of suspersion-feeding macrobenthos near abyssal hydrothermal vents at oceanic spreading centers. Deep-Sea Res 24:857–863
22. Makogon YF (1966) Special characteristics of the natural gas hydrate fields exploration in the zone of hydrate formation (in Russian). TsNTI MINGASPROMa, Moscow
23. Marchant J (2001) Sunk without trace. New Sci 171(2310):12
24. Matsumoto R, Okuda Y, Aoyama C et al (2005) Methane plumes over a marine gas hydrate system in the eastern margin of Japan Sea: a possible mechanism for the transportation of subsurface methane to shallow waters. In: Proceedings of international conference on gas hydrates 5, Trondheim, 13–16 June, pp 749–754
25. May DA, Monaghan JJ (2003) Can a single bubble sink a ship? Am J Phys 71(9):842
26. Milkov AV (2004) Global estimates of hydrate-bound gas in marine sediments: how much is really out there? Earth-Sci Rev 66:183–197
27. Murray D, Kleinberg R, Sinha B, Fukuhara M (2005) Formation evaluation of gas hydrate reservoirs. SPWLA 46th annual logging symposium, 26–29 June, New Orleans, 2005-SSS
28. Pohlman JW, Canuel EA, Chapman NR et al (2005) The origin of thermogenic gas hydrates on the northern Cascadia margin as inferred from isotopic ($^{13}C/^{12}C$ and D/H) and molecular composition of hydrate and vent gas. Org Geochem 36(5):703–716
29. Sassen R, MacDonald IR (1994) Evidence of structure H hydrate, Gulf of Mexico continental slope. Org Geochem 22(6):1029–1032
30. Sassen R, Joye S, Sweet ST et al (1999) Thermogenic gas hydrates and hydrocarbon gases in complex chemosynthetic communities, Gulf of Mexico continental slope. Org Geochem 30(7):485–497
31. Sassen R, Roberts HH, Carney R et al (2004) Free hydrocarbon gas, gas hydrate, and authigenic minerals in chemosynthetic communities of the northern Gulf of Mexico continental slope: relation to microbial processes. Chem Geo 205(3–4):195–217
32. Sloan ED, Koh CA (2008) Clathrate hydrates of natural gases, 3rd edn. CRC Press, Boca Raton
33. Spence GD, Chapman NR, Hyndman RD, Cleary C (2002) Fishing trawler nets massive 'catch' of methane hydrates. EOS 82(50):621–627
34. Taviani M (1994) The 'calcari a Lucina' macrofauna reconsidered: deep-sea faunal oases from Mioocene-age cold vents in the Romagna Apennine. Geo-Mat Lett 14:185–191
35. Trehu AM, Long PE, Torres ME et al (2004) Three dimensional distribution of gas hydrate beneath southern hydrate Ridge. Earth Planet Sci Lett 222:845–862

36. Trofimuk AA, Cherskiy NV, Tsarev VP (1973) Accumulation of natural gases in zones of hydrate—formation in the hydrosphere (in Russian). Doklady Akademii Nauk SSSR 212:931–934
37. Trofimuk AA, Cherskiy NV, Tsarev VP (1975) The reserves of biogenic methane in the ocean (in Russian). Doklady Akademii Nauk SSSR 225:936–939
38. Vardaro MF, MacDonald I, Bender L, Guinasso N Jr (2006) Dynamic processes observed at a gas hydrate outcropping on the continental slope of the Gulf of Mexico. Geo-Mar Lett 26:6–15
39. Woodside JM, Modin DI, Ivanov MK (2003) An enigmatic strong reflector on subbottom profiler records from the Black Sea-the top of shallow gas hydrate deposits. Geo-Mar Lett 23(3–4):269–277
40. Zhang X, Walz PM, Kirkwood WJ et al (2010) Development and deployment of a deep-sea Raman probe for measurement of pore water geochemistry. Deep Sea Res I 57(2):297–306

Chapter 7
Hydrates Seen as a Problem for the Oil and Gas Industry

7.1 The Problems Caused by Gas Hydrates for Industry

For many decades after their discovery, gas hydrates were simply considered to be a scientific curiosity. The possibility that hydrates existed outside the laboratory was not recognized. This changed in 1934. The processing and transportation of natural gas in the presence of water vapor was troubled by formation of what appeared to be snow. This solid material would build up and lead to blockages (or plugs) in onshore and offshore pipelines. Originally thought to be ice, it was observed during operations that these snow-like solids were forming above the ice point. This observation led to efforts to find another explanation. Hammerschimdt [4] identified gas hydrates as the solid forming the *snow* in the pipelines and the culprit for these pipeline blockages (Fig. 7.1).

The economic implications of pipeline blockages were quickly recognized by the oil and gas industry. Systemic research was organized and funded to better understand and avoid formation of gas hydrates. In a relatively short time, extensive thermodynamic phase behavior was measured and correlations were developed to predict the pressure and temperature at which hydrates were stable for a given natural gas. This was followed by the identification of the different crystal structures of gas hydrates and a statistical thermodynamic model was developed for improved hydrate stability predictions. The ultimate goal was originally to avoid hydrate formation, especially in the most prone locations such as subsea or river crossings (Fig. 7.2). As drilling operations have moved to deeper and deeper water (Fig. 7.3), the increased pressure and low seafloor temperatures have made fully avoiding hydrates impractical. The paradigm of complete hydrate avoidance is shifting to the development of ways to manage gas hydrates without pipeline plugging.

Beyond economic concerns, Sloan and Koh [17] cite several industrial incidents, including serious injuries and fatalities, due to hydrates. Hydrates have a density and texture similar to ice. One way to try and remove a hydrate plug is to depressurize and dissociate the hydrate. During this process, the hydrate plug can

C. Giavarini and K. Hester, *Gas Hydrates*, Green Energy and Technology,
DOI: 10.1007/978-0-85729-956-7_7, © Springer-Verlag London Limited 2011

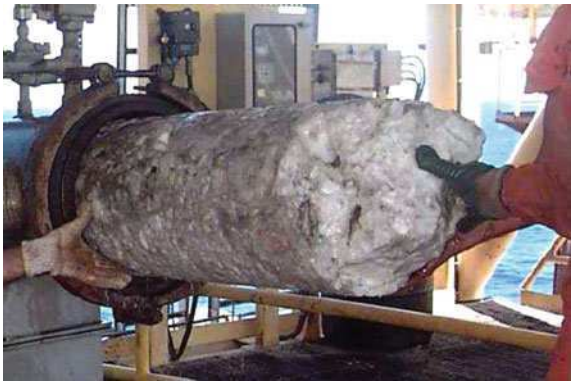

Fig. 7.1 A hydrate plug forming inside a pipeline (photo from Petrobras and reproduced by Sloan and Koh [17])

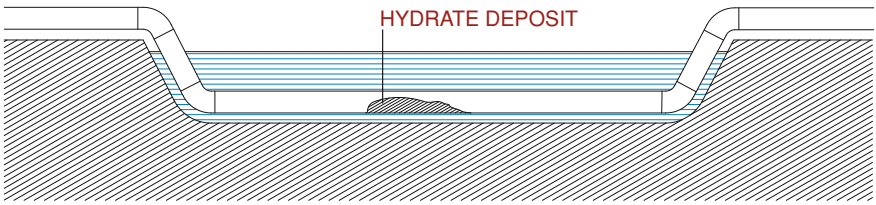

Fig. 7.2 Hydrate formation in subsea pipelines. It is an example of a river or lake crossing in winter

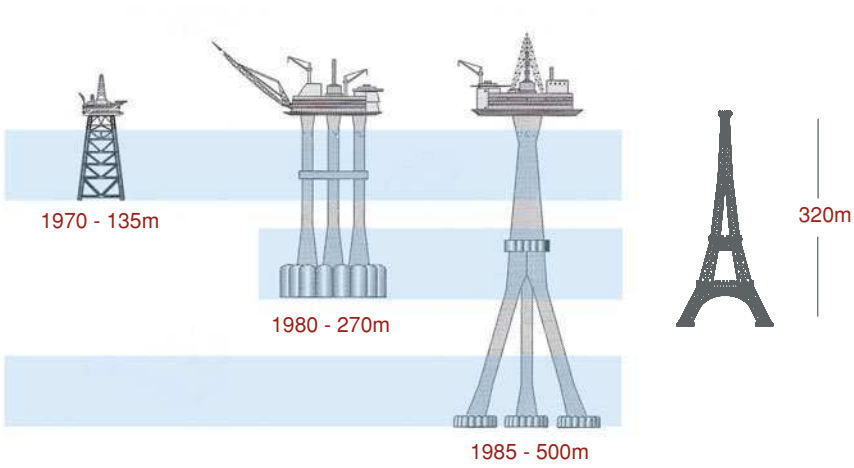

Fig. 7.3 Development of extraction platforms in the North Sea [16]

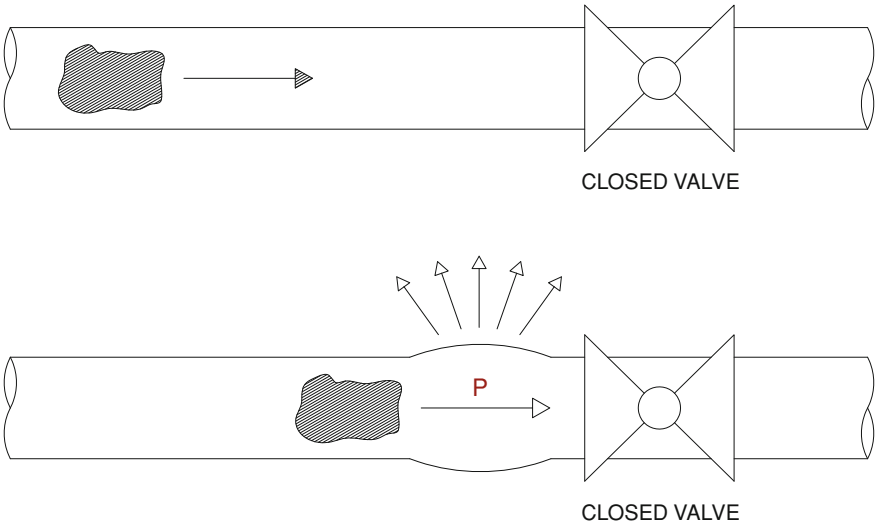

Fig. 7.4 A ruptured pipe caused by a hydrate plug

dislodge from the pipe wall and become mobile. If only one side is depressurized, the pressure gradient across the plug can turn it into a high-speed projectile. Any bends, valves, or other restrictions can lead to pipeline rupture by the hydrate *bullet* (Fig. 7.4). Another option is to heat the hydrate plug. Considering that each volume of gas hydrate can contain 160 volumes of gas, extreme care must be taken to avoid excess pressure buildup and pipeline explosion. These scenarios help highlight the risk hydrates pose to both men and equipment.

In addition, accidental hydrate formation during drilling can occur with certain drilling fluids. The hydrate formation will drastically change the rheological properties of the fluids and even, while infrequent, lead to line blockages. In other cases, drilling through hydrate-bearing sediment can lead to dissociation and possible uncontrollable gas release [3].

7.1.1 Role of Hydrates in the BP Deep Water Horizon Oil Spill

On May 6–8, 2010, an operation was executed to attempt to lower a large containment dome, also called a cofferdam, over the leaking well (Fig. 7.5). A pipe at the top of the cofferdam was designed to channel oil and gas to a ship above [14]. These cofferdams have been used previously. However, they were used in shallow water, where hydrate formation was not an issue.

The possible problems associated with hydrate formation were recognized. When natural gas comes in contact with cold seawater, a hydrate shell can quickly form around the gas bubble. An example of this is shown in Fig. 7.6. In this

Fig. 7.5 Cofferdam used by BP during the deepwater horizon oil spill response (Photo credits: USCG, BP)

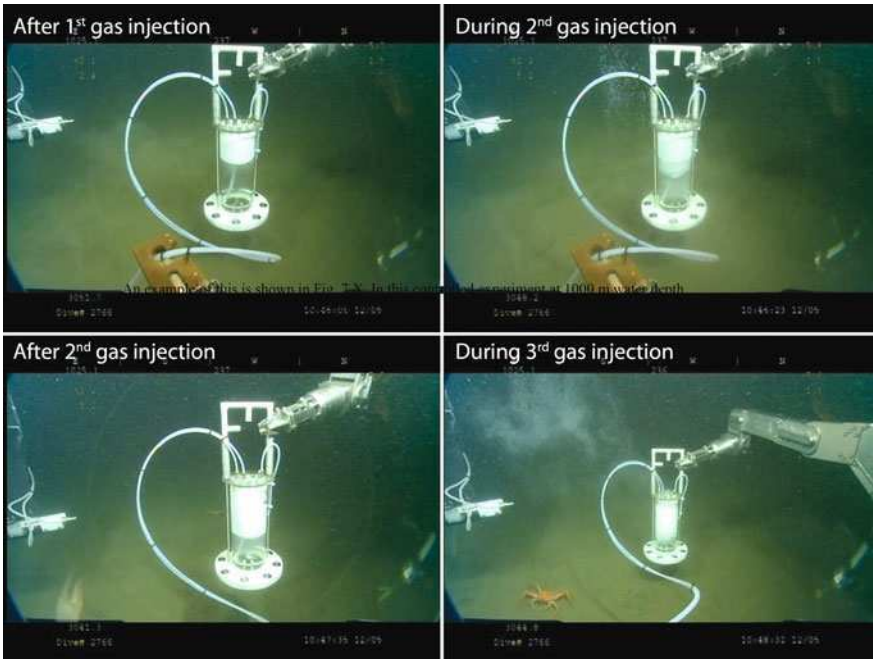

Fig. 7.6 Controlled experiment at 1,000 m depth (10 MPa) and 4°C showing immediate hydrate formation on the gas bubble during injections of natural gas into a chamber full of cold seawater ([7], Photos courtesy of MBARI). This could be representative of how hydrate formation occurred in the BP cofferdam

controlled experiment at 1,000 m water depth using a remotely-operated vehicle, natural gas is injected into a glass chamber [7]. Immediately, hydrate forms around the gas bubbles creating a white mass of hydrate at the top of the chamber. When they come into contact with one another, these bubbles can stick together and agglomerate to form a large mass of hydrate. Without the use of inhibitors, the hydrate-coated gas and oil droplets from the well had a high probability of causing a plug as it entered the cofferdam and the pipe leading from the seafloor to the ship above. While BP had planned for methanol injection to prevent hydrate from forming after the cofferdam was in place, they had no inhibitor injection capability during installation.

As the enormous 98-ton dome was positioned over the leaking well on May 7, hydrates almost immediately plugged the line and the cofferdam began filling with hydrates, gas, and oil. BP's CEO of exploration and drilling was quoted as saying in disgust, "If we had tried to make a hydrate collection contraption, we couldn't have done a better job". As the containment dome filled with very buoyant gas, along with hydrate and oil, the crew lost control of the cofferdam. Another potential disaster loamed as the large dome began to float up towards the ships above, filled with flammable material. Fortunately, the personnel were able to regain control of the cofferdam and avert disaster. When the smaller *top hat* collection device was put into place on June 3, methanol injection was started at the beginning and hydrate plugging was avoided.

Based on the events of the Deep Water Horizon disaster, both government and industrially funded work has begun on addressing the role of hydrates in any future containment operation. A not for profit consortium, mainly of major oil companies, called the Marine Well Containment Company (http://marinewellcontainment.com/index.php) has been started to create an effective containment system if one is ever needed again. They have recently introduced an interim containment system capable of handling 60,000 barrels of oil/day in 8,000 ft of water. There are plans for a future expanded containment system with a 100,000 bbl/day capacity. These containment systems are using injection lines to introduce methanol for preventing hydrate growth and plugging. More on how methanol works will be given later in the chapter.

7.2 Hydrate Formation and Where it Occurs

To form hydrates, there must be low temperature and high pressure, along with water and a hydrate-forming gas. The goal of oil and gas production is to produce hydrocarbons, which contain hydrate formers. Water is often present during this production of oil and natural gas. During the lifetime of a well, the water content tends to rise. High pressures are often present due to hydrostatic head (depth) and pipeline operating pressures for flow. Low temperatures can be from the external environment, e.g., pipelines on the seafloor, or Joule–Thompson cooling during gas expansion.

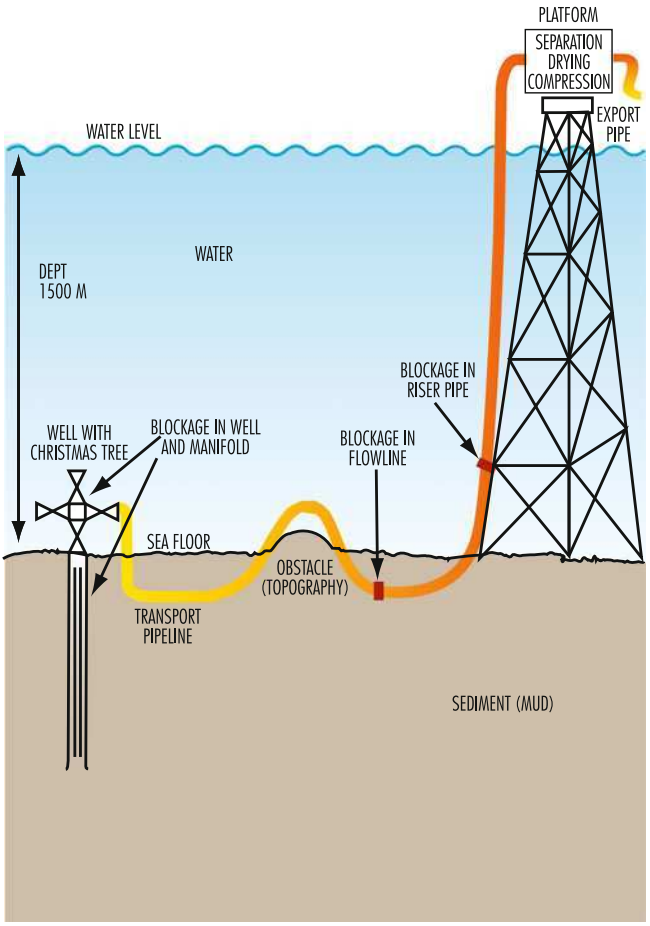

Fig. 7.7 Points of hydrate formation in an offshore process [18]

In the ocean, pipelines can run for tens of kilometers. Below 500–1,000 m depth, the ocean temperature is fairly uniform and cools to around 3°C. For a typically natural gas at these temperatures, less than 0.7 MPa or ($\sim$100 psi) is needed to stabilize hydrate. This pressure is much lower than typical pipeline operating pressures.

Figure 7.7 shows a typical offshore process with a well, a submerged pipeline, and a platform [18]; most hydrate problems occur between the well inlet and the platform. Prior to the well, the normally high reservoir temperatures prevent hydrate formation.

7.3 Ways to Prevent Hydrates

The traditional methods for preventing hydrate formation fall under three approaches:

- Water removal from the gas mixture,
- temperature control,
- addition of inhibitors.

Lowering the pressure, and consequently fluid flow, would be another method to prevent hydrate formation in some situations. However, this approach is generally not economically feasible. Depressurization is a technique used for remediating and removing a hydrate blockage. While this chapter focuses on hydrates, other materials such as wax and scale can add and compound the problems caused by hydrates.

7.3.1 Water Removal

Water removal (dehydration/drying) is theoretically the best approach for ensuring hydrates will not form, as it eliminates a necessary component for hydrate formation. Drying gases can be achieved by a number of well-known engineering processes (e.g., glycol absorption, adsorption on solids, permeation through membranes, etc.). The drying requirements are quite stringent as hydrate formation can occur directly from water vapor, even in the parts per million (ppm) range. While possible, formation from water vapor is a slower process due to the limited amount of water and the decrease in the hydrate stability temperature for a given pressure (See Fig. 3.13).

Care must be taken when deciding the level of drying needed for a particular gas stream. The correlations that define maximum water content on the basis of dew point are not entirely reliable, as they do not take into account the equilibrium between hydrates and water vapor. Thermodynamic models can also be inaccurate. Therefore, requesting gas based on dew point specifications may not be sufficient. A more logical approach, based on experience, is to set limit on moisture content.

While the techniques for drying are well known, they can be challenging from an economic standpoint given the large volumes that need to be treated. This is especially true in the case of production in remote locations, offshore installations, and connections between wells and processing facilities.

7.3.2 Temperature Control

Hydrates are controlled with temperature by heating a zone to ensure the temperature does not fall below the hydrate stability temperature. However, heating electrically or with hot fluids is not often feasible or practical considering

some pipelines can be in the hydrate formation region for sections hundreds of kilometers long. One approach for reducing the zone in the hydrate formation region for subsea production is to bury the pipeline or add insulation. This thermal insulation keeps the hot fluid from the wellhead warmer during transposition through the pipeline. However, any stoppage in production lasting over several hours will allow the fluid in the pipeline to cool into the hydrate stable region. Startup of production in these situations is particular hazardous for hydrate formation and blockage.

7.3.3 Addition of Inhibitors

When heating or drying the fluid is not possible or economically infeasible (which unfortunately is most often the case), additives (or inhibitors) can be added to prevent hydrate formation. They are often convenient to use in locations such as subsea pipelines where other additives are already routinely added (e.g., corrosion inhibitors, wax inhibitors).

In order to understand why inhibitors are effective in prevent hydrate formation, let's discuss how they work. From a thermodynamic point of view, a phase transition occurs based on the Gibb's free energy of the system:

$$\Delta G = \Delta H - T\Delta S \tag{7.1}$$

To prevent hydrate formation (meaning to shift hydrate stability to lower temperatures at a given pressure), we must try to increase the system free energy by introducing an additive. In this case, the energy term, ΔH (enthalpy), remains relatively constant even with additives. However, the *structural* term, ΔS (entropy) for the phase transition:

$$\text{Gas} + \text{water} \leftrightarrow \text{hydrate} \tag{7.2}$$

at a given pressure and temperature, is likely to change if the additive disrupts the way the water molecules bond and structures themselves. This increased disorder causes the entropy term in become more negative, resulting in an overall increase in free energy.

The most commonly used inhibitors (e.g., alcohols, glycols) have an affinity for water, as they themselves form hydrogen bonds with the water molecules, and interfere with the ordering of the water. This has the desired effect of lowering the hydrate formation temperature. Other effective inhibitors for hydrates include salts such as sodium chloride (NaCl). However, salts are not added to pipelines due to increased problems they cause with corrosion and scale.

The inhibitors mentioned above are called thermodynamic hydrate inhibitors as they shift the hydrate stability line. There are other hydrate inhibitors which are designed to either delay/slow the growth of hydrate or to prevent hydrates from sticking together to form a plug.

Table 7.1 Main characteristics of some thermodynamic hydrate inhibitors

	Methanol	EG*	DEG**
Formula	CH_3OH	$C_2H_6O_2$	$C_4H_{10}O_3$
Molecular weight	32	62	106
Boiling point (°C)	64.7	198	245
Vapor pressure at 20°C (KPa)	12.5	0.01	< 0.01
Melting point (°C)	−98	−13	−10
Density at 20°C (g/l)	792	1,116	1,118
Viscosity at 20°C (cP)	0.59	21	35.7

* EG = ethylene glycol HO–CH_2–CH_2–OH
* DEG = diethylene glycol HO–CH_2–CH_2–O–CH_2–CH_2–OH

Let us briefly review the main classes of hydrate inhibitors. They are as follows:

- Thermodynamic inhibitors
- Kinetic inhibitors
- Anti-agglomerants

7.4 Hydrate Inhibitors

7.4.1 Thermodynamic Hydrate Inhibitors

Thermodynamic inhibitors are compounds which lower the hydrate formation temperature when mixed with water. The effect is similar to adding salt to roads in the winter, de-icer (mainly NaCl and $MgCl_2$) on planes, and glycol to a car's radiator. These chemical additives disrupt hydrogen bonding in water and the freezing point of water is lowered (or depressed) and ice is no longer stable at 0°C. Based on the additive chosen (which include salts, glycols, and alcohols), one can vary the amount of freezing point depression achieved.

Table 7.1 shows the thermodynamic properties of some common hydrate thermodynamic inhibitors. Because of its effectiveness, low cost, and easy availability, methanol is often used to prevent hydrate plugs (continuous injection into the pipeline) or to remediate (dissociate) a hydrate plug that has formed.

Glycols are also commonly used as thermodynamic hydrate inhibitors. Monoethylene glycol (MEG) is the most effective, based on molecular weight. However, diethylene glycol (DEG) may be justified as it is easier to recover and better at dehydrating natural gas.

The typical measure of inhibitor effectiveness is the subcooling (difference between the hydrate formation temperature with inhibitor subtracted from the formation temperature without inhibitor). Figure. 7.8 shows the subcooling for various inhibitors as a function of aqueous concentration. As shown in the figure, the inhibitor concentration increases the amount of subcooling achieved.

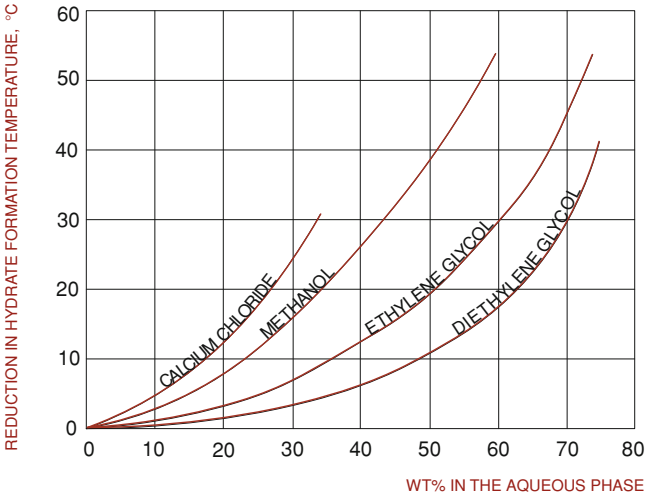

Fig. 7.8 Effect of some thermodynamic hydrate inhibitors on methane hydrate stability as a function of concentration. The hydrate is stable to the left of each curve

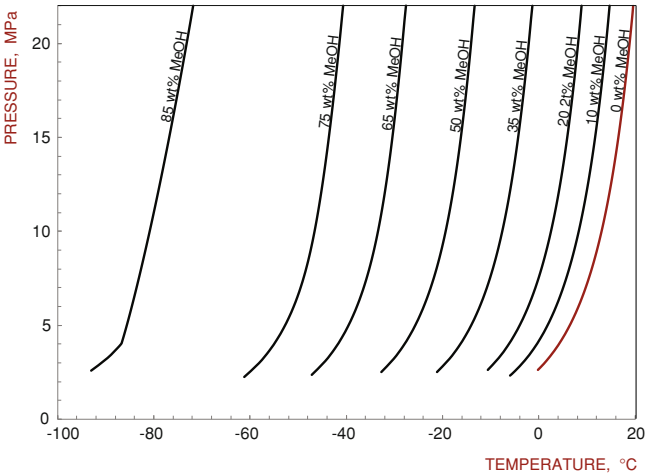

Fig. 7.9 Effect of methanol (MeOH) on hydrate inhibition at different pressures and temperatures. The hydrate formation temperature (for a given pressure) decreases as methanol concentration increases, given as weight % in the aqueous phase [2]

The amounts of inhibitor needed can be significant. As shown in Fig. 7.9, 5°C of subcooling requires methanol concentrations of 10 wt% in the aqueous phase. There is a simple equation developed by Hammerschmidt [5] for predicting the amount of subcooling an inhibitor provides based on concentration:

$$\Delta T = \mathrm{K_H} W / [M(100 - W)] \tag{7.3}$$

where ΔT is the subcooling in °C, W is the wt% of inhibitor in the aqueous phase, M is the molecular weight of the inhibitor (g/mol) and K_H is a constant and a function of the inhibitor used (methanol, ethanol = 1.297; ethylene glycol: between 1.297 and 2.222; diethylene glycol: between 2.222 and 2.427; triethylene glycol: between 2.222 and 3.000) [2]. The equation was reported to be applicable for methanol concentrations below 30 wt% and glycol concentrations below 20 wt% [5].

The Hammerschimdt equation is a good starting point in estimating inhibitor effects. In addition, there have been other empirical equations developed and more rigorous methods for determining the inhibitor effect [2, 17]. It should be noted that equations such as the one above from Hammerschimdt only calculate subcooling. Therefore, knowing the actual hydrate formation temperature also relies on the prediction without inhibitors. Caution should be used when combining these empirical predictions.

As mentioned, given the low cost and effectiveness, methanol is widely used in extraction wells and pipelines. However, it does have its drawbacks. The quantities often required are, in fact, huge. Tons per day can be used even in small to medium sized offshore operations. In addition to being flammable and quite volatile, methanol is a toxic compound and does not easily biodegrade. Because of it chemical nature, methanol tends to partition more into the hydrocarbon phase than other inhibitors such as glycols. This methanol is considered lost as it does not contribute to inhibiting hydrate formation. There are also restrictions on the amount of methanol in the hydrocarbon stream allowed to reach the downstream refineries. Fines can be assessed typically for methanol values in the hydrocarbon above 100 ppm. If you focus on LPG (liquefied petroleum gas, containing mainly propane and butanes), methanol leads to azetropes and products can no longer be fully separated using distillation. Methanol can also strip corrosion inhibitors added to the oil, and itself is slightly corrosive. In the long run, this can lead to corrosion problems.

As mentioned above, even ionic solids (e.g., inorganic salts) inhibit hydrate formation. The effect of brine on hydrate formation can be described as a first approximation by an equation proposed by McCain [13], which is valid for salt concentrations up to 20 wt% and gas densities between 0.55 and 0.68

$$\Delta T = AS + BS^2 + CS^3 \tag{7.4}$$

where ΔT is the subcooling (°F), S is the salinity (in wt%) and the coefficients A, B and C are functions of the gas density, γ:

$$A = 2,20919 - 15,5746\gamma + 12,160\,\gamma^2 \tag{7.5}$$

$$B = -0,106056 + 0,722692\gamma - 0,85093\gamma^2 \tag{7.6}$$

$$C = 0,00347221 - 0,0165564\gamma + 0,049764\gamma^2 \tag{7.7}$$

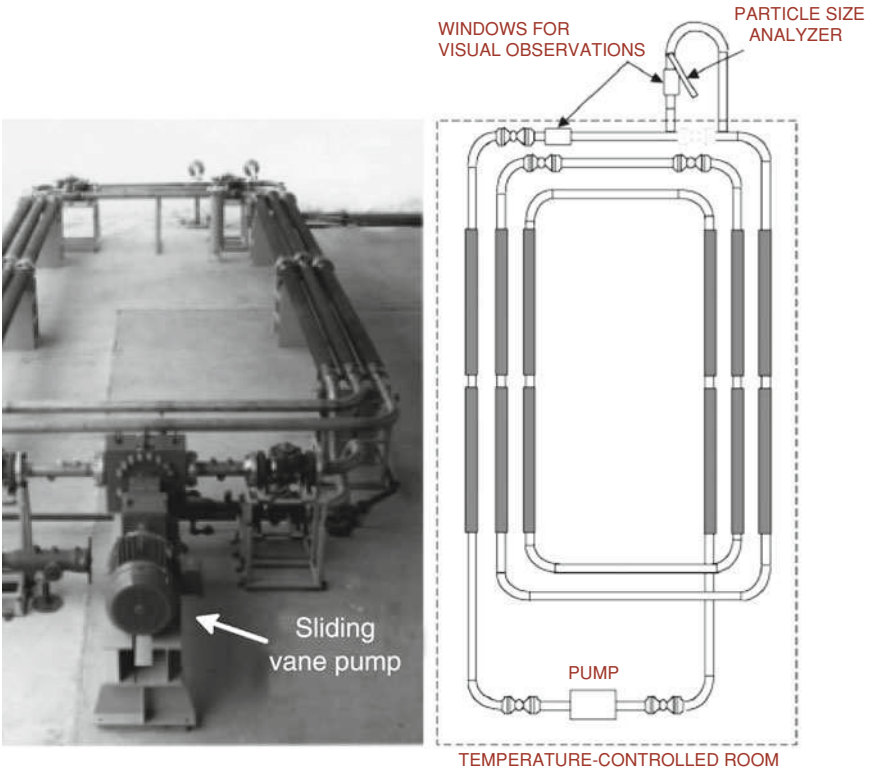

Fig. 7.10 The flowloop at the ExxonMobil Friendswood facility in Texas. Its design allows for a relatively small footprint while achieving an overall length of nearly 100 m [19]

Estimating the effect of salinity is important as saltier water typically begins to be produced (in increasing quantities) during the lifetime of a producing reservoir.

Oil companies and engineering service companies often rely on experimental measurements to better understand how these systems behave, using laboratory equipment as seen in Chap. 5 or even larger flow loops to simulate the behavior of fluid in pipes. These flow loops can reach considerable size, from a few meters to hundreds of meters long.

The following are some of the flow loops worldwide used to study gas hydrates. The ExxonMobil Friendswood flow loop in Texas (Fig. 7.10) is 93 m long with an internal diameter of 9.7 cm [19]. The flow loop installed at the research center of the French Petroleum Institute (IFP) in Solaize (Fig. 7.11) is 140 m long with a 5 cm inner diameter and can go up to 10 MPa (1,450 psi). There is an even larger flow loop at SINTEF Multiphase Flow Laboratory in Trondheim, Norway (Fig. 7.12). SINTEF also uses an interesting wheel-shaped flow loop (2 m diameter) which rotates to simulate pipeline flow. The University of Tulsa flowloop (Fig. 7.13) in Tulsa,

Fig. 7.11 The flowloop used for experimental research on hydrates installed at the research center of the French Institute of Petroleum in Lyon

Fig. 7.12 The large flowloop at the SINTEF Multiphase Flow Laboratory in Trondheim, Norway

Fig. 7.13 The 49 m flowloop at the University of Tulsa. The flowloop is jacketed and glycol is circulated for cooling. The movable platform allows the flowloop to be inclined

Oklahoma has an internal diameter of 7.6 cm and a flow path of 49 m. It is mounted on a movable platform that allows the flowloop to be rocked back and forth up to $\pm 8^{\circ}$.

7.4.2 Low-Dosage Hydrate Inhibitors

The use of methanol and other thermodynamic hydrate inhibitors often requires significant quantities of the inhibitor to be injected into the pipeline. Beginning in the early 1990s, work began on new classes of hydrate inhibitors. Instead of preventing growth based on thermodynamics, these inhibitors rely on delaying nucleation, slowing growth, and preventing hydrate agglomeration to prevent hydrate plugs.

These new types of inhibitors are effective at much lower doses than thermodynamic inhibitors and are often called *low-dosage* hydrate inhibitors (LDHI). The benefits, both from an economic and environmental standpoint, can be significant and the industry has shown marked interest in their development.

LDHI's are classified on the basic of their mechanism for preventing hydrate plugs. There are kinetic hydrate inhibitors and anti-agglomerants.

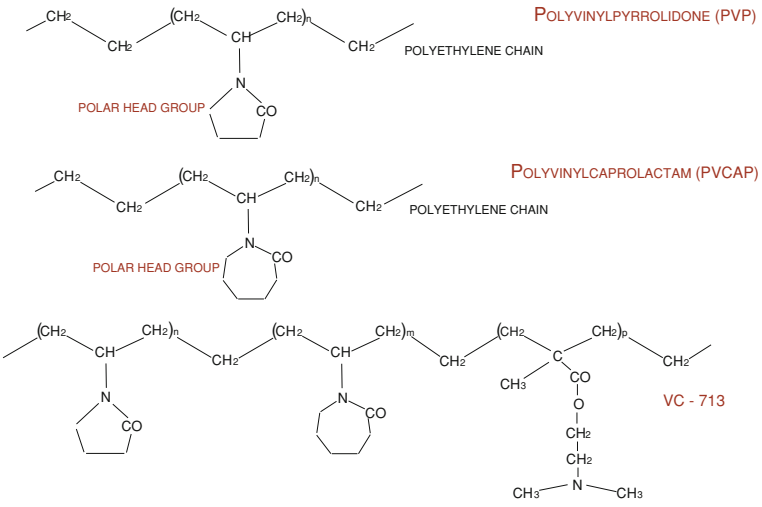

Fig. 7.14 Molecular structures for some kinetic inhibitors consisting of a polymer chain and one or more polar groups

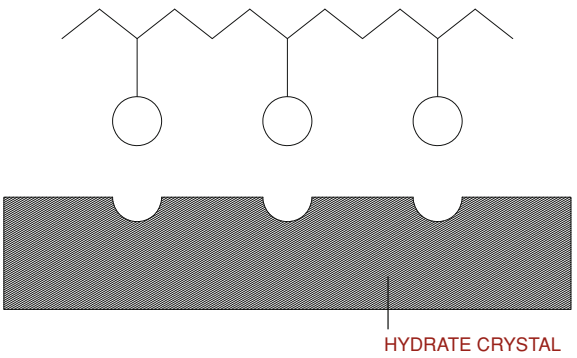

Fig. 7.15 Kinetic inhibitor absorbed on the hydrate surface

7.4.2.1 Kinetic Hydrate Inhibitors

Kinetic hydrate inhibitors (KHIs) affect the induction time and slow down the formation of hydrates. They work by binding to the surface of the hydrate, opposing the formation and growth of crystalline hydrate nuclei. The goal is to suppress hydrate formation for longer than the residence time of the water in the hydrate formation region. KHIs tend to be low molecular weight polymers, usually a polyethylene (or polyvinyl) backbone chain with attached polar groups (typically amides with carbon numbers of 5–7) (Fig. 7.14).

The exact mechanism of KHIs is not fully understood. It is thought that when the inhibitor is in contact with a hydrate, the polar groups interact with the partially formed cages on the hydrate surface [6]. The polymer chain then stretches over the

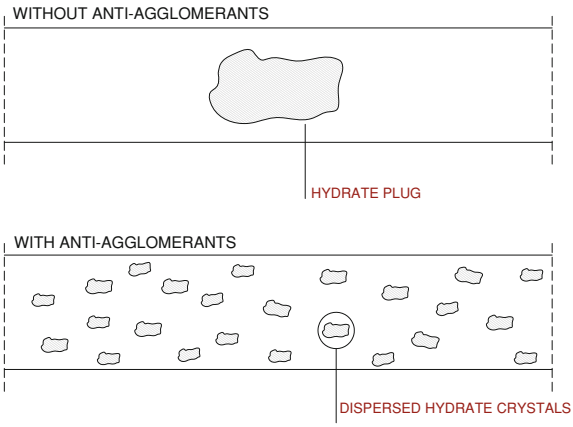

Fig. 7.16 Schematic on the effect of using anti-agglomerants

hydrate surface, blocking further growth (Fig. 7.15). However, the KHI is not truly adsorbed onto the hydrate.

Early research on KHIs was performed largely at the Colorado School of Mines in the late 1980s [12, 17] with the introduction of molecules such as polyvinyl pyrrolidone (PVP) and polyvinylcaprolactam (PVCap). Their work continued as several other inhibitors were proposed, often used in combination with other synergistic materials [9].

The effective capability of KHIs is limited to small subcoolings and residence time. PVP has been shown effective for less than 10°F (5–6°C) of subcooling with residence times of less than 20 min. However, more complex additives, i.e. VC-713 and PVCap can allow up to 18°F (10°C) subcooling and residence time of up to several days. The performance of KHIs is strongly affected by temperature, pressure, and salinity. It has also been shown that the hydrate crystal structure can affect KHI performance. A KHI developed for sII hydrates is not necessarily (and likely not) effective for sI hydrates.

While the cost per weight of KHIs is generally higher than tradition thermodynamic inhibitors, aqueous concentrations of KHIs need to be generally less than 1 wt% versus 10–60 wt% for methanol. This leads to a 50% savings when using KHIs.

Despite initial enthusiasm for these inhibitors, their application has been limited and work continues on finding KHIs with a large effective subcooling range and longer residence time capabilities. In most cases (e.g. deep water operations), subcoolings can be over 20°C. There has been some reports by BP in the North Sea of synergistic effects with KHI's combined with anti-agglomerants [1].

Hybrid inhibitors are also studied based on compounds like polyether amines, which have synergistic effects on hydrate inhibition properties when applied concurrently with polymeric kinetic inhibitors or thermodynamic inhibitors [15].

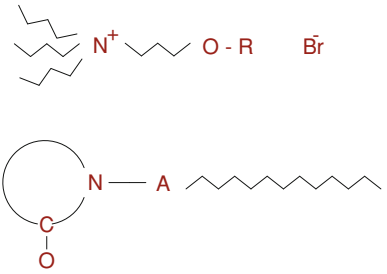

Fig. 7.17 Typical structure of an anti-agglomerant. *Top*: quaternary ammonium salt with three short chains (butyl and pentyl) and a longer alkyl chain (R) with 12–14 carbon atoms

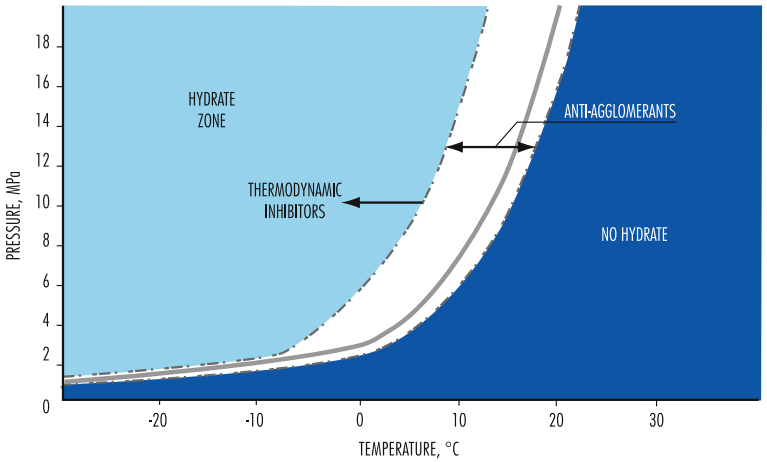

Fig. 7.18 Typical PT diagram showing the regions where the low dosage (anti-agglomerants) inhibitors can be used. (1) No inhibitor needed, (2) an anti-agglomerant can be used, (3) a thermodynamic inhibitor should be used

7.4.2.2 Anti-Agglomerants

The inhibition technique using anti-agglomerants is based on preventing hydrate crystals from sticking together and/or depositing on the pipe walls. It is used to basically form a slurry of hydrate particles that can flow through the pipe (Fig. 7.16). The goal here is not to prevent hydrate from forming, but to prevent hydrates from growing larger and plugging the pipeline.

Generally, to be effective, they must be oil-soluble. Industrial interest in these compounds began in the 1980s, initially by the French Petroleum Institute (IFP), and then by Shell, who had realized the kinetic hydrate inhibitors had their limitations.

Work started with classic surfactants, such as alkylsulphonic compounds, and moved to more effective types of anti-agglomerants, such as quaternary ammonium and phosphonium salts. From this, we can define anti-agglomerants are effective when their structures contain two or three short butyl- or pentyl-chains and one or two longer chains (more than eight carbons long) [10,11]. Other authors

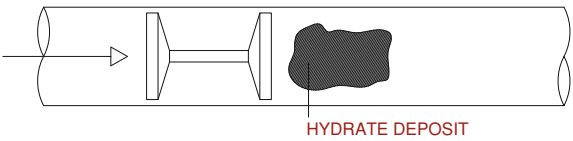

Fig. 7.19 The use of a *pig* which serves to clean pipelines of deposits, including wax and hydrates

[8] studied anti-agglomerants based on molecules similar to kinetic hydrate inhibitors (Fig. 7.17)

In practice, effective anti-agglomerants have a hydrophilic (polar group) head and a hydrophobic (hydrocarbon-based) tail. They are positioned at the interface between the water and the hydrocarbon when hydrates begin to form. The steric hindrance of the long tails in the hydrocarbon phase prevents continued hydrate growth or agglomeration of the hydrate particles.

While much less quantities of these compounds are needed versus thermodynamic hydrate inhibitors, most are still considered toxic for the environment and their usage is limited.

7.4.3 How to Use the Inhibitors

Some oil companies have implemented proprietary software tools that give quick information on hydrate formation in oil and gas facilities. Algorithms can be developed to estimate the thermodynamic conditions of hydrate formation in different media, suggesting how and when to use the inhibitors. Such tools are normally based on experimental tests on the use and dosage of various types of additives. Diagrams can be created that suggest which type of inhibitor should be used. As an example, Fig. 7.18 shows a typical PT diagram where hydrate formation is possible on the left of the equilibrium curve. The central area, including the equilibrium curve, is typical for the use of low-dosage inhibitors (especially anti-agglomerants) and depends on the type of inhibitor. On the left of such area only a thermodynamic inhibitor can be effective. On the right of the central area, no inhibitor is necessary

7.5 Remediation and Removal of Hydrate Plugs

Once a plug has formed in a pipeline, it must be remediated as quickly as possible to minimize economic losses. There are a number of options available and the recommended remediation strategy is selected (typically by a flow assurance engineer) based on the specific situation. If hydrate formation is gradual and flow is still possible, one option is to use a *pig*. A pig (Fig. 7.19) is a pipeline tool that is used to sweep out and clean pipelines. They are used to remove deposits, such as wax, and can be used for hydrates as well. Other options include injecting

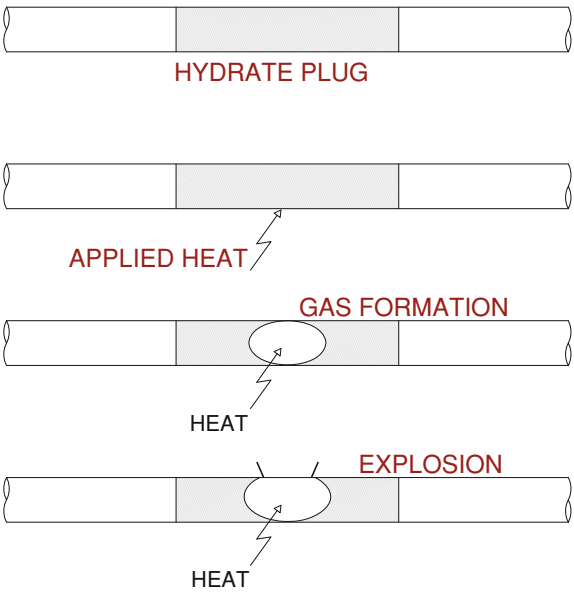

Fig. 7.20 Pipeline rupture due to excessive pressure buildup generated by hydrate dissociation

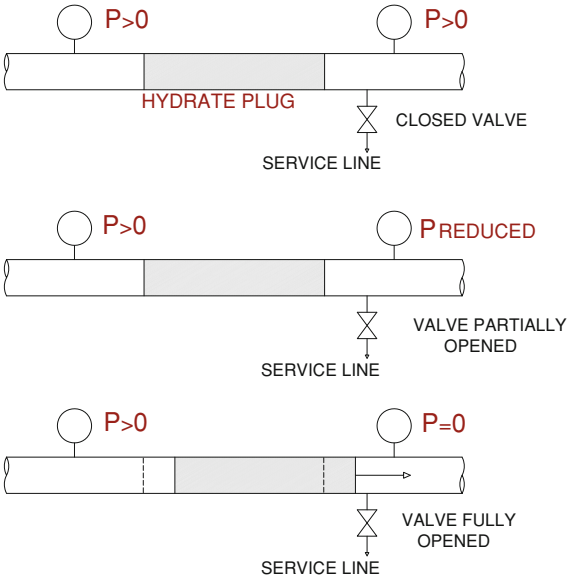

Fig. 7.21 Depressurization downstream of a hydrate plug which can cause the plug to be released as a dangerous projectile in the pipeline

inhibitor, heating, or depressurization. One or a combination of methods can be used. Each of these approaches has potential risks. When heating, caution was be used to prevent excessive pressure build-ups and possible rupture and explosion (Fig. 7.20). Depressurization, especially when only from one side of the plug, can lead to dislodging of the plug and moving through the pipe as a projectile

(Fig. 7.21). Inhibitor injection is often effective but large quantities of chemicals can be needed.

References

1. Argo CB, Blain RA, Osborne CG, Priestley ID (1997) Commercial deployment of low dosage hydrate inhibitors in a southern North Sea 69 km wet-gas subsea pipeline. In: International symposium on oilfield chemistry, Houston, 18–21 February 1997, SPE 37255
2. Carroll J (2009) Natural gas hydrates. a guide for engineers, 2nd edn. Gulf-Elsevier, Oxford
3. Collett TS, Dallimore SR (2002) Detailed analysis of gas hydrate induced drilling and production hazards. In: Proceedings of international conference on gas hydrates 4, Yokohama, 19–23 May 1997, pp 47–52
4. Hammerschmidt EG (1934) Formation of gas hydrates in natural gas transmission lines. Ind Eng Chem 26(8):851–855
5. Hammerschmidt EG (1939) Gas hydrate formation in natural gas pipe lines. Oil Gas J 37(50):66–71
6. Hawtin RW, Moon C, Rodger PM (2005) Simulation of hydrate kinetic inhibitors: the next level. Proceedings of international conference on gas hydrates 5, Trondheim, 13–16 June, Paper 1048
7. Hester KC, Dunk RM, Walz PM et al (2007) Direct measurements of multi-component hydrates on the seafloor: pathways to growth. Fluid Phase Eq 261:396–406
8. Huo Z, Freer F, Lamar M et al (2001) Hydrate plug prevention by anti-agglomeration. Chem Eng Sci 56:4979–4991
9. Kelland MA (2006) History of the development of low dosage hydrate inhibitors. Energy Fuels 20(3):825–847
10. Klomp UC, Kruka VR, Rejnhart R, Weisenborn AJ (1995) A method for inhibiting the plugging of conduits by gas hydrates. International Patent WO 95/17579, 29 June, international application number PCT/EP94/04248
11. Klomp UC, Rejnhart R (1996) Method for inhibiting the plugging of conduits by gas hydrates. International Patent WO 96/34177, 31 October 1996, international application number PCT/EP96/01732
12. Ledermos JP, Long JP, Sum A et al (1996) Effective kinetic inhibitors for natural gas hydrates. Chem Eng Sci 51(8):1221–1229
13. McCain WD (1990) The properties of petroleum fluids. PennWell Books, Tulsa
14. National Commission on the BP Deepwater Horizon Oil Spill and Offshore Drilling (2011) Deepwater: the gulf oil disaster and the future of offshore drilling. US Government, January, http://www.gpoaccess.gov/deepwater/index.html
15. Pakulski M, Szymczac S (2008) Twelve years of laboratory and field experience for polyether polyamine gas hydrate inhibitors. In: Proceedings of international conference on gas hydrates 6, Vancouver, 6–10 July 2008, Paper 5347
16. Rojey A, Jaffret C (1997) Natural gas: production processing transport. Technip, Paris
17. Sloan ED, Koh CA (2008) Clathrate hydrates of natural gases, 3rd edn. CRC Press, Boca Raton
18. Sloan ED, Koh CA, Sum AK (2010) Natural gas hydrates in flow assurance. Elsevier, New York
19. Turner DJ, Kleehammer DM, Miller KT et al (2005) Formation of hydrate obstructions in pipelines: hydrate particle development and slurry flow. In: Proceedings of international conference on gas hydrates 5, Trondheim, 13–16 June 2005, Paper 4004

Chapter 8
Hydrates as an Energy Source

8.1 Why Gas Hydrates?

The potential use of gas hydrates as an energy resource should be viewed from two perspectives. The first concerns global energy needs from a relatively long term point of view (about 50 years). The second is related instead to geopolitical concerns and national energy security.

Natural gas reserves (see Chap. 1) are abundant and growing due to new discoveries. The current rate of natural gas consumption versus production should ensure availability for more than 60 years. This is without even considering the so-called *unconventional* gas from coal seams (coal bed methane), shales, and tight gas sands. Today, large quantities of natural gas associated with oil production are still being flared or re-injected into the reservoir due to lack of local markets or adequate means to transport the gas to market. With that being said, the largest conventional natural gas reserves are found in regions of political instability or controlled by countries who do not always deliver in a reliable and/or predictable fashion. This is true at a time when major consumers like the United States, Canada, and parts of Europe are seeing their production decline. In addition, with the economic rise of countries such as India and China, market demand will increase likely making it more difficult and costly to adequately supply gas to the western world.

Transportation of natural gas by sea over long distances is now typically done in liquefied form, a method that is very expensive (plants are needed upstream to liquefy the gas and downstream for re-gasification) and potentially vulnerable to attack. Inter-regional pipeline systems used for over-land transportation are fixed infrastructure and are vulnerable as well. The defense of pipelines and liquefaction facilities, as well as LNG tankers, from terrorist attacks is an open problem.

Gas hydrates are present in large amounts in all of World's oceans on the continental shelves and in permafrost areas. Whether onshore (including Canada, Russia, China, USA) or offshore (USA, Japan, India, and others), hydrates are present in countries which are large consumers and importers of energy.

C. Giavarini and K. Hester, *Gas Hydrates*, Green Energy and Technology,
DOI: 10.1007/978-0-85729-956-7_8, © Springer-Verlag London Limited 2011

As an energy resource, gas hydrates are considered together with other unconventional hydrocarbon resources which are either expensive to recover and/or requiring special technology for extraction. However, in recent years, production has begun on many of these unconventional resources. Besides the tar sands and extra heavy oils, other examples are shale gas and coal bed methane which were once seen as uneconomic resources and now considered important energy commodities. It was necessary to better understand the geology and properties of the reservoirs to address the production challenges.

While hydrates for some are a potential future energy resource in the coming decades, countries like Japan have already identified hydrates as a strategic resource and have well-defined projects ongoing to commercially produce hydrates in less than 10 years.

Besides the best known countries working on hydrates (Canada, China, India, Japan, South Korea, USA, etc.), other countries (e.g., Bulgaria, Taiwan, and Turkey) are undertaking research to evaluate and define their national reserves of gas hydrates.

8.2 Identifying the Ideal Hydrate Reservoirs

Methane hydrates form spontaneously wherever there are suitable conditions of pressure and temperature, as well as sufficient water and gas supply. While much of the World's oceans are within the hydrate stability field, hydrates are found primary on the continental margins and in the permafrost, as this is where enough gas supply existed. Hydrates are also found in geological formations such as mud volcanoes or cold gas vents. More details on hydrate distribution in nature are contained in Chap. 6.

The makeup of the sediment itself, or the *container* for the hydrates, greatly influences hydrate distribution and saturation. This is one key factor contributing to the high variability in hydrate deposits. Hydrates found in clays or silts, for example, typically have low saturations (on the order of 1–5 vol%) with only occasionally higher saturations appearing in small fractures. Hydrates preferentially form in coarse-grained sediments and sands. The low capillary pressure likely helps gas migration and leads to hydrates being concentrated in these layers. Hydrate saturations in coarse grained sands can exceed 80 vol% of the pore space. Globally, the vast majority of hydrates are disseminated across vast areas in low saturations. Economic production from gas hydrates will selectively target coarse sandy layers with medium to high hydrate saturations.

8.2.1 Hydrate Reservoirs Classified by Types

A simple hydrate reservoir classification system has been developed by Moridis and Collett [15] and allows for a general assessment to be made about hydrate production potential for a particular reservoir.

Class 1 reservoirs are hydrate deposits underlain by a two-phase zone involving mobile gas and water. Class 1 reservoirs are further divided into two subclasses (class 1G and class 1W). Class 1G hydrate deposits have gas filling the pore space in the hydrate zone and are the best candidates for producing gas from hydrates. Class 1W reservoirs have water filling the remaining pore space in the gas hydrate stability zone (GHSZ). Class 1W systems perform nearly as well as class 1G wells but heating is required to prevent secondary hydrate formation near the well bore [2].

Class 2 and class 3 reservoirs both have water filling the hydrate-bearing sediment. Class 2 reservoirs have a mobile free water phase below the GHSZ, while class 3 reservoirs have an impermeable boundary (e.g., shale under burden). While not as good as class 1, reservoir simulated production from both class 2 and 3 type reservoirs have been shown to be feasible economically using depressurization as the production method [16, 17].

Class 4 reservoirs contain dispersed hydrates in low-saturations in marine sediments. While globally there are vast quantities of methane trapped in this class of hydrate deposits, reservoir simulations have shown that production volumes and rates are orders of magnitude below accepted standards for economic viability [18].

8.3 Amount of Gas They Trap

Almost as soon as hydrates were discovered in nature, people began to estimate the global amount of methane in hydrates. Estimates were speculative and ranged more than three orders of magnitude, from about 2.8×10^{15} to 8×10^{18} m^3 of gas (Table 8.1).

Until actual investigations of natural hydrates were done, the validity of these estimates (and the assumptions they made) could not be evaluated. Most of our learning about natural hydrates has come from drilling. With the success of the International Ocean Drilling Program (IODP), including Leg 164 (offshore South Carolina, USA at Blake Ridge in 1995), Leg 204 (offshore Oregon, USA at Hydrate Ridge in 2004) and Expedition 311 (offshore Vancouver Island, Canada on the Northern Cascadia Margin in 2005), there have been a number of major marine drilling projects: the JIP drilling in the Gulf of Mexico, the India National Gas Hydrate Program expedition, the Chinese exploration in the South China sea, and the first Korean expedition. Exploration-style gas hydrate drilling has also been conducted in the Nankai Trough by the Japanese Hydrate Program. Much has

Table 8.1 Estimates of methane contained in hydrates, differentiating between hydrates in permafrost and oceanic areas

Volume (m^3)	Year
Permafrost	
1.4×10^{13}	Meyer (1981)
3.1×10^{13}	McIver (1981)
5.7×10^{13}	Tromufik et al. (1977)
7.4×10^{13}	MacDonald (1990)
3.4×10^{13}	Dobrynin et al. (1981)
Volume (m^3)	References
Ocean	
3.1×10^{15}	Meyer (1981)
$3–5 \times 10^{15}$	Milkov et al. (2003)
$5–25 \times 10^{15}$	Tromufik et al. (1977)
125×10^{15}	Klauda and Sandler (2005)
2×10^{16}	Kvenvolden (1988)
2.1×10^{16}	MacDonald (1990)
4×10^{16}	Kvenvolden and Claypool (1988)
7.6×10^{18}	Dobrynin et al. (1981)

More details and references are given by Collett [6], Collett et al. [7], Kvenvolden [9], and Milkov [14]

also been learned from inland drilling at Mallik (Mackenzie Delta, Canada; two tests in 2002 and 2007/2008) and Mt. Elbert (North Slope, Alaska, USA) in 2007. The first successful gas hydrate production test was performed at Mallik.

One of the fundamental changes in the understanding of gas hydrates accumulations is that they have to be regarded as a component of a traditional petroleum system. Exploration for potential gas hydrate production areas has to follow the established petroleum system analysis path to detect and map the hydrocarbon source migration pathways and host sediments [25].

During the last decade, the knowledge obtained from actual measurements of hydrate reservoirs (largely from the drilling programs) both in the marine and permafrost zones has allow for a refined hydrate resource estimate. The current estimate has converged around 20,000 trillion m^3 (TCM, 2×10^{16} m^3) of methane in hydrates. By comparison, conventional gas is estimated to be about 2×10^{14} m^3. Methane trapped in hydrates is over two orders of magnitude higher than the estimate for conventional natural gas reserves. It should be noted that these estimates represent in-place quantities of methane in the hydrate. None of the global assessments published up until now have estimated how much gas could actually produced from hydrates [7].

Better estimates have been made for hydrate production potential in the United States. They were reported by the National Research Council [21] and by the AAPG [7]. The in-place volume of gas in gas hydrates for the Gulf of Mexico has been estimated to be about 600 TCM (6×10^{14} m^3) of which 190 TCM occurs as relatively highly concentrated accumulations within sand reservoirs. Technically

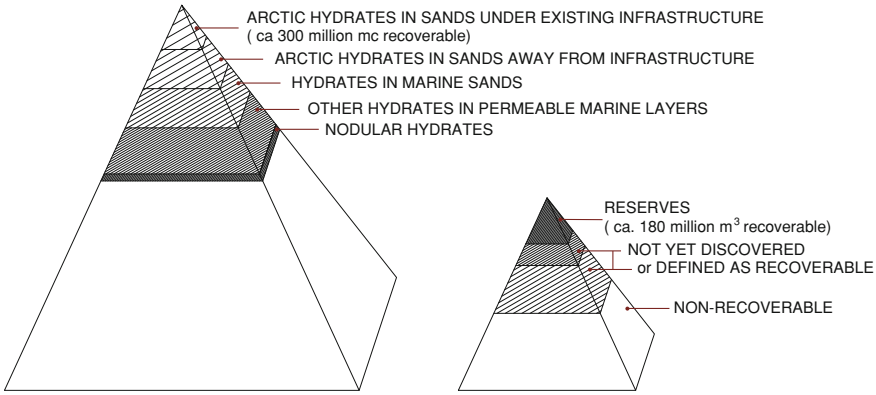

Fig. 8.1 A resource pyramid related to hydrates (*left*) and gas from other sources (*right*)

recoverable hydrate resources on the North Slope of Alaska range between 0.71 and 4.5 TCM [7] with a mean estimate of 2.4 TCM.

Other data on US and world gas hydrate occurrences are given by Collett et al. [7]. Gas hydrates are practically present on all continents. Besides studies of accumulations in the Americas, offshore hydrate deposits in Japan and India have been especially well studied. In 2009, China discovered a huge on shore deposit in Qinghai province and the Tibet plateau, at a depth of 130–300 m below the permafrost.

8.4 The Pyramid of Methane Resources in Hydrates

Different geological substrates produce different types of hydrate deposits. In turn, the hydrate reservoir type affects the likelihood of economic gas recovery. The porosity of the deposit plays an important role. Precisely defining which hydrate deposits can be considered resources, of course, is of fundamental importance.

Boswell and Collett [3] introduced a hydrate resource pyramid to represent the relationship between the deposit type and recovery potential (Fig. 8.1), and related hydrates to conventional gas deposits. Another version of this representation is reported by Collett et al. [7]. These pyramids, of which an example is also given in Chap. 1, are sometimes used to emphasize the quantity and accessibility related to different sources of gas within the same category of reserves.

The most promising and easy to recover resources, or the *low-hanging fruit*, are located at the upper vertex. For hydrates, the top of the pyramid represents high quality reservoir sands with high hydrate saturations located close to existing infrastructure. These are likely on-land deposits in the permafrost regions, e.g., North Slope of Alaska. The next class immediately below the top of the pyramid is composed of hydrates in less well-defined accumulations and existing in similar

Fig. 8.2 Example of a hydrate-bearing core (from the NGHP expedition 01 India, reproduced from Boswell and Collett [3])

geological contexts (i.e., on-land permafrost hydrates), but far from existing infrastructure. The next group includes marine hydrates formed in good quality sand or sandstone reservoirs with medium to medium–high hydrate saturations (Fig. 8.2). The costs for producing these reservoirs will likely be high, considering the necessity of working offshore at certain depths in the ocean. The most favorable accumulations of this type appear to be in the Gulf of Mexico, located near existing infrastructure, and in the Japanese Nankai Trough.

Further down towards the base of the pyramid, there are massive deposits, often with a high degree of hydrate saturation, but are usually found in unconsolidated, low-permeability clay and silt sediments. Some of these accumulations are in fracture zones within clays and grow as nodules (Fig. 8.3) or layers. The recovery of these deposits is challenging, at least based on current technology, for many reasons including the low in situ permeability.

A special class of natural hydrates contains mud volcanoes and diapirs that form from deeper gas rising and forming massive hydrate mounds that crop out on the seafloor or are covered by a thin layer of sediment (Fig. 8.4). These structures are likely very dynamic and are commonly found in places such as the Gulf of Mexico and in general all along active continental margins. The recovery of methane from these geological structures may be very problematic, both for safety reasons and the damage it could cause to the marine ecosystem and the environment in general.

The reserves that are the most difficult technically to recover are also the most abundant ones and make the base of the pyramid. These hydrate accumulations are scattered over large areas in large volumes but with very low saturations (<10 vol%). They represent the largest reserves of hydrates, but there is little to no chance for producing gas from them.

Fig. 8.3 Example of a nodual of massive gas hydrate (from the NGHP expedition 01 India, reproduced from Boswell and Collett [3])

Various international research programs have a priority to establish the hydrate accumulations with the highest potential for production, which will particularly be deposits in sand and sandstone reservoirs. The goal is to decide on the ones that commercial production should be attempted. The top candidates will likely be deposits with continuous zones of high hydrate saturations having a large lateral extent, appropriate reservoir conditions, and sufficiently low costs.

8.5 Some Problems to be Solved

The science and knowledge of natural hydrates has progressed tremendously in the recent years. However, much remains to be done to link and scale what occurs in nature to hydrates formed and measured in the laboratory, which remains the main basis for knowledge on gas hydrates. In the laboratory, we are unable to reproduce the various conditions that led to hydrate formation and occurred over natural timescales. Natural hydrates are complex and formed over a slow process of hundreds of thousands of years. The scientific community is still struggling to find a way to produce representative analogs to natural hydrates. Certain properties, such as the geomechanical strength of hydrate-bearing sediments, are some of hardest to obtain. In addition, the *upscaling* or transition to the industrial scale is far from easy. One difficulty in this comes from the challenge in obtaining actual cores of hydrates in their native state. As hydrates are cored and recovered,

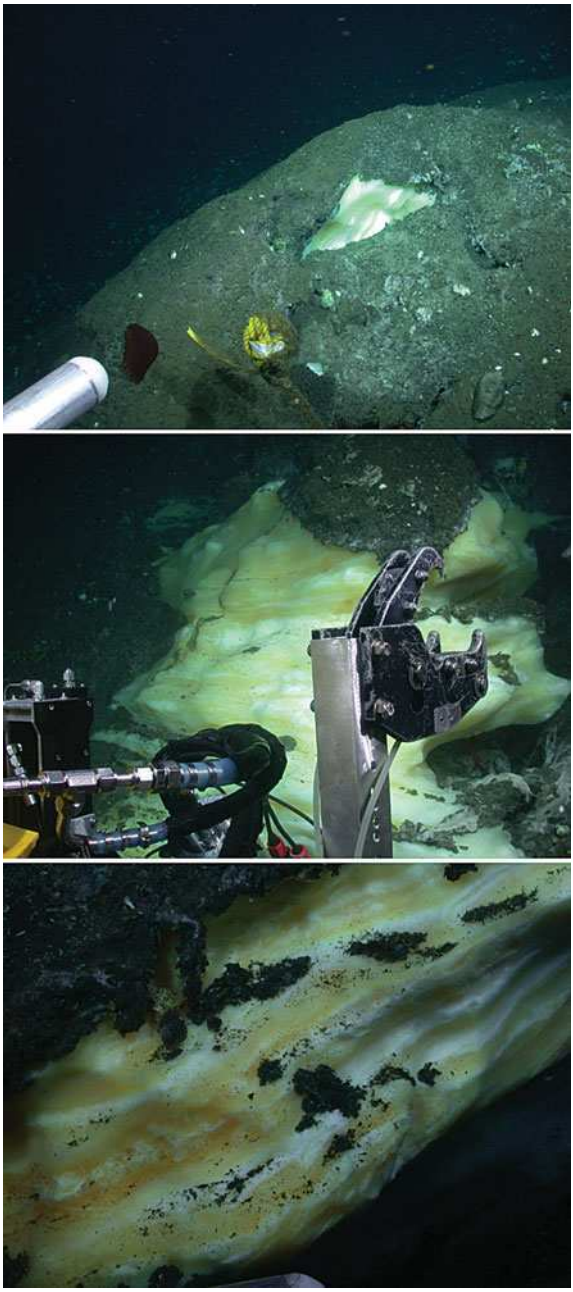

Fig. 8.4 Gas hydrate mounds on the seafloor at Barkley Canyon (Photos courtesy of MBARI)

variations in pressure and temperature cause dissociation and other changes to core. Cores are traditionally stored in liquid nitrogen, which keeps the remaining hydrate stable, but likely significantly alters the sediment matrix. Consequently,

information such as how the hydrate resides in the pore space is lost. Pressure coring techniques (which keep the hydrate core under reservoir pressure conditions) are advancing and hold promise for the future [23].

Following the scientific foundation, it will be the responsibility of engineers to produce hydrates in a safe and economic way. In the field of gas hydrates, scientists and engineers often work closely together and the gap between these two categories of specialists is ever decreasing. According to Max et al. [13], the following issues related to commercial development of gas hydrates need to be better addressed:

- ability to better identify and characterize hydrate deposits with remote sensing technologies;
- ability to define the amount of recoverable gas from a given reservoir and the expected gas production rates (the latter is particularly critical);
- safety and environmental concerns;
- development of production technologies;
- reduction in research, development, and production costs.

Regarding the first two points, one of the biggest problems comes from the dissemination of hydrate accumulations and low permeability. In addition, various sediments containing hydrates do not have the mechanical strength to sustain gas production at commercial rates. Remote sensing techniques at this time (such as using the bottom simulated reflector from seismic surveys) cannot predict the volume or quantity of hydrates and are not even so reliable at identifying potential hydrate deposits [24].

The safety and environmental aspects of hydrate production involve the geology of the local sediment and possible methane gas emissions [21]. During production, the mechanical strength of the sediments can be dramatically reduced, even to value less than a quarter of the original strength. This is especially true if the hydrates are cementing the sediment grains and contributing to its overall strength. There exists the possibility to create slumps or even landslides. The industry is considering the risks carefully and the possible environmental and safety implications, even as each particular hydrate field will be different. In particular, the goal is to safely produce gas from hydrates without large emissions of methane gas, disturbance to the marine ecosystem, or hazardous slumping or seafloor collapse.

Much of the techniques for gas hydrate production can be built on the experience from conventional oil and gas production. In the permafrost, hydrate production could use almost the same technologies as used for conventional gas production. In the marine setting, the need for new technologies and procedures is likely guaranteed. Given the greater complexity, lessons learned from onshore hydrate production will be studied and applied; this is in fact already being done. In addition, the fundamental aspects of processing and transporting gas produced offshore should not be underestimated. A valid path for commercial development of hydrates could likely look like this:

1) perform basic research to study the characteristics of the reservoir;
2) accurately assess the hydrate saturations in place and the amount of recoverable gas;
3) define the economic feasibility;
4) perform logging and production tests to determine the hydrate-rich zones;
5) develop the industrial technologies for the extraction, processing, storage, and transportation of the produced gas.

8.6 How Do We Get Gas from the Hydrates?

It is easy to foresee that the first recovery of methane from gas hydrates will rely on existing infrastructure for conventional oil and gas production, in areas where access roads, gas processing facilities, and pipelines are in place.

At a technical level, well-proven drilling and completion processes for oil and gas drilling and production will be used, along with production strategies specific to dissociating hydrates. Methane from hydrates first has to be released by dissociation. This can be accomplished by lowering the pressure (depressurization), heating the deposit (thermal stimulation), or injecting inhibitors to shift the hydrate stability line. A combination of these approaches could be used as well. The most suitable approach or combination of approaches will be based on local environmental and economic considerations.

8.6.1 Depressurization

Depressurization is the simplest and cheapest method to dissociate in-place hydrates. It is how conventional gas is produced and can be undertaken largely employing current technologies used in conventional oil and gas production. This method is directly applicable when hydrate accumulations overlay a free gas zone (i.e., class 1 type reservoir). One of the simplest schemes is shown in Fig. 8.5, where gas is produced below the GHSZ. Lowering the reservoir pressure will eventually lead to hydrate dissociation and a gradual release of methane supplementing the gas supply.

This is likely what occurred during conventional gas production at the Messoyakha field in Siberia, where hydrates were discovered in the 1960s. It has been established that gas production from dissociated hydrates occurred from 1969–1979 at Messoyakha [5, 6, 12]. The field consisted of two zones, communicating with each other, as shown in Fig 8.5. The upper zone contained hydrates (about 24 m thick) and the lower zone contained free gas with an initial pressure of about 7.8 MPa (1130 psi). For 2–3 years, the pressure followed a gradually and regular decrease, as expected. Then, the pressure stabilized and this stabilization

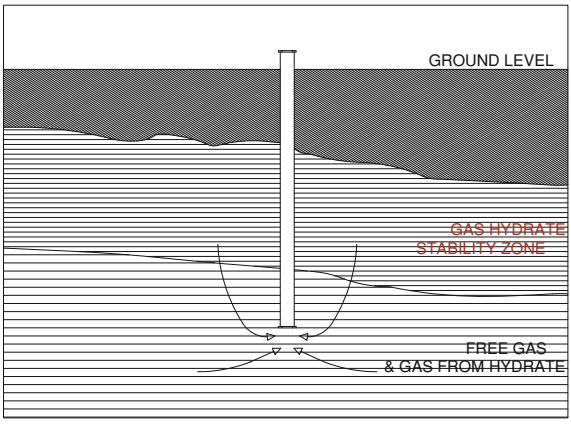

Fig. 8.5 Production by depressurization below the hydrate-bearing sediments (permafrost zone)

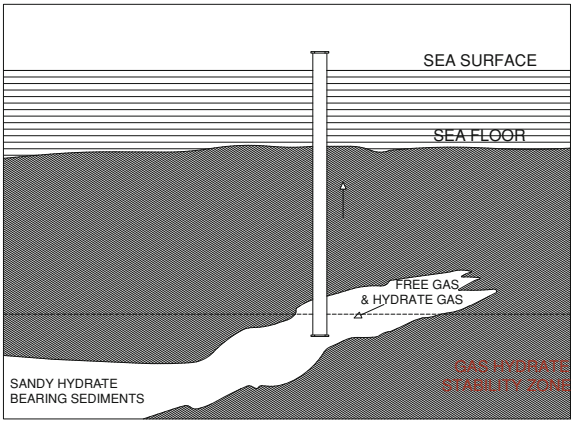

Fig. 8.6 Production by depressurization in marine hydrate

was attributed to gas release from dissociating hydrates. To put it in the right perspective, there are estimates that 36% of the gas produced ($\sim$5 billion m^3) came from hydrate [5].

Figure 8.6 illustrates a similar situation. The production is accomplished by lowering the reservoir pressure through gas production. New gas is gradually supplemented by hydrate dissociation. The process requires that a free gas phase is in contact with the hydrate. We have to note that hydrate dissociation is an endothermic process, meaning that it takes heat from the surroundings. Therefore, as hydrate dissociates, there is a cooling effect around the hydrate. The hydrate will continue to dissociate until it reaches the hydrate stability pressure at the surrounding temperature.

Production of hydrate by depressurization may be hampered by the formation of ice and/or the reformation of secondary gas hydrate, especially around the well bore. This requires controlling the rate of depressurization (how hard you drive the system) or other external intervention, such as heating around the well bore.

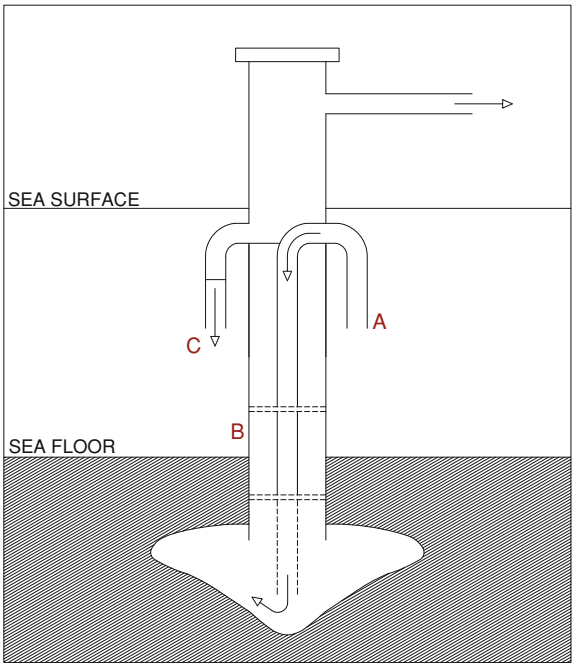

Fig. 8.7 Production of methane from hydrates by injecting warm water (into A) and the gas is produced through the annular space, B [8]

8.6.2 Thermal Stimulation

Thermal stimulation, possibly coupled with depressurization, utilizes a heat source to increase the reservoir temperature, destabilizing the hydrate. The heat may be provided by warm fluid injection (such as brine or steam) or by electrical heating. Heating the injection fluid could be accomplished through heat recovery of neighboring conventional oil and gas operations. The injection fluid could also be warm surface water, in areas where temperatures are at least 18–20°C, as shown in Fig. 8.7 [8]. Warm 20°C water is pumped through Pipe A to the hydrate zone, causing dissociation. The resulting brine in the Annular Space B transports the recovered methane as bubbles, which can be easily separated and produced out of Pipe D. Following the separation, the used injection fluid is pumped out of the system through Pipe C. The patent that proposed this process claims no additional input of energy is required [8].

Steam injection, produced at the surface, is feasible only if the reservoir has a high permeability and porosity. This technique, however, consumes a large part of the energy produced [28]. It is therefore not likely to be economical, but could be an option if steam was produced by natural geothermal heating.

Injecting hot brine (e.g., saturated solutions of $CaBr_2$ or $CaCl_2$) is more effective than pure water as it also acts as a hydrate inhibitor and reduces the hydrate stability temperature. The brine can be sent under pressure to create and maintain an ice-free zone around the well bore. The injection of hot fluids can be

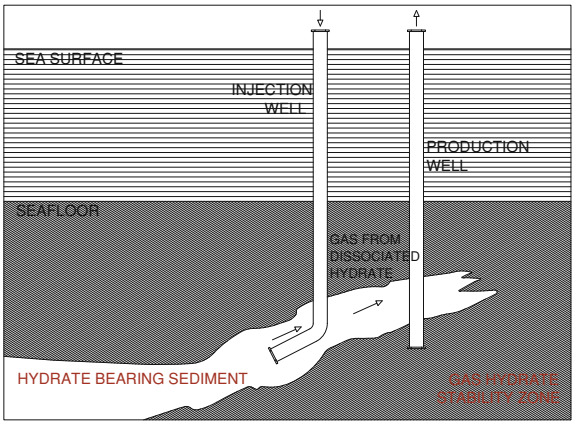

Fig. 8.8 Production of methane from hydrate by heating. Heating is required when there is no free gas in contact with the hydrate

achieved in a single well or through multiple wells. With multiple wells, warm fluid could be introduced into the formation on a continuous basis through an injection well, while methane is extracted from the production well (Fig 8.8). Heat could also be supplied by in situ combustion. Hydrocarbon is burned in a controlled fashion in an injection well and the heat front dissociates methane hydrate, which is then recovered by a production well (Fig. 8.8). Other heat sources, such as using electromagnetic or microwaves, have also been explored.

8.6.3 Use of Inhibitors

Hydrate dissociation can also be initiated by the injection of inhibitors, usually combined with one or more of the other production techniques like depressurization and thermal stimulation. The choice of inhibitors could include traditional ones used in pipeline flow assurance (See Chap. 7) such as methanol or glycols. Other compounds like ionic solutions (e.g., chloride and bromides) could also be used. The inhibitors disrupt bonding the water and cause a lowering of the hydrate stability temperature. Such methods were attempted at Messoyakha and during the first production test at Mallik. While it can cause hydrate dissociation, there are a number of drawbacks to using inhibitors to produce hydrates. They may harm the environment, especially in the marine ecosystem. Their cost and possible corrosion problems should also not be underestimated. Finally, compounded with the above concerns, inhibitors work only if they are present in sufficient concentrations in the aqueous phase. Hydrates are around 86 mol% water and they quickly dilute the inhibitor making them ineffective and requiring significant volumes to be injected.

Most recent studies have shown that in the majority of cases, depressurization most often has the highest efficiency and is the preferred method for producing gas

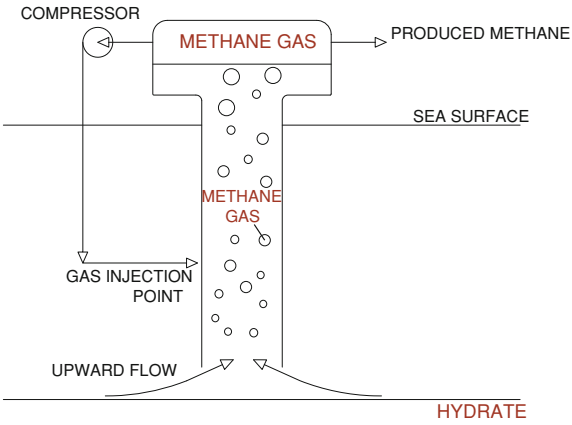

Fig. 8.9 Recovery of methane from hydrate by gas-lift technology, i.e., the creation of upward gas flow caused by lowering the density of the produced fluid

from hydrates. It may be advantageous to combine depressurization with thermal stimulation in some situations.

8.6.4 Other Possible Production Techniques

Beyond the three approaches listed above, others have been proposed and could have the potential to provide an unconventional approach to producing this unconventional resource. In one, gas is injected through a pipe drilled into a layer of gas hydrate (Fig. 8.9). The rising bubbles from the injected gas create an upward flow, causing a vacuum that *sucks* the methane hydrate to the surface [22]. Another method involves the injection of CO_2 into a hydrate reservoir. The CO_2 prefers the hydrate phase and exchanges with the methane. This allows for simultaneous energy production from methane and CO_2 sequestration.

8.7 International Projects for Gas Hydrate Production

8.7.1 Onshore in the Permafrost

Hydrates in nature were discovered in Siberia in July 1961; although, the official announcement was not given until 1969. The Siberian permafrost is, in fact, rich in hydrates [10]. We have seen that the first production of methane from hydrates occurred in the 1970s in the Messoyahka field during normal operation of conventional gas production. This was unexpected. Anomalous patterns in reservoir pressure allowed scientists and engineers to conclude that hydrates were indeed contributing to the gas being produced.

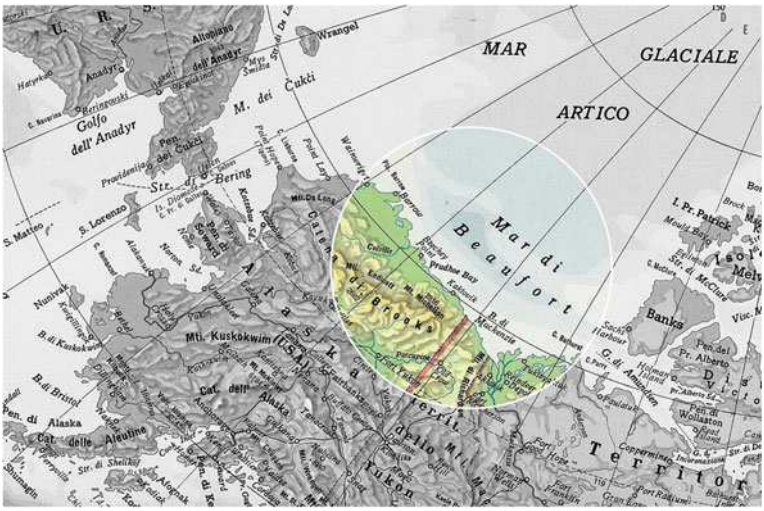

Fig. 8.10 The site of the first gas hydrate production test, Mallik, in the Mackenzie River Delta, Canada

Messoyahka represents an important event because it sparked research towards the exploitation of hydrates as an energy research and the publication of the first modern book on hydrates [11]. It would be almost 30 years before the first production test was conducted specifically designed to produce gas from natural hydrates. In fact, the first test at the Mallik well occurred in 2002 on Richard Island in the Mackenzie River Delta in the Canadian arctic (Fig. 8.10). An on-land permafrost location was chosen for this test and represents the hydrate resource at the top of the pyramid as shown in Fig. 8.1.

Mallik provided the first reservoir studied in enough detail to permit analysis of the production rate and volume of gas purely from dissociating hydrate. Hydrates were first discovered at Mallik in 1972. In this area, deposits of oil (210 million tons) and gas (280 billion m^3) were found. However, without a pipeline, the conventional gas (nor the hydrate) was produced.

The Mallik site was revisited in 1998 by a project designed to drill and test gas production from hydrates. This project was part of a joint program between the Japanese national oil company (JNOC) and the Canadian Geological Survey, with participation from Japan Petroleum Exploration Co (JAPEX) and the US Geological Survey (USGS). In 2001, the partnership grew to include India and other countries. Based on its reservoir characteristics, Mallik was identified as an ideal candidate. The hydrate reservoir at Mallik was in fact very similar to hydrate reservoirs identified offshore Japan.

Three wells were drilled down 1150 m into the sediment during the winter of 2001–2002: one production well and two observation wells. It was ascertained that the reservoir was capable of producing about 110 billion m^3 of gas. Gas hydrate was found primarily as a pore-filling material within the sands with hydrate saturations

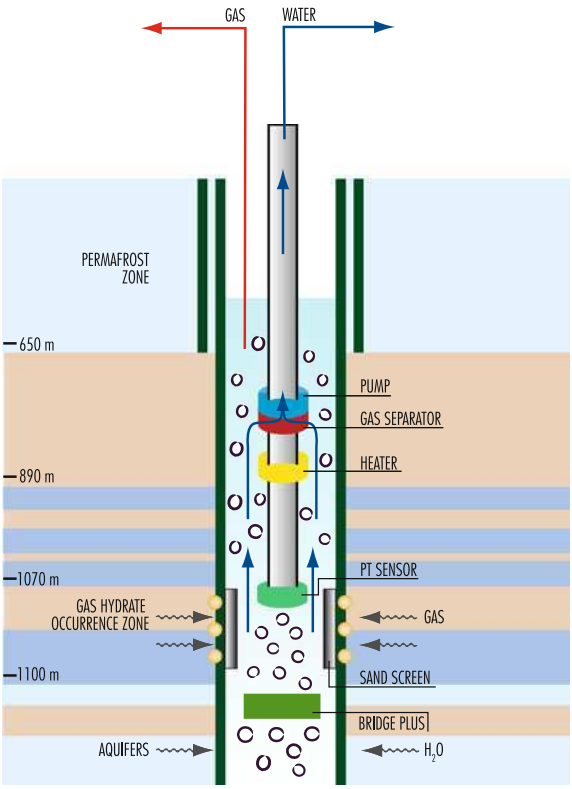

Fig. 8.11 Simplified scheme of the depressurization system in Mallik 2007–2009 [31]

between 50 and 90 vol%. Two carefully planned and monitored production tests were carried out, by means of depressurization and by thermal stimulation. Both tests led to the production of gas from hydrates making it possible to evaluate production strategies and commercial viability, experience which is transferable to other sites [19].

Simple depressurization was sufficient to extract the gas from the hydrates. Thermal stimulation with warm drilling fluids (around 50°C) improved the gas production rate. This first test was scientific in nature and not intended to produce gas at commercial rates. Over the limited testing duration, about 500 m^3 of gas was produced and flared (as they did not have the ability to store and transport the gas).

Five years later, Canadian and Japanese researchers undertook a second longer test utilizing a simple depressurization technique. The two-winter research program was successfully completed in April 2008 and represents a new step forward towards the use of gas hydrates as a viable energy resource [31].

An ice road was built on the Mackenzie River and Beaufort Sea to connect Inuvik with the Mallik site, and allow mobilization of drilling rigs and other equipment. The reservoir gas was depressurized by dropping the water level in the well and the water was re-injected into aquifers below the GHSZ (Fig. 8.11).

Fig. 8.12 The Mallik site in April 2007 [31]

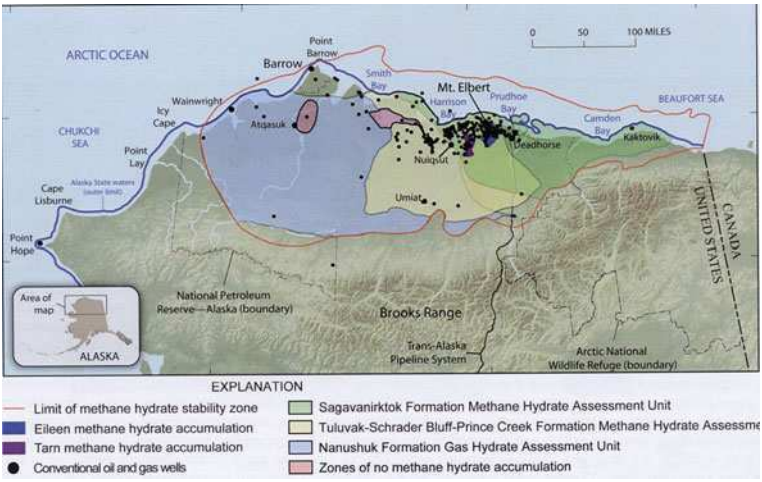

Fig. 8.13 Map of the North Alaska region with hydrocarbon resources [21]

Six days of continuous operation established stable pressure conditions in the well and regular flow to the surface. The volume of produced gas was about 13,000 m^3 and the continuous flow ranged from 2,000 to 4,000 m^3/day. This production test clearly confirmed that the depressurization method was the correct approach. Figure 8.12 shows a view of the Mallik site, in April 2007 [31].

The Mallik program proved that gas production from hydrates was technically feasible (at least from a sand-dominated reservoir) advancing the potential for

Table 8.2 Examples of potentially exploitable marine reserves of hydrates

Region	Area (km^2)	Depth (m)	Reserve (m^3)	Concentration (m^3/km^2)	Hydrate saturations (vol%)
Hydrate Ridge (USA)	375	700–1000	9×10^9	2.4×10^7	From 1–8 to 40
Gulf of Mexico (USA)	23000	440–2500	$8–11 \times 10^{12}$	$3.5–4.8 \times 10^8$	From 20–30 to 100
Blake Ridge (USA)	26000	1000–4000	2.8×10^{13}	1.1×10^9	From 2 to 14
Nankey Trough (Japan)	32000	700–3500	6×10^{13}	1.9×10^9	From 10 to 30

hydrates to be regarded as a recoverable energy resource in the permafrost. The future of gas production in the permafrost will probably hinge on the construction of a gas pipeline connecting the arctic north to markets in Canada and the US. At this time, without an adequate means to transport gas, even conventional gas is not being exported and is largely re-injected at this time to maintain oil reservoir pressures. Beyond the Mackenzie Delta, the North Slope of Alaska is one of the areas with excellent potential for the discovery of additional oil and gas, as well as hydrate reserves (Fig. 8.13).

In the North Slope of Alaska, there have been attempts to refine sampling, site analysis, and drilling with the purpose to build a more *green* production platform. A Joint Industry Project (JIP, Maurer and Anadarko) investigated the use of platforms on pylons and special vehicles that operate on thin ice to minimize environmental damage. These structures allow for greater flexibility and have potential at other sites. One such platform was installed in February 2003 and immediately became operational with no discharges or emissions into the atmosphere. The temporary abandonment season did not produce marked environmental impacts on the surrounding plant and animal life. Among the ambitious goals of this project, involving not only hydrates, the possibility of extending the operating window on permafrost from 3–4 months/year to 9 months or more was explored.

8.7.2 Offshore

For hydrates to truly be a source of future energy, the largest hydrates reserves found in the marine environment need to be exploited (Table 8.2). Developing technologies for offshore production from marine hydrates is of paramount importance.

This is actively being pursued by the Japanese who are aiming for commercial before 2020. Their focus is on large hydrate deposits in the Nankai Trough, located with the Japanese archipelago to the east, Nagoya to the southeast, and Tokyo Bay to the southwest. The interest of Japan is understandable when you consider that

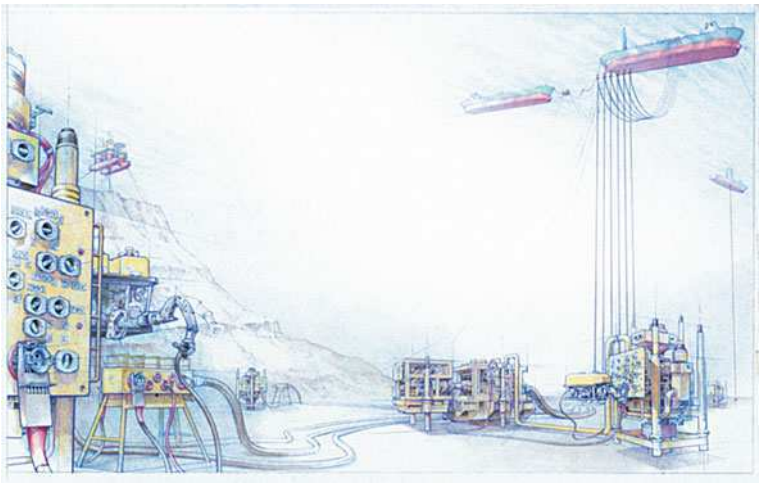

Fig. 8.14 Example of mobile drilling equipment (from Argomenti Esso, year 18 n°45, 2006)

Japan imports nearly 100% of its fossil fuel needs. To increase energy security, Japan started an aggressive program in 1995 to study and assess the potential of natural hydrates. As the largest national hydrate program, they have been involved in a number of international partnerships, included Mallik and work in the Gulf of Mexico. In 1999, field evaluations of the Nankai Trough have confirmed the presence of highly concentration accumulation of natural hydrate in the marine sediments. While not very thick, these deposits have a large lateral extent. In 2001, they began a 16 year strategic exploration (HETI) project with the goal of hydrates commercially supplying energy to Japan. The program funding is over $100 million and involves more than 250 people and 30 organizations [29].

Studies have also been made for other hydrate reservoirs in various parts of the globe. This includes off the coast of Oregon in the US northwest and in the Gulf of Mexico. Studies have been carried out to assess the feasibility of such reservoirs, including processing and transportation requirements for the produced gas [1, 20]. Some of the findings have been extrapolated to other marine situations at medium depths (700–1000 m). Normal fixed leg platforms, possibility linked to anchored or floating support structures, are economically challenging. Hydrate extraction is complex and hard to justify for deposits not related to conventional oil and gas.

Given the characteristics of hydrate deposits and the need to cover large areas at medium to shallow water depths (< 900 m), mobile offshore production facilities are a more functional choice. These wells are connected my means of a multi-functional complex mooring system. The equipment on the seafloor is controlled by remotely operated motors (Fig. 8.14). The main components are the umbilical connection to a support platform and pipelines to transport the gas from the well. The produced gas could be received and processed by an Floating Production, Storage, and Offloading (FPSO) vessel. The FPSO contains gas storage tanks to

temporarily store the produced gas. The system is served by tankers that transport the produced gas to the shore.

The presence of hydrates has been reported in large areas of the Gulf of Mexico, especially off the coast (500 km) of Louisiana and Texas [27]. Hydrates are known to occur in this area as mounds on the seafloor. Conventional oil and gas operations had drilled thousands of wells through the hydrate stability zone in this area. However, it was not known until 2004 if deeper reserves of hydrates in high saturations existed in the sandy layers. Chevron discovered in 2004 a thick sandstone layer saturated with hydrates while drilling an area known as Tiger Shark [4].

A US Department of Energy sponsored JIP project is currently underway with the aim of collecting data on hydrate deposits in the Gulf of Mexico and to develop the most suitable technologies for producing gas hydrates from this area. The participants of this project include major oil companies from the US, India, France, Korea, Norway, and the Japanese hydrate consortium. Leg I of this project in 2005 focused on possible drilling hazards related to gas hydrates. During this leg, information was collected on subsurface heat flux, salinity, stratigraphy, and geochemistry which has also been used to assess the energy potential of marine hydrates. In 2009, a 21-day expedition confirmed high hydrate saturations in quality reservoir sands in at least two of the three sites drilled.

8.7.2.1 Harvesting Production Method

Due to a number of reasons, such a slow hydrate concentration and low driving pressure, low productivity is expected from marine sediments. Only a large number of low cost wells could support an offshore production facility at shallow depths. The method of harvesting natural gas from sea floor gas hydrates is a combination of several new concepts [32].

The released hydrate or free gas can be captured with an overhead receiver as shown in Fig. 8.15. Electrical heating is used to warm the sediment and melt the hydrate. The produced gas is accumulated in the overhead receiver and transported to the surface in the form of hydrate; in fact, the gas will form hydrates when moving through the cold sea water and inside the receiver. No pumps, tubing, subsea pipelines are needed and there are no flow assurance challenges. Many wells can be drilled using low cost technology.

8.8 Processing and Transportation of the Gas Produced

While hydrate can concentrate a lot of methane, it is still mainly water. Producing methane hydrates results in water production as well as a wet gas. In some areas, appreciable amounts of CO_2 or H_2S, along with higher hydrocarbons, might be present in the produced gas. Depending on the transportation method chosen

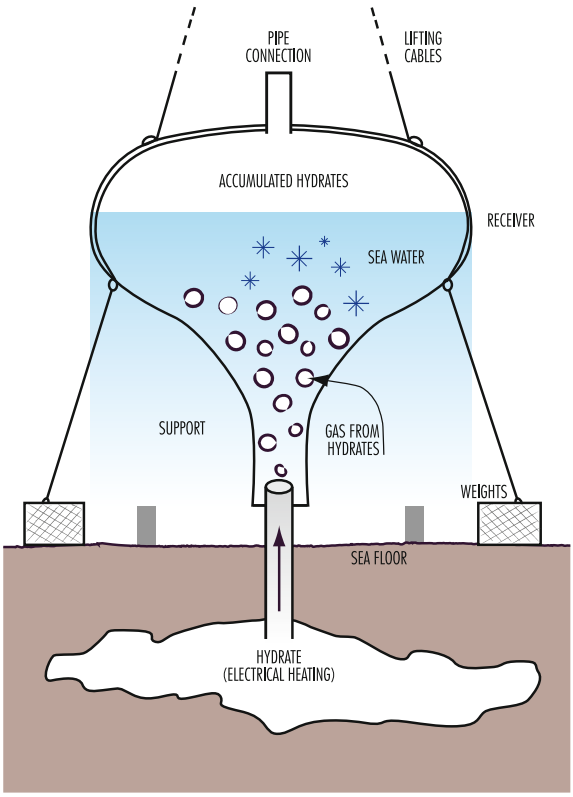

Fig. 8.15 Overhead receiver to capture gas and hydrate particles from a heated well [32]

for the gas, an initial pre-treatment of dehydration, sweetening, separating higher hydrocarbon [26] might need to be performed directly on the offshore production platform.

Gas transportation from the production site could be done in several ways (See Chap. 9). A pipeline would be the best option but will likely not be available in many of these sites. Other techniques exist or are being developed such as liquefying or compressing the natural gas or converting the gas using gas-to-liquid technologies. One possibility, which could be economical and practical, is to transport the gas in the form of hydrate. As will be discussed in more detail in Chap. 9, this technology is still being developed. In this case, the produced gas could be re-converted back to hydrate with little to no pre-treatment.

It appears that the most critical phase for offshore production of methane hydrate is found paradoxically in the transportation. However, the growing intensity of research in the recent years leaves hope that this matter might be resolved in the not so distant future.

8.9 Economics of Gas Production from Gas Hydrates

Up to now there are limited studies of the economics of gas production from onshore and offshore gas hydrates. The existing ones suggest that a number of factors interact to make production more expensive and costly than from traditional gas reservoirs.

Among these factors, the most critical ones include:

- single well production would likely result in low gas production rates;
- the gas must be compressed from the start;
- the well will be more complex because of sand and water production;
- inhibitors will need to be injected to prevent hydrate plugs in the well.

It should also be noted that many of the countries with the relatively *easiest* hydrates to produce, on land in the permafrost, also have significant other resources. For example, Russia has oil and vast reserves of conventional natural gas. Canada has oil and gas, as well as the tar sands. While exploring hydrates as a potential resource, these countries may not be in a hurry to push for construction of infrastructure in the near term to produce and transport gas from hydrates.

A preliminary economic evaluation on gas hydrate's commercial viability was published in 2009 [30]. Based on 2010 US$, they estimated that the viable price for producing gas from hydrate would be around $9.9/Mscf (thousand standard cubic feet). This price drops to around $6.2/Mscf if a free gas zone is present along with the hydrate. At the time this book was written, natural gas was being traded at around $4/Mscf so there is still a way to go before the economics are favorable. However, new discoveries and technological advancements could lower the cost of producing gas from the hydrates.

The most likely countries to first produce gas commercially from hydrates will be those with limited hydrocarbon reserves. This includes Japan, India, and possibly China. At this time, Japan leads the World in spending for hydrate-related research and plans to commercially produce hydrate by 2018.

References

1. Alexander G, Almarri M, Eren E et al (2004) An assessment of methane hydrate recovery and processing at hydrate ridge. College of Earth and Mineral Science (Pennstate), Report FSc 503, Team 1, November
2. Alp D, Parlaktuna M, Moridis GJ (2007) Gas production by depressurization from hypothetical class 1G and class 1W hydrate reservoirs. Energy Conv Manag 48(6):1864–1879
3. Boswell R, Collett TS (2006) The gas hydrates resource pyramid. Fire in the Ice, Spring, vol 6, issue 3
4. Boswell R, Shelander D, Lee M et al (2009) Occurance of gas hydrate in Oligocene Frio sand: Alaminos Canyon block 818: Northern Gulf of Mexico. Mar Petrol Geol 26(8):1499–1512

5. Collett TS, Ginsburg GD (1998) Gas hydrate in Messoyakha gas field of the west Siberian basin: a re-examination of geologic evidence. Int J Offshore Polar Eng 8(1):22–29
6. Collett TS (2003) Natural gas hydrates as a potential energy resource. In: Max MD (ed) Natural gas hydrates in oceanic and permafrost environments. Kluwer Academic Publishers, New York
7. Collett T, Johnson A, Knapp G, Boswell R (2009) Natural gas hydrates: energy resource potential and associated geological hazards. AAPG Memoir 89, Tulsa
8. Elliott GRB, Barraclough BR, van der Bourgh NE (1984) US patent 4.424.858, 10.01.1984
9. Kvenvolden KA (1993) Gas hydrate as a potential energy resource: a review of their methane content. In: Howell DG (ed) The future of energy gases. US geological survey professional paper 1570:555–561
10. Kuznetsov FA (2000) Gas hydrates in Siberia. In: Holder GD, Bishnoi PR (eds) Gas hydrates. Annals of the New York Academy Sciences, vol 912. pp 101–111
11. Makogon YF (1974) Hydrates of natural gases (in Russian). Nedra, Moscow
12. Makogon YF (1997) Hydrates of hydrocarbons. PennWell Books, Tulsa
13. Max MD, Johnson AH, Dillon WP (2006) Economical geology of natural gas hydrates. Springer, Dordrecht
14. Milkov AV (2004) Global estimates of hydrate-bound gas in marine sediments: how much is really out there? Earth-Sci Rev 66:183–197
15. Moridis GJ, Collett TS (2004) Gas production from class 1 hydrate accumulations. In: Taylor C, Qwan J (eds) Recent advances in the study of gas hydrates, sec I, vol 6. Springer, USA, pp 75–88
16. Moridis GJ, Reagan MT (2007a) Strategies for gas production from oceanic class 3 hydrate accumulations. In: Proceedings of offshore technical conference, Houston, 30 April–3 May, OTC-18865
17. Moridis GJ, Reagan MT (2007b) Gas production from oceanic class 2 hydrate accumulations. In: Proceedings of offshore technical conference, Houston, 30 April–3 May, OTC-18866
18. Moridis GJ, Sloan ED (2007) Gas production of disperse low-saturation hydrate accumulations in oceanic sediments. Energy Conv Manag 48:1834–1849
19. Mroz TM (2004) Mallik results presented in Chiba, Japan. Fire in the Ice, Winter, vol 4, issue 1
20. Naredi P, Narkiewicz M, Strohm T et al (2004) Optimal recovery of methane hydrates of the hydrate ridge, offshore Oregon. College of Earth and Mineral Science (Pennstate), Report FSc 503, Team 3, November
21. National Research Council (2010) Realizing the energy potential of methane hydrate for United States. National Academic Press, Washington, DC.
22. Ohta K, Ohtsuka Y, Matsukuma Y et al (2002) Basic study on recovery system of methane hydrate. In: Proceedings of international conference on gas hydrates, vol 4, Yokohama, 19–23 May, pp 206–209
23. Parkes RJ, Derek M, Armann H et al (2009) Technology for high-pressure sampling and analysis of deep sea sediments, associated gas hydrates, and deep-biosphere processes. In: Collett TS, Johnson A, Knapp G, Boswell R (eds) Natural gas hydrates: energy resource potential and associated geological hazards. AAPG Memoir 89, Tulsa
24. Pecher IA, Holbrook WS (2003) Seismic methods for detecting and quantifying marine gas hydrate/free gas reservoirs. In: Max MD (ed) Natural gas hydrates in oceanic and permafrost environments. Kluwer Academic Publishers, London
25. Riedel M (2008) Recent advancements in marine gas hydrate drilling. In: Proceedings of international conference on gas hydrates, vol 6, Vancouver, 6–10 July, Paper 7000
26. Rojey A, Jaffret C, Cornot-Grandolphe S (1997) Natural gas production processing and transport. Editions Technip, Paris
27. Sassen R, Losh SL, Cathles L III (2001) Massive vein-filling gas hydrate: relation to ongoing gas migration from the deep subsurface in the Gulf of Mexico. Mar Petrol Geol 18:551–560
28. Sawyer WC, Boyer CM, Frantz T, Yost AB (2000) Comparative assessment of natural gas hydrate production models. SPE/CERI gas technical symposium, Calgary, 3–5 April, 62513-MS

29. Tanaka S (2003) Introduction of research consortium for methane hydrate resources in Japan. Mallik International Symposium, Chiba, Japan, 8–10 December
30. Walsh MR, Hancock SH, Wilson SJ et al (2009) Preliminary report on the commercial viability of gas production from natural gas hydrates. Energy Econ 31:815–823
31. Yamamoto K, Dallimore S (2008) Aurora-Jogmec-NRCan Mallik 2006–2008 gas hydrate research project progress. Fire in the Ice, Summer, vol 7, issue 2
32. Zhang H-Q, Brill P, Sarica C (2008) A method of harvesting gas hydrates from marine sediments. In: Proceedings of international conference on gas hydrates, vol 6, Vancouver, 6–10 July, Paper 5587

Chapter 9
Industrial Applications

9.1 Introduction

For many decades in the energy industry, hydrates have been considered primarily as a problem with the potential for serious economic consequences in lost production due to pipeline blockages and even potentially harmful and fatal consequences to humans. Therefore, the generally followed paradigm has been hydrate avoidance with most studies focused on how to prevent hydrate formation and reduce possible harm. In contrast, rather than absolute avoidance, some recent research has been focused on considering the formation of hydrates in a controlled manner.

One of the most interesting aspects of this new research could lead to major changes in natural gas transportation with the possibility of gas transport by sea in solid hydrates, rather than via liquefied natural gas (LNG) carriers (or gas tankers). Other research for the beneficial utilization of hydrates industrially include: seawater desalination, use in refrigeration cycles, the production of concentrated (powder or dehydrated) food and heavy water, separation and recovery of toxic agents and pollutants (e.g., H_2S and chlorinated solvents), gas compression without mechanical means, and separation and disposal of CO_2 from flue gas.

In the following sections, we will consider some of the more interesting and sophisticated applications utilizing hydrates, especially those for gas transportation, which are already in the development stages for industrial use.

9.2 Transportation of Methane

As discussed in the first chapter, among current energy sources, natural gas has the greatest potential for development in the present and immediate future. Even if one assumes a future based on hydrogen fuel, the role of natural gas will remain important as a raw material for the production of hydrogen itself.

C. Giavarini and K. Hester, *Gas Hydrates*, Green Energy and Technology,
DOI: 10.1007/978-0-85729-956-7_9, © Springer-Verlag London Limited 2011

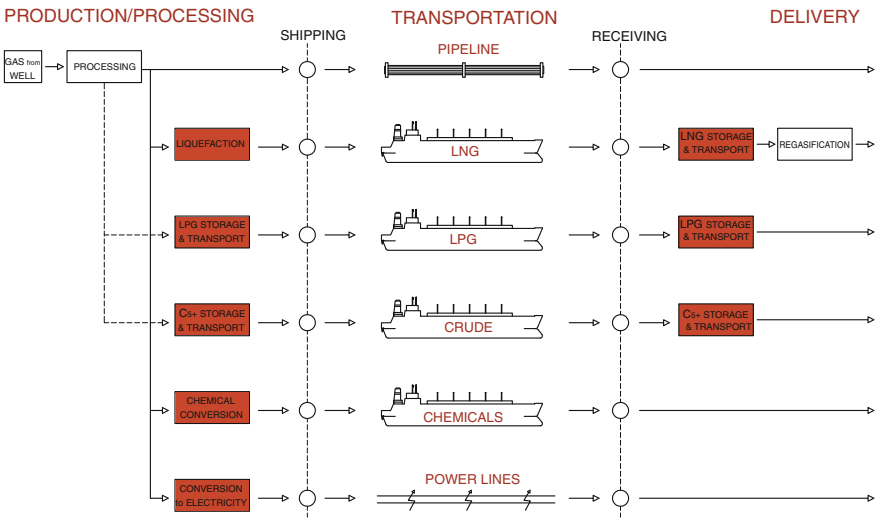

Fig. 9.1 The systems used to transport natural gas [29]

The major problem limiting the spread of natural gas to more markets is that gas transportation is far more technically and economically challenging than liquid fuels. In fact, only a small fraction of gas produced (about 25%) is subject to international trade. Several approaches have been applied to make the transport and storage of natural gas more economic and practical. Of those, only two transport systems (via pipelines and LNG), have been widely applied. Figure 9.1 and Table 9.1 show the current gas transportation systems and their main features.

Compressing natural gas and transporting it through a pipeline is the most simple and widespread approach and is applied whenever possible. Today, it is possible to overcome some water crossings, laying the pipes on the seafloor to depths exceeding 2,000 m. About 75% of all natural gas is transported via pipeline. This approach requires the use of a fixed network of pipes that connect the areas of production to consumption, which results in high installation, operation, and maintenance costs. Subsea pipelines cost around twice the amount of those on land; this amount can become 4–5 times higher if the installation depth exceeds 500 m. Land and/or subsea pipelines over long distances are often limited by economic and well as geopolitical factors. In addition, accumulation of water, hydrates, sand, wax, and corrosion products can occur, significantly increasing operational and maintenance expenses.

Transportation of natural gas in liquefied form is very favorable from an energy density standpoint as liquidation causes over a 600x reduction in volume: one ton of LNG (2.2 m^3) is equivalent to 1,350 m^3 of gas at STP. However, the cost of natural gas liquefaction is high and requires specialized ships and gas carriers built from material capable of handling the low temperatures needed (−161°C).

Table 9.1 Characteristics of natural gas in the various forms it is transported

	Temperature (°C)	Pressure (bar)	Overall density (g/cm^3)	Density relative to CH_4 gas
Natural gas	25	1	0.00065	1
Compressed, Medium pressure	25	35	0.0234	36
Compressed, High pressure	25	200	0.15	230
LNG	−160	1	0.45	690
Absorbed on solids	25	35	0.13	200
Gas to liquid	25	1	0.82	1,260

Furthermore, the point of delivery must have a regasification plant, not particularly complex, but regarded with suspicion by local authorities.

It was calculated that for an annual flow of 10^9 m^3 of gas, a transportation distance of 4,000–6,000 m is needed for LNG to be economically preferred over an on-land pipeline [19]. This distance would be less if the pipeline was located subsea. Overall, both pipeline and LNG operations require significant investments and are only economically justified for large volumes of gas. Obviously, such systems are not applicable for small deposits in remote areas (stranded gas).

An alternative to liquidation is to compress the gas to pressures of 200 bar and transport it (still as a gas) in special coiled line. This technology is known as compressed natural gas (CNG). While a compression system is cheaper than the liquefaction/regasification process, over long distances, the cost to transport the same amount of energy by ship is significantly higher than LNG. This is due to vessel requirements to cope with such high pressures: a vessel used to transport 9 million m^3 of gas must have over 1,700 km of high-pressure coiled line, weighing nearly 50,000 tons [3]. Initiatives to build CNG carriers capable of transporting gas at higher pressures are still in progress, as it is thought that such systems can be beneficial for short distances and for smaller fields.

Another growing possibility is to transform the gas through chemical processes into more valuable liquid products, such as methanol or higher molecular weight hydrocarbons, which are easily transportable (by land or sea) as normal liquid fuels. This technology is often referred to as *gas to liquids* (GTL). Large GTL systems have arisen in Qatar, one of the richest countries in natural gas. Again, the cost of processing is one of the most important aspects. The GTL technology has the advantage of delivering an intermediate liquid stream easily used or processed into finished products.

In addition to the applications in practice above, there are various other proposals, most in the pilot stages. These include the adsorption of the gas on solid matrices [adsorbed natural gas, (ANG)] [23] or transformation to electricity through combustion [gas to wire, (GTW)] cable transport. These solutions thus far have not been widely applied, although they look promising in certain situations.

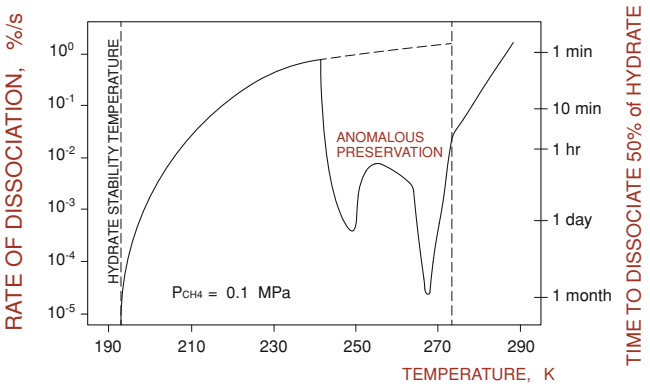

Fig. 9.2 The range of the anomolous *self-preservation* of methane hydrate, at atmospheric pressure, between −30°C and 0°C [32]

9.3 Transportation of Gas in the Form of Methane Hydrate

The idea of transporting natural gas in the form of hydrate is not new; hydrates are attractive due to their ability to concentrate gas. A cubic meter of hydrate may contain more than 160 m^3 of methane. In addition, while the gas in hydrates is flammable, it is not explosive giving it a significant safety advantages over CNG or LNG.

The use of hydrates for gas transportation has long remained a hypothesis, given the difficult technical (and economic) challenges in development of a process that must include the production and preservation of hydrates at high pressure and relatively low temperatures. However, in the 1990s, an anomaly was discovered, whereas under certain conditions hydrates may be relatively stable even at ambient pressure. This ignited much research in the field [11]. The classic work of Stern et al. [32] and subsequent works that followed [5, 31] better defined the range of hydrate *self preservation* (Fig. 9.2).

In practice, in the temperature range between approx. −30°C (243 K) and 0°C (273.15 K), methane hydrate shows the abnormal behavior of remaining relatively stable at temperatures 50–80°C above its equilibrium temperature (−80°C at 1 bar). It is interesting to note that the maximum preservation occurs within a few degrees below 0°C. One possible explanation for this phenomenon is that during depressurization a thin film of ice forms and temporarily blocks the gas molecules escape. Dissociation occurs but at a very slow rate. A recent study showed that self-preservation was directly related to the permeability of the ice film formed on the dissociating hydrate surface [4]. The work of Giavarini and Maccioni [5] showed that using a pressure slightly higher than atmospheric (2–3 bar) and temperatures from 3–5°C below zero, it can take over 40 days for complete hydrate dissociation. The use of mixed hydrates, e.g., the addition of tetrahydrofuran (THF), can further increase this hydrate preservation [6].

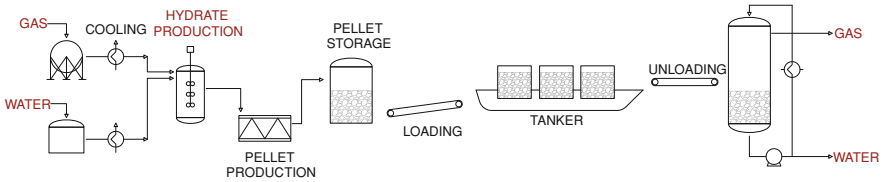

Fig. 9.3 The complete process of transporting natural gas in the form of gas hydrate as proposed by MEC [25, 36]

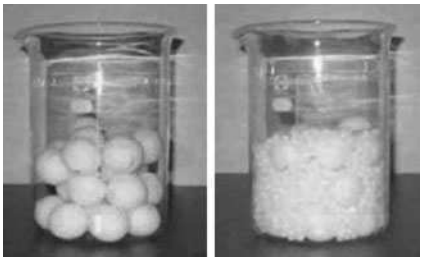

Fig. 9.4 The production of hydrate by Mitsui Eng and Shipbuilding in the form of pellets (diameters of a few centimeters) prepared for transport (Photo: Mitsui-Eng. and Shipbuilding)

Table 9.2 Differences between gas transportation as NGH and LNG

	NGH	LNG
Phase	Solid (pellets)	Liquid
One m^3 composed of:	160 m^3 gas + 0.8 m^3 water	600 m^3 gas
Temperature required	−20°C	−161°C
Specific gravity	0.85–0.95	0.42–0.47

The Norwegian J.S. Gudmundsson (NTNU) was the first to try to commercially exploit this discovery in collaboration with the Japanese Mitsui Engineering and Shipbuildings Co. (MES) [18, 34, 35]. Together with the Norwegian Aker Kvaerner, the whole chain was developed from production to final gasification (Fig. 9.3).

In fact, for smaller scale gas fields, the transportation of natural gas in the form of natural gas hydrate (NGH) is a new means that enables easier formation and milder transport conditions than LNG. MES has operated a 5,000 kg/day pilot plant. Using a relatively simple approach, the hydrate is produced at about 70 bar in the form of pellets (Fig. 9.4), with a controlled mechanical press. Hydrate powder is more sensitive than pellets to sticking and to temperature fluctuations. Storage capacity is increased by producing pillow shaped NGH pellets of different sizes [25]. Table 9.2 summarizes the differences between NGH and LNG transportation systems. Figure 9.5 shows the first MES pilot plant.

Dedicated NGH pellet carriers were also developed by MES. The ship's tanks (Fig. 9.6) are designed with insulation capable of maintaining the load at −20°C. The gas produced by partial hydrate dissociation during transport (approximately 0.05% per day) can be used as fuel for the propulsion of the vessel or can be

Fig. 9.5 The pilot plant for the production of hydrate from natural gas [36]

compressed and stored at the unloading port [25, 35]. Also, procedures for loading and unloading were developed as well as the design of NGH export and receiving terminals [26].

The Japanese have verified that the transportation costs in the form of gas hydrate are on average lower by about 20%, compared to LNG [18]. Two scenarios were considered: distances of 1,500 and 3,500 nautical miles with a volume of 1 million tons of gas a year. A distance of 3,500 nautical miles is equivalent to ~6,000 km, or a distance slightly less than that which connects the Persian Gulf to Japan [30]. The NGH chain is an appropriate means of transportation from Indonesia to Japan. Figure 9.7 summarizes the conclusions and extrapolations of various feasibility studies on the transport of natural gas.

In practice, a more flexible transportation method, based on gas hydrates, intermediate liquids (GTL), or CNG is preferable for short to medium distances and for smaller deposits. LNG remains preferable for long distances by sea and for large reserves. As already mentioned, many gas reserves yet to be developed are small to medium in size and the challenge still remains for efficient transport of stranded gas, located in places far from infrastructure and/or in small quantities [1].

Together with the Chugoku Electric Power Co, MES has also developed in 2008 a land transportation chain based on a 5 ton/day NGH plant. For the production of NGH, the cold sink created from LNG vaporization is utilized by the Yanai power station (one of the largest LNG importers in Japan). The produced NGH pellets are loaded on newly designed pellet containers and transported by

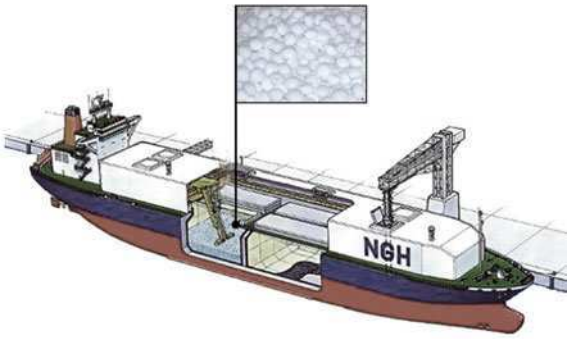

Fig. 9.6 The vessel for transportation of natural gas in the form of hydrate [35]

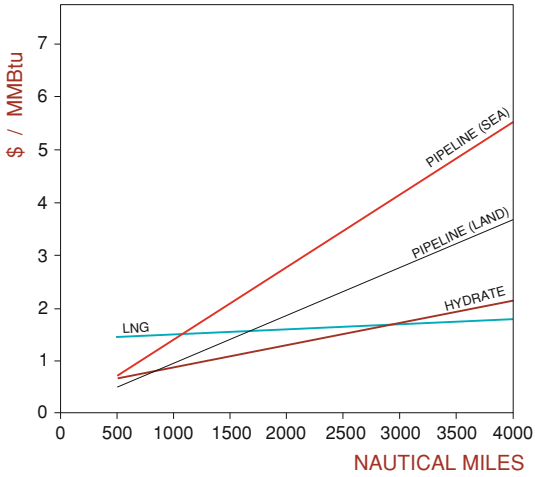

Fig. 9.7 Cost of natural gas transportation by sea for short and medium distances

trucks to the gas consumers; one of them is a gas engine power generation system and a housing complex about hundred kilometers from Yanai station. Figures 9.8 and 9.9 show, respectively, the block flow diagram of the NGH plant at Yanai station and the explanatory diagram of the land transportation chain [39].

9.4 Desalination Using Hydrates

Desalination of water through the formation of hydrates is based on the fact that salts are excluded during hydrate formation. In a saturated saline solution, formation of hydrate causes the crystallization of salt, producing two solid phases: hydrate and salt. These phases have different densities and can be readily separated by gravity.

In a saline solution, hydrate is formed in contact with a gas former (e.g., ethane, propane, CO_2). The hydrate crystals are separated, washed, and melted. Pure water and residual brine are then degassed. Depending on its stability conditions, the

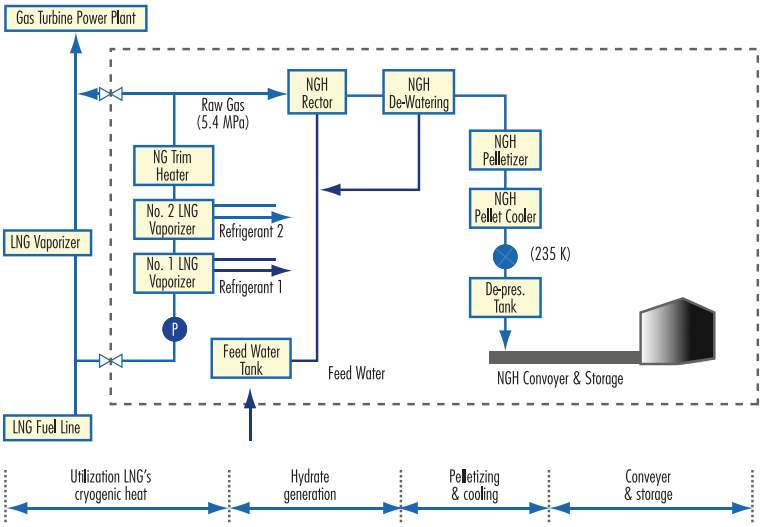

Fig. 9.8 Flow diagram of the NGH production process at Yanai station [39]

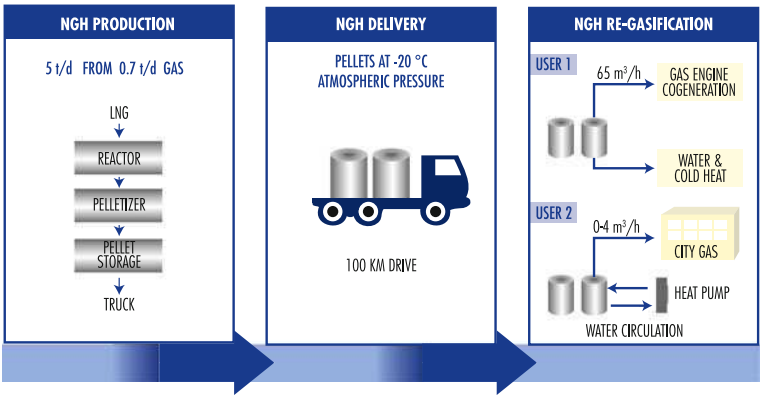

Fig. 9.9 Explanatory diagram of the hydrate production process and land transportation chain at the Yanai site [39]

choice of the gas former is adaptable to the desired mode of desalination. For these applications, propane and freon-free ozone are traditionally the favorite gas formers. A hydrate-based desalination/separation process can be considerably cheaper than other methods such as multistage distillation and membranes. A more complete presentation on desalination with hydrates is given by Makogon [24].

On the same principle described above, it is also possible to produce anhydrous powders and concentrates from fresh fruits and vegetables.

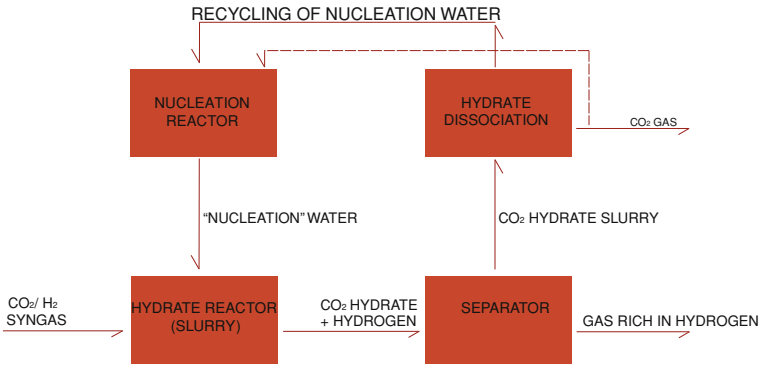

Fig. 9.10 Schematic of the SIMTECHE process for separating CO_2 produced by the IGCC process [2]

9.5 Sour Gas Separation

Hydrogen sulfide (H_2S) and carbon dioxide (CO_2) are often referred to as acid or sour gases for their ability to moderately acidify aqueous solutions. They are present in most of the oil and natural gas produced and must be handled and processed. CO_2 is also present in the flue gas from burning fossil fuels.

Traditional methods for acid gas separation, as mentioned above, are processes based on absorption with liquid solutions (e.g., amines or other solvents), adsorption on solids, and the use of membranes.

H_2S and CO_2, however, can also easily form hydrates and this property can be exploited to separate from gas mixtures [8, 16, 27]. Processes have been proposed for the separation of CO_2 from combustion fumes [17] and gas (mainly CO and H_2) from the Integrated Gasification Combined Cycle process (IGCC) [2].

IGCC is a process that converts low value fuels such as coal, petroleum coke, and residues into high value, environmental friendly gaseous fuels, also called *syngas*. Syngas, mostly composed by hydrogen and carbon monoxide, can be converted by a shift reaction into a mixture of H_2 and CO_2.

Figure 9.10 shows the block diagram of the SIMTECHE process. Syngas, after complete oxidation of carbon monoxide to CO_2, is sent to the hydrate formation reactor at about 70 bar using liquid ammonia as a refrigerant. Hydrogen does not form hydrates (except under much higher pressure conditions) and is readily separated. Therefore, the CO_2 can be sent for *disposal* as a hydrate or returned to its gaseous state by allowing the hydrate to dissociate.

Kumar et al. [21] proposed an integrated process for CO_2 separation from IGCC plants (Fig. 9.11). The fuel gas mixture is mixed with propane (2.5%) and then subjected to gas hydrate crystallization. The role of propane is to reduce the hydrate formation pressure from 7.5 to 3.8 MPa at 273.7 K. A membrane separation unit would then be used to recover pure hydrogen from the CO_2-lean stream. Two hydrate formation and decomposition stages, together with the membrane

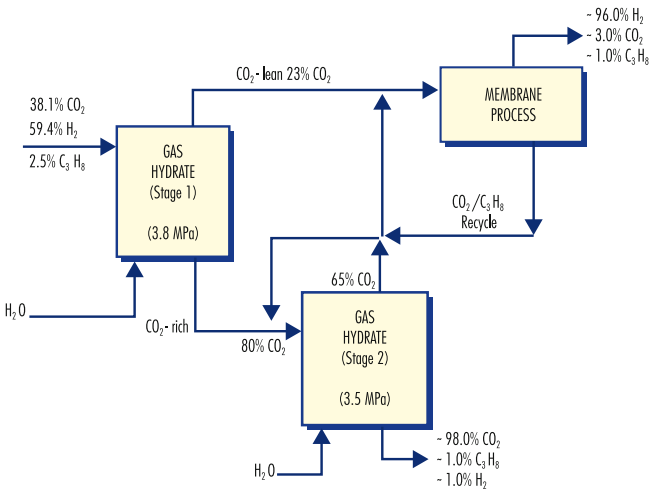

Fig. 9.11 Block flow diagram of a hybrid hydrate membrane process for carbon dioxide recovery from fuel gas in the presence of propane [21]

step, enable the recovery of two streams: one containing 98% pure CO_2 and the other containing 96% pure H_2.

The application of a process based on hydrate formation for the separation of carbon dioxide from the power plants flue gases could be especially interesting when associated to an oxy-coal process [9]. In oxy-coal processes, coal is burned with oxygen instead of with air. The resulting flue gases, after condensation of the water vapor, are almost entirely composed of carbon dioxide. In 2010, the US Department of Energy started a based on oxy-combustion project at a large coal-burning power plant. The high CO_2 concentration greatly facilitates its capture and transport to the storage site. In this case, only a small increase in the pressure could produce a concentrated CO_2 hydrate. In fact, CO_2 acts as a co-former for the production of hydrates containing also nitrogen; therefore, the presence of high concentrations of N_2 could be disturbing to the process. Figure 9.12 shows a simplified scheme of an integrated process for coal combustion with oxygen (or with O_2-enriched air) and CO_2 sequestration through hydrate formation and disposal [9].

9.6 Carbon dioxide Sequestration and Disposal

The term *carbon sequestration*, mainly related to CO_2, refers to the removal of greenhouse gases from anthropogenic sources (e.g., power plant flue gas) and long-term storage without environment problems. Various techniques have been suggested for the removal of carbon dioxide from emission sources. The ones that

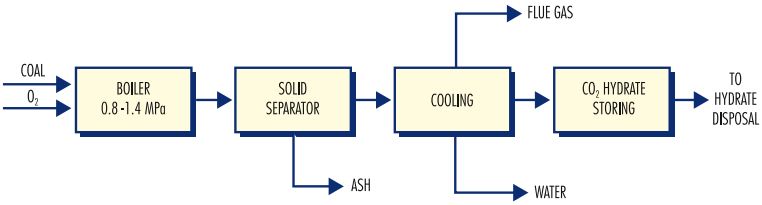

Fig. 9.12 Simplified scheme of an integrated process for coal combustion with oxygen and CO_2 sequestration through hydrate formation and disposal

have currently entered into commercial use include absorption of gases by solids or liquids, separation with membranes, and cryogenic fractionation. Several options have also been proposed for the disposal of CO_2 following separation. These include storage on the ocean floor and in suitable geological basins [12, 37]. Another intriguing possibility is to use the formation of CO_2 hydrates for its separation and/or for storage.

CO_2 hydrates in contact with sea water are stable in the ocean when the pressure and temperature are within the hydrate formation region ($P > 45$ bar, $T < 10°C$). However, it must be kept in mind that even under P, T conditions for hydrate stability, hydrate can only form if the surrounding sea water is saturated with CO_2. Otherwise, the CO_2 dissolves forming carbonic acid leading to increased acidity of the water. For this reason, seafloor storage of CO_2 is not likely a viable option.

The sequestration capacity under the ocean floor can also be increased by the buffering effect of marine sediments, i.e., by their ability to react with CO_2 [13]. Certain types of rocks in natural cavities (e.g., natural basins of wollastonite are already being used) may interact with CO_2 to give calcium carbonates and silicates, provided an appropriate amount of reaction time is given [40]. The storage of CO_2 in gas hydrates in the subsea sediments and geological reservoirs could help exploit this opportunity. However, a number of scientists think that geological and oceanic sequestration technologies are only a temporary response to the problem of CO_2 capture and sequestration.

More than pressure, which is very important for methane hydrate preservation, temperature affects the preservation of CO_2 hydrate. However, CO_2 hydrate may be stored for a relatively long time under less stringent conditions than methane hydrate (i.e., $-3°C$ and almost atmospheric pressure). The dissociation of methane hydrate requires less energy than CO_2 hydrate and therefore methane hydrates are less stable [6, 7].

A method of CO_2 sequestration from combustion flue gases that does not require a gas separation process has been proposed by Komai et al. [20]. The results of their study suggest that it would be feasible to use CO_2–N_2 mixtures for vast amount of storage capacity in sediments. The fuel gas is introduced into the reservoir to capture CO_2 and to form gas hydrates, which selectively concentrate CO_2 over N_2; therefore, the nitrogen separation occurs in situ (Fig. 9.13). Carbon

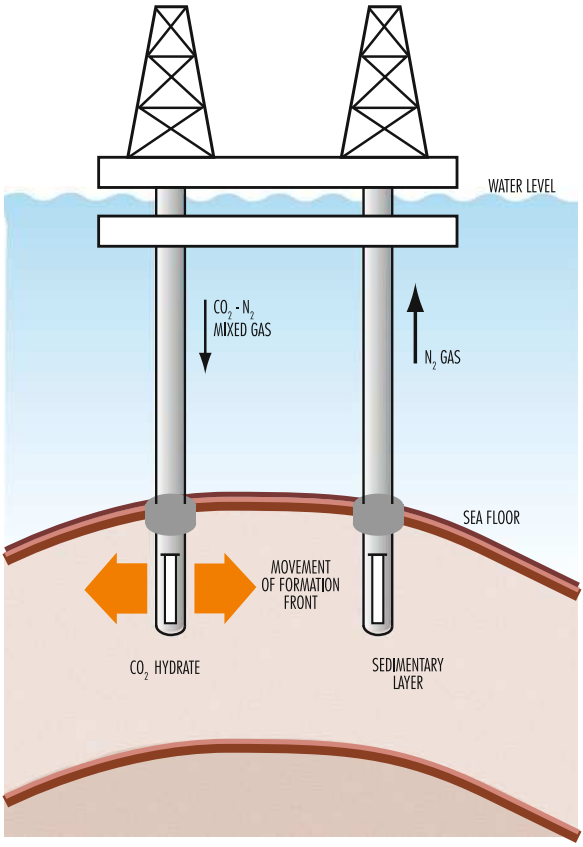

Fig. 9.13 Direct CO_2 sequestration from flue gas mixtures containing nitrogen [20]

dioxide is trapped in sediments as solid hydrate, as nitrogen migrates through the porous media into production wells.

If formed in deep sediments, similar to deep natural methane hydrate deposits, there is a high likelihood that successful long-term sequestration could be achieved by forming CO_2 hydrates. One technology to accomplish this is to directly exchange CO_2 for the methane in natural hydrate reservoirs. Thermodynamically, it has long been known that CO_2 is more stable than methane in the hydrate phase. However, little was known about if CO_2 would replace methane in an existing hydrate and how fast this exchange would occur. In laboratory studies, methane hydrate was exposed to CO_2 (either in gas or liquid form). It was observed that the exchange rate was rapid on surface of the hydrate and over 70% of the methane in the hydrate could be replaced with CO_2 [22, 28]. Figure 9.14 shows a conceptual drawing of the methane being released to the gas phase as CO_2 replaces it in the hydrate phase [28].

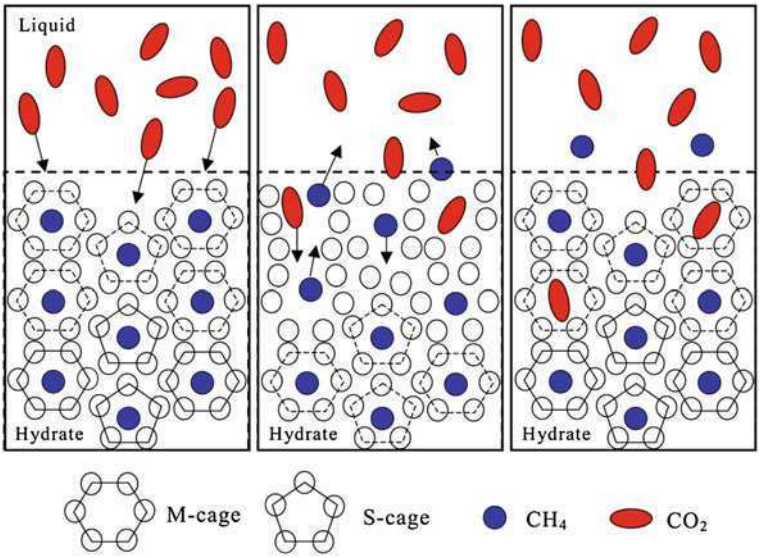

Fig. 9.14 Conceptual drawing of the CO_2 exchange process with methane hydrate [27, 28]

To test in a more realistic situation similar to a natural hydrate reservoir, methane hydrate was formed in a sandstone core inside a Magnetic Resonance Imager (MRI) [10, 14, 15, 33]. The MRI can detect methane gas and liquid water but is insensitive to the solid hydrate, making it basically *invisible*. As shown in Fig. 9.15a, water is distributed throughout the sandstone core. As hydrate forms, the water signal disappears and only the methane gas in the middle spacer is visible to the MRI (Fig. 9.15b). When CO_2 (also invisible to MRI, Fig. 9.15c) is injected into the middle spacer, there is initially no signal detected in the core as it contains only methane hydrate and liquid CO_2. Though over time, as shown in Fig. 9.15d, methane gas diffuses into the middle spacer clearly indicating that CO_2 is exchanging with methane in the hydrate. One of the most interesting results from these experiments (also shown in Fig. 9.15d) is that no free water phase was detected during the exchange process. From Fig. 9.14, one might expect the hydrate undergoes a solid–liquid-solid transition during the exchange process. However, from the MRI evidence, the methane hydrate is not dissociating to liquid water and then forming CO_2 hydrate. The water remains in a solid-like form during the exchange process. At the same time, the process is effective at recovering the methane in the hydrate with the ability to recover over 70% of the methane originally trapped in the hydrate.

This proposed technology seems promising for simultaneous CO_2 sequestration as well as energy production from the natural hydrates. ConocoPhillips, an US energy Company, and the US Department of Energy are planning on conducting a field trial to determine the feasibility of the CO_2 exchange technology in an actual hydrate reservoir. Drilling of the well for this field trial is planned for the winter of

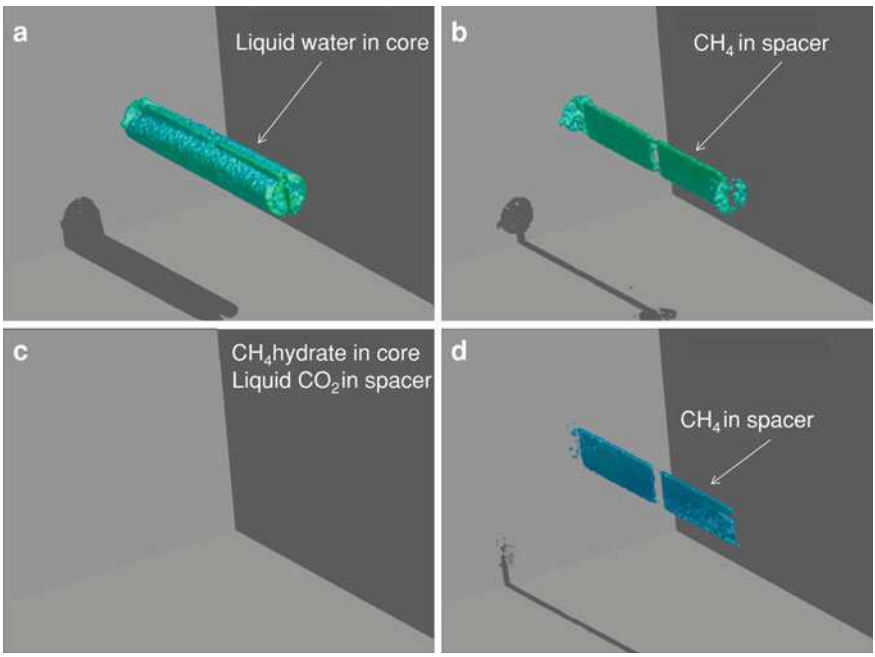

Fig. 9.15 MRI images of a sandstone core with a middle spacer. **a** The core is saturated with water, with methane gas in the spacer. **b** Following methane hydrate formation, only methane gas in the spacer is detected. **c** Following liquid CO_2 into the spacer, no signal is detected by the MRI. **d** CH_4 gas is detected filling the spacer and the CO_2 exchanges with methane in the hydrate (Adapted from Housebo et al. [15])

2011 with the CO_2 injection test occurring in 2012 in the Prudhoe Bay on the North Slope of Alaska.

9.7 Other Processes

A technique for separating hydrogen from synthetic ammonia plant tail gas mixtures through hydrate formation/dissociation has been proposed by Wang et al. [38]. Ammonia plant tail gas is normally composed by hydrogen, methane, nitrogen, and argon; the recovery of hydrogen through the use of membrane or other conventional processes is quite costly. Hydrates are utilized because hydrogen has very little affinity for the hydrate phase and will remain largely in the gas phase. The partitioning coefficient of H_2 between gas and hydrate phases is improved by adding tetrahydrofuran. The use of an anti-agglomerant is necessary to disperse the hydrate particles in the condensate phase and to create a water-in-oil emulsion system. Hydrogen content can be enriched up to about 80 mol%,

while reducing the methane concentration to less than 2 mol%. The process temperature is slightly above 273 K and the pressure below 10 MPa.

In recent years, a number of attempts have been made to develop a novel hydrate-based refrigeration system. The phase equilibrium conditions in the system of cyclopentane and water plus difluoromethane seem to satisfy the required conditions for a hydrate-based refrigeration system for residential air conditioning [36].

References

1. Chang S (2001) Comparing exploitation and transportation technologies for monetization of offshore stranded gas. SPE Asia Pacific oil and gas conference, Jakarta, 17–19 April, 68680
2. Currier RP, Young JS, Anderson GK et al (2003) High-pressure carbon dioxide separation from shifted synthesis gas. In: Proceedings of 225th ACS national meeting, New Orleans, 23–27 March
3. Economides MJ, Mokhatab S (2007) Compressed natural gas. Another solution to monetize stranded gas. Energy Tribune, Posted on October 18
4. Falenty A, Kuhs WF (2009) "Self-Preservation" of CO_2 gas hydrates-surface microstructure and ice perfection. J Phys Chem B 113:15975–15988
5. Giavarini C, Maccioni F (2004) Self-preservation at low pressure of methane hydrates with various gas contents. Ind Eng Chem Res 43:6616–6621
6. Giavarini C, Maccioni F, Politi M, Santarelli ML (2007) CO_2 hydrate: formation and dissociation compared to methane hydrate. Energy Fuel 21:3284–3291
7. Giavarini C, Maccioni F, Politi M, Santarelli ML (2008) Formation and dissociation of CO_2 and CO_2-THF hydrates compared to CH_4 and CH_4 THF hydrates. In: Proceedings of international conference on gas hydrates 6, Vancouver, 6–10 July, P-048
8. Giavarini C, Maccioni F (2010) Process for the purification-sweetening of natural gas by means of controlled dissociation of hydrates and use thereof separators. WO/2010/018609. Int Appl PTC/IT2009/000376
9. Giavarini C, Maccioni F, Santarelli ML (2010) CO_2 sequestration from coal fired power plants. Fuel 89(3):623–628
10. Graue A, Kvamme B, Baldwin B et al (2006) Magnetic resonance imaging of methane-carbon dioxide hydrate reactions in sandstone pores. SPE annual technical conference, San Antonio, 24–27 Sept, 102915-MS
11. Gudmundsson JS, Borremaug A (1996) Frozen hydrate for transport of natural gas. In: Proceedings of international conference on gas hydrates 2, Tolouse, 2–6 June
12. Herzog HJ (2001) What future for carbon capture and sequestration? Environ Sci Tech 35(7):148–153
13. House KZ, Schrag DP, Harvey CF, Lackner KS (2006) Permanent carbon dioxide storage in deep-sea sediments. Proc Natl Acad Sci U S A 103(33):12291–12295
14. Husebo J (2008) Monitoring depressurization and CO_2–CH_4 exchange production scenarios for natural gas hydrates. University of Bergen, Deptment of Physics, Ph.D. thesis
15. Housebo J, Graue A, Kvamme B et al (2008). In: Proceedings of international conference on gas hydrates 6, Vancouver, 6–10 July, Paper 5636
16. Kamata Y, Ebinoma T, Oyama H et al (2005) Hydrogen sulfide separation using TBAB hydrate. In: Proceedings of international conference on gas hydrates 5, Trondheim, 13–16 June, Paper 4033
17. Kang SP, Lee H (2000) Recovery of CO_2 from flue gas using gas hydrate: thermodynamic verification through phase equilibrium measurements. Environ Sci Tech 34(20):4397–4400

18. Kanda H, Uchida K, Nakamura K, Suzuki T (2005) Economics and energy requirements on natural gas ocean transport in form of natural gas hydrate pellets. In: Proceedings of international conference on gas hydrates 5, Trondheim, 13–16 June, Paper 4023
19. Karnic J-L, Valais M (1990) Natural gas. In: Masseron J (ed) Petroleum economics. Technip, Paris, pp 433–482
20. Komai T, Sakamoto Y, Kawamura T et al (2008) Formation kinetics of CO_2 gas hydrates in sandy sediment and change in permeability during crystal grouth. Carbon capture and storage system using gas hydrates. In: Proceedings of international conference on gas hydrates 6, Vancouver, 6–10 July, Paper 5019
21. Kumar R, Englezos P, Ripmeester J (2008) The gas hydrate process for separation of CO_2 from fuel gas mixture: macro and molecular levels studies. In: Proceedings of international conference on gas hydrates 6, Vancouver, 6–10 July, Paper 5451
22. Lee H, Yongwon S, Sea Y-T et al (2003) Recovering methane from solid methane hydrate with carbon dioxide. Angewandte Chemie. doi:10.1002/anie.200351489
23. Lozano-Castelló D, Alcañiz-Monge J, de la Casa-Lillo MA et al (2002) Advances in the study of methane storage in porous carbonaceous materials. Fuel 81(14):1777–1803
24. Makogon YF (1997) Hydrates of hydrocarbons. PennWell Books, Tulsa
25. Nakata T, Hirai K, Takaoki T (2008) Study of natural gas hydrate carriers. In: Proceedings of international conference on gas hydrates 6, Vancouver, 6–10 July, Paper 5539
26. Nogami T, Oya N, Ishida H, Matsumoto H (2008) Development of natural gas ocean transportation chain by means of natural gas hydrate. In: Proceedings of international conference on gas hydrates 6, Vancouver, 6–10 July, Paper 5547
27. Ota M, Seko M, Endou H (2005) Gas separation process of carbon dioxide from mixed gases by hydrate production. In: Proceedings of international conference on gas hydrates 5, Trondheim, 13–16 June, Paper 4032
28. Ota M, Morohashi K, Abe J et al (2005) Replacement of CH_4 in the hydrate by use of liquid CO_2. Energy Conserv Manag 46(11–12):1680–1691
29. Rojey A, Jaffret C (1997) Natural gas: production, processing, transport. Technip, Paris
30. Sanden K, Rushfeld P, Graff OF et al (2005) Long distance transport of natural gas hydrate to Japan. In: Proceedings of international conference on gas hydrates 5, Trondheim, 13–16 June, Paper 4035
31. Shirota H, Aya I, Namie S et al (2002) Measurement of methane hydrate dissociation for application to natural gas storage and transportation. In: Proceedings of international conference on gas hydrates 4, Yokohama, 19–23 May, pp 972–977
32. Stern L, Circone S, Kirby S, Durham W (2001) Anomalous preservation of pure methane hydrate at 1 atm. J Phys Chem B 105:1756–1762
33. Stevens JC, Howard JJ, Baldwin BA et al (2008) Experimental hydrate formation and gas production scenarios based on CO_2 sequestration. In: Proceedings of international conference on gas hydrates 6, Vancouver, 6–10 July, Paper 5635
34. Takahashi M, Iwasawi T, Katoh Y, Uchida K (2005) Experimental research on mixed gas hydrate pellet production and dissociation. In: Proceedings of international conference on gas hydrates 6, Trondheim, 13–16 June, Paper 4027
35. Takaoki T, Hirai K, Kamei M, Kanda K (2005) Study of natural gas hydrate carriers. In: Proceedings of international conference on gas hydrates 6, Trondheim, 13–16 June, Paper 4021
36. Takeuki F, Ohmura R, Yasuoka K (2009) Statistical-thermodinamics modelling of clathrate hydrate-forming systems suitable as working media of a hydrate-based refrigeration system. Int J Thermophys 30(6):1838–1852
37. Teng H, Yamasaki A, Chun MK, Lee M (1997) Why does CO_2 hydrate disposed of in the ocean in the hydrate-formation region dissolve in seawater? Energy 22(12):1111–1117
38. Wang XL, Chen GJ, Tang XL et al (2008) Recovery of H_2 from synthetic ammonia plant tail gas. In: Proceedings of international conference on gas hydrates 6, Vancouver, 6–10 July, Paper 5361

39. Watanabe S, Takahashi S, Mitzubayashi H, Murata S, Murakami H (2008) A demonstration project of NGH land transportation system. In: Proceedings of international conference on gas hydrates 6, Vancouver, 6–10 July, Paper 5442
40. Wu JCS, Sheen JD, Chen SY, Fan YC (2001) Feasibility of CO_2 fixation via artificial rock weathering. Ind Eng Chem Res 40(18):3902–3905

Chapter 10
Environmental Issues with Gas Hydrates

10.1 Why are Hydrates of Environmental Concern?

We have seen in the previous chapters that gas hydrates seem to be an extensive resource of methane, much greater than conventional accumulations of natural gas. Hydrates form in Arctic permafrost, where the near-surface temperature is low. These hydrates can form a seal preventing gas from seeping toward the surface. Methane hydrates are also stable in deep ocean sediments at water depths greater than about 500 m. Most accumulations are expected to be in submarine sediments along continental margins.

Safety and sea floor stability are important issues related to gas hydrates. Sea floor stability is related to the susceptibility of the sea floor to collapse and slide during gas hydrate dissociation. The safety issues, which already affect current conventional oil and gas production, are of concern when considering future production from hydrate reservoirs, both onshore and offshore.

Energy companies have reported various drilling and production problems due to the presence of gas hydrates, such as gas releases during drilling and the collapse of well casings. Gas leakage to the surface in marine environments can cause local sea floor subsidence and loss of support for drilling platforms. These kinds of problems are frequently caused by the dissociation of gas hydrates due to heating from hot hydrocarbons as they are produced from great depths.

These processes of gas leakage and subsidence have the potential to release large volumes of methane into the atmosphere. Methane is a greenhouse gas many times more effective than carbon dioxide at accelerating global warming. Most methane is oxidized to carbon dioxide in the water column. However, if the release is shallow or large enough, the amount of methane could overwhelm the natural oxidation processes causing methane to reach the atmosphere.

Much of the information on gas hydrate-related safety is currently proprietary. However, many of the safety issues associated with the production of methane from gas hydrates appear to be similar to those encountered during production from a conventional gas field.

C. Giavarini and K. Hester, *Gas Hydrates*, Green Energy and Technology,
DOI: 10.1007/978-0-85729-956-7_10,

10.2 Gas Hydrates and Climate Change

10.2.1 Methane in the Atmosphere

Methane is present in the atmosphere in very small quantities (best estimates are around 0.00017% based on volume). Methane is produced naturally by fermentation of organic matter in the absence of oxygen (anaerobic microbial degradation), volcanoes, geothermal fluids, rudimentary animals such as cows, and exploitation of coal and oil fields.

Methane has an atmospheric residence time of more than 8 years. Since the methane molecule (CH_4) is very compact and stable it undergoes little change as it moves up through the atmosphere. It is only broken down through ultraviolet radiation when it reaches the troposphere.

Methane is a powerful greenhouse gas (10–20 times more effective than carbon dioxide). Despite its small concentration in the atmosphere, it seems to have a measurable effect on global warming. Similar to carbon dioxide, methane concentration has significantly increased since 1800 (Fig. 10.1). The composition of the atmosphere in recent geological time was measured through scientific drilling of the Greenland (GRIP Project, [2]) and Antarctica [10] ice sheets [6]. Air bubbles trapped in the ice allowed scientists to know atmospheric conditions based on when the air was buried. As shown in Fig. 10.2, methane was more abundant during periods of warmer climate. Global warming since the last deglaciation, from 20,000 to 10,000 years Before Present (BP) has been accompanied by a corresponding increase in atmospheric methane. This trend of increasing methane has continued in the post-ice age through the Holocene (10,000 years BP) and the advent of our modern industrialized civilization. Investigations of the ice record have resulted in a clear correlation between higher temperature and increasing atmospheric methane during the recent evolution of the Earth.

10.2.2 The Clathrate Gun Hypothesis

The Clathrate Gun Hypothesis, formulated by Kennett et al. [15, 16], was developed following a series of observations of microfossil shell compositions (foraminifera) preserved in marine sediments. Foraminifera are small single-celled organisms that live both on the seafloor (benthic foraminifera) and in the water column (planktonic foraminifera). The shells of these organisms are made up of calcium carbonate ($CaCO_3$) which formed their shells using calcium and carbonate ions available in seawater. Studies into the stable carbon isotopes present in these shells were of particular interest.

The carbon atoms present in carbonate ions were derived from organic matter that was metabolized by communities of bacteria producing carbon dioxide. The carbon dioxide dissolves in the seawater, producing carbonate ions. The two main

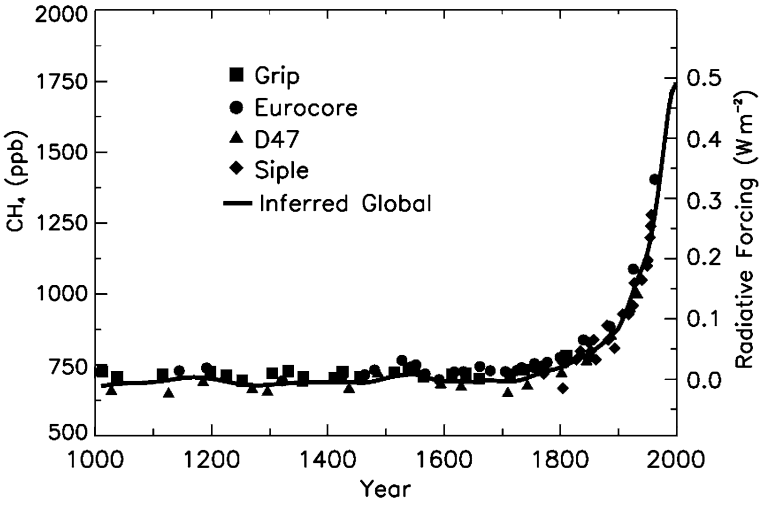

Fig. 10.1 Increasing atmospheric methane concentrations over the last 1,000 years [12]

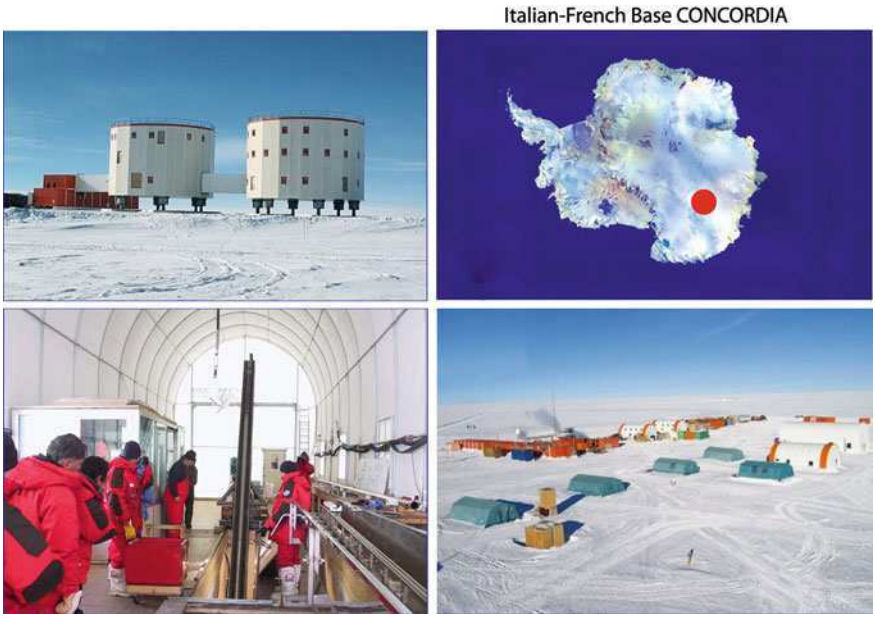

Fig. 10.2 Drilling rig at the Italian-French Concordia Base in Antarctica. The base is jointly operated by the French Polar Institute Paul-Emile Victor (IPEV) and the Italian National Antarctic Research Program (PNRA). The EPICA project is funded through the Research Networking Programs of the European Science Foundation [6]

carbon isotopes observed from this process are ^{12}C (98.9%) and ^{13}C (1.1%). Variations in the $^{12}C/^{13}C$ ratio are used as indicators for changes in the nature of the organic matter over geological time. In practice, the shells of foraminifera living near methane seeps on the seafloor have an anomalous carbon isotope ratio, with an enrichment in ^{12}C [1]. This isotopic fractionation is caused by the actions of the bacterial communities which preferentially metabolize the methane over other forms of organic material. Methane is lighter (or has higher concentrations of ^{12}C) than the other organic material and results in $CaCO_3$ with a higher $^{12}C/^{13}C$ ratio.

Short intervals of time over the last 60,000 years were identified to have foraminifera greatly enriched in ^{12}C. According to some authors [15, 16], these enrichments can only be explained by a massive release of methane from the seafloor. In addition, these intervals appear to coincide with periods of global warming measured in the ice record [4, 7].

Following this hypothesis, the episodic atmospheric methane emissions that contributed to large temperature increases during the late Quaternary period were attributed to instability of the marine methane hydrate reservoirs. The model involves punctuated releases of methane from hydrate reservoirs and, therefore, was named *Clathrate Gun Hypothesis*.

The major elements of the model are illustrated in Fig. 10.3. The changes in upper intermediate waters intersecting the continental slopes caused temperature changes of sufficient magnitude to partially destabilize the methane hydrate reservoirs. The released methane provided the amplification of rapid warming at glacial terminations. The action of the methane was reinforced by other greenhouse gases, including water vapor. These changes were able to shift the climate system into an interglacial state. According to this model, late Quaternary instability of methane hydrates occurred as well during times of sea-level stability, caused by frequent upper intermediate water temperature oscillations on wide areas of the upper continental margins, in the zones of hydrate instability.

These temperature oscillations led to successive intervals of hydrate stability and instability. Consequently, the methane hydrate reservoirs (clathrate guns) were periodically loaded (recharged) during cold intervals when cold waters were in contact with continental slopes.

The instability of the hydrate reservoirs caused catastrophic methane releases. This release of gas in turn resulted in sediment disruption. The Clathrate Gun Hypothesis predicts extensive instability of upper continental slopes during rapid atmospheric temperature increases. Such instability is reflected in developments of debris flows, slumps, and other mass sediment transport phenomena as represented by turbidite and nepheloid layer deposits found in the oceans.

The Clathrate Gun Hypothesis proposes a connection between methane hydrates and global climate change during the last 800,000 years of the Quaternary. The cycles of methane release into the atmosphere from hydrates below the seafloor occurred on $\sim$100,000 year intervals. However, there is evidence of further short duration releases (around 1,000 years). These relatively *short* episodes on a geological timescale show that the Earth's climate can drastically

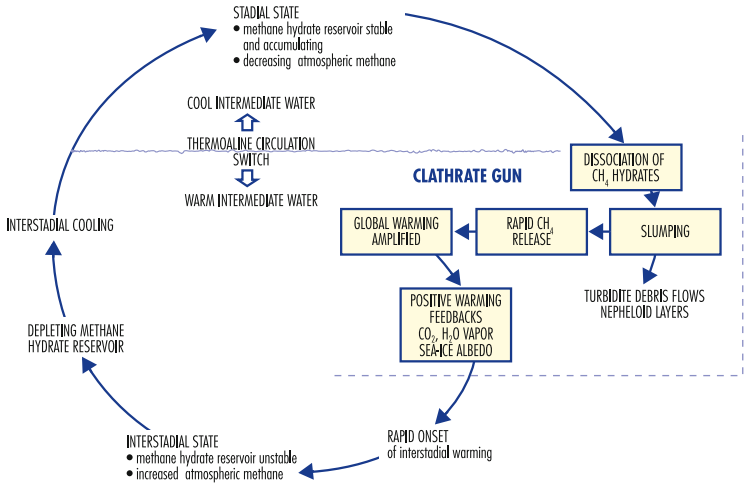

Fig. 10.3 Simplified diagram illustrating the clathrate gun hypothesis (Kennett et al. [16]. Changes in atmospheric methane concentration result from changes in the stability of the methane hydrate reservoir. Oscillations occur between stadial (glacial) and interstadial (interglacial) states

change naturally (i.e., without action due to man). Some argue that massive methane releases from the seafloor would have also occurred in other periods of global warming such as during the early Eocene epoch (about 55 million years ago, [9]), the middle of the Cretaceous period (about 120 million years ago, [13]), in the Jurassic (about 190 million years ago, [11]), and the transition between the Permian and Triassic periods (about 250 million years ago, [28]). Other studies are underway to clarify the relationship between hydrates in the permafrost and climate change [29].

While the Clathrate Gun Hypothesis offers an explanation for climate change due to hydrate destabilization, others have refuted whether hydrates were responsible for late Quaternary events. The hydrogen to deuterium (^{2}H) isotopic ratios (H/D) from the ice record suggests hydrates were stable during the late Quaternary [27]. Hydrates have a distinct H/D ratio and a massive dissociation event should have caused the H/D ratio to increase in the atmosphere. However, this was not observed. Another study investigated the ice record during the Younger Dryas-Preboreal transition around 10,000 years BP [25]. Concentrations of ^{13}C were found to be inconsistent with marine gas hydrate dissociation. The increase in methane was likely attributed to increased methane production from the wetlands.

10.3 Destabilization of Submarine Slopes

10.3.1 Hydrates as a Possible Cause of Submarine Landslides

The idea that hydrate dissociation could trigger potentially catastrophic submarine landslides has aroused the concern of academics, companies involved in offshore operations such as pipeline and cable laying, and public safety officials.

Underwater landslides can be not only damaging to seafloor infrastructure but also to coastal areas. The landslide could extent from the submarine environment to the exposed coastal zones or cause deadly tsunamis. Historically, submarine landslides are responsible for about 20% of know tsunamis. Important examples of recent landslides include the Grand Banks (Canada) in 1929, the airport of Nice (France) in 1979, and the Sciara del Fuoco at Stromboli (Italy) in 2002. These events caused great material damage and some casualties. More tragically in 1998, a landslide-triggered tsunami killed over 2,000 people in Papua New Guinea.

The mechanism by which hydrate dissociation could cause a submarine landslide is shown in Fig. 10.4. In most areas, hydrates are found deep in the sediments and increases in ocean bottom water temperatures do not cause hydrate dissociation because the pressures and temperatures make the hydrate very stable. The situation is different on parts of the continental slope and arctic regions where hydrates are close to the seafloor and the temperatures are closer to the hydrate stability temperature. Small water temperature increases will quickly be transmitted to the hydrate causing dissociation. Studies have shown changes of as little as 1°C for shallow hydrate deposits can result in a large methane release [23, 24]. The effect of the sudden and rapid expansion of gas in the sediment pore space is an increase in pore pressure over lithostatic conditions. As the pore pressure reaches the lithostatic load pressure, the sediment loses its mechanical strength and flows like a fluid. When this occurs on a flat area of the seafloor, several meter deep depressions (called *pockmarks*) can form. This could be a serious problem if an offshore platform was resting on one of these areas and the loss of mechanical stability of the seafloor sediment could threaten the platform. If this kind of sediment destabilization event occurs at the bottom of a sloping seafloor, a submarine landslide could occur.

The hypothesis that climate change and warming of seawater triggers hydrate dissociation and subsequent submarine landslides has been strengthened by a group of British researchers [18]. From the submarine landslides analyzed in the North Atlantic sector, it was found that over 70% by volume took place during two periods of global warming in the last deglaciation, between 8,000 and 15,000 years ago. The two periods coincide with times of increased atmospheric methane and agree with the ideas in the Clathrate Gun Hypothesis for glacial-interglacial transitions.

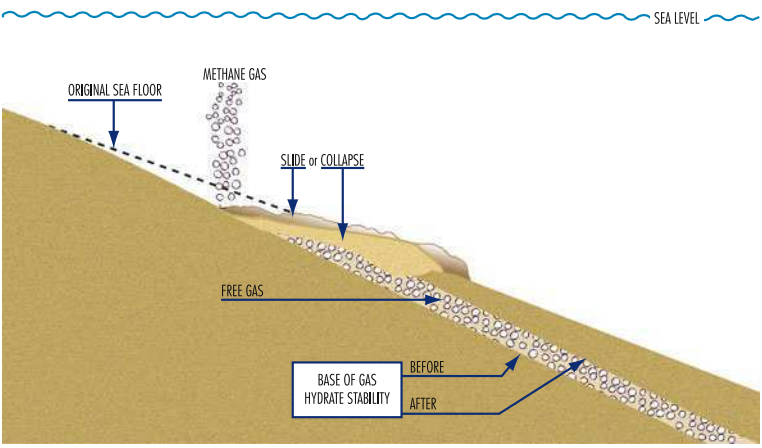

Fig. 10.4 Schematic of how a submarine landslide could be triggered due to hydrate dissociation caused by climate change

10.3.2 The Storegga Slide

The most important opportunity to test the relationship between marine hydrate dissociation and submarine landslides came from a study sponsored by a consortium of oil companies led by Norsk Hydro. This large research project was a collaboration between oil companies, universities, and research institutes to study the catastrophic geological event known as the Storegga Slide, which occurred on Norway's continental shelf over 8,000 years ago. This submarine landslide, almost 300 km in length, caused a slope collapse and moved thousands of cubic kilometers of mud and rock from the slope to the abyssal plain [26] (Fig. 10.5). The landslide generated an avalanche of mud that reached the continental margin of Iceland. The movement of water, in turn, triggered a tsunami that impacted the coasts of Norway, Iceland, and Scotland. The height of this tsunami was estimated to have reached tens of meters. The impetus for commissioning this study by the consortium was that a large gas field was discovered just below the detachment of the Storegga Slide. Being very deep water, pumping facilities and pipelines would need to be installed on the seafloor and it was necessary to determine the likelihood of causing another landslide by drilling and extracting the gas. The study focused on understanding the root causes of the landside and the conditions of slope stability.

Among the various possible causes of the landslide, dissociation of methane hydrates was considered. At the time of the landslide, seawater temperature had risen around 8°C since the last deglaciation in part due to the onset of the Gulf Stream, which brings relatively warm water from the tropical Atlantic to the shores of Northern Europe. Dissociation and thinning of the hydrate zone due to climate change was thought to be a possible trigger for the landslide.

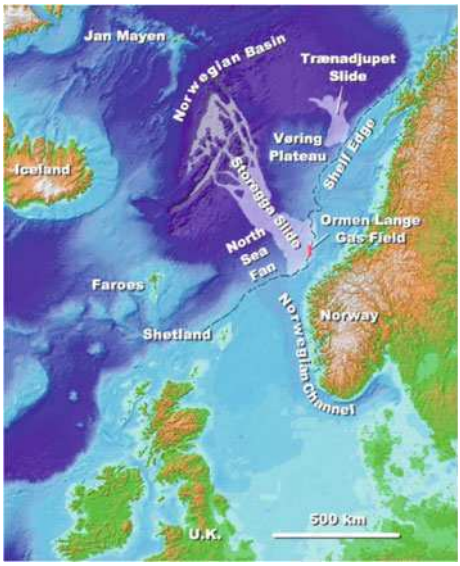

Fig. 10.5 The area of the Storegga slide, which occurred around 7,000 years ago in the Norwegian continental margin [5]

However, from the study, the landslide was found to have originated at the base of the slope and eventually spread upward to the top of slope, where sediments have more strength and are more stable. The likely cause of the landslide was attributed to a major earthquake. While hydrates were not the cause of the Storegga Slide, such submarine landslides can release enormous quantities of methane in the atmosphere. Recent studies of the area show large amounts of methane hydrates near the slide area. However, no evidence of hydrate was found in the slide deposits themselves [21]. It is not clear whether all the methane hydrate was released during the landslide events or if they were never present there to begin with.

10.4 Environmental Impact Studies for Production from Marine Hydrates

The two hydrate production tests at Mallik (see Chap. 8) have allowed for evaluation of environmental risks of onshore hydrate production. On land hydrate production largely involves similar issues common to conventional natural gas and oil recovery. On the other hand, due to lack of experience in the marine setting, it is difficult to fully evaluate all possible risks and their magnitude.

Given the scenarios we have considered in the previous chapters, the primary potential environmental risk factors for the development of a gas production from a marine hydrate reservoir are the following:

- methane leakage from the seafloor around the production wells;
- seafloor subsidence;

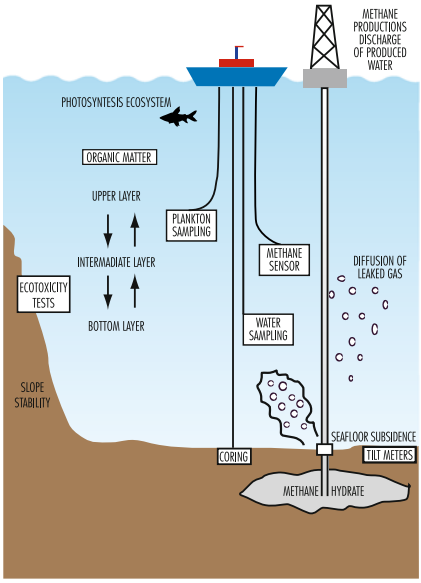

Fig. 10.6 Schematic diagram of the marine environment and remote monitoring to be performed

- submarine landslides;
- discharge of production water into the ocean.

As gas hydrates are destabilized, they produce significant amount of water. Containments in the produced water will likely be diluted through the freshening effect of hydrate dissociation. However, this production water could still be capable of causing detrimental effects in the marine environment.

During Japan's Methane Hydrate R&D Program established in 2001, fundamental research was conducted to develop tools and approaches for conducting the environmental impact assessment and investigate countermeasures [20]. A management plan was proposed for safe commercial production from methane hydrates, prior to onset of any full field development.

Figure 10.6 shows a schematic diagram of the marine environment and of the monitoring to be performed before, during, and after the production tests. In particular, methane leakage is monitored near or on the deep seafloor to detect any increase of dissolved methane concentration. Seafloor deformation is detected by tilt meters and pressure sensors. The quality of the water is controlled as well.

We should remember that methane hydrate dissociation is an endothermic reaction. Therefore, the surrounding sediments are cooled during the process which is naturally self-limiting. In practice, it needs continual energy input to continue. Moreover, the spatial scales of currently identified methane hydrate reservoirs for production are not even remotely comparable to events such as Storegga.

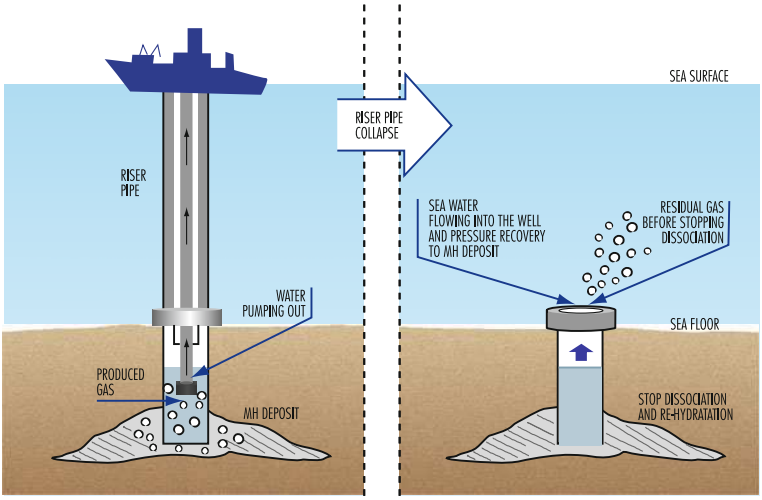

Fig. 10.7 Schematic of the natural fail safe mechanism during offshore production tests [20]

The use of the depressurization method in sandy sediments fully mitigates the risk of gas blowouts from the seafloor, as shown in Fig. 10.7 [20]. If an accident similar to that of the 2010 Gulf of Mexico Deep Water Horizon was to happen, seawater would flow into the production well. The pressure on the deposit would be restored and the hydrate dissociation would soon stop.

10.5 Carbon dioxide Sequestration

The Kyoto Protocol was signed in Japan on 11 December 1997 by 160 nations as an UN initiative (United Nations Framework Convention on Climate Change). Its objective was to control the man-made contribution (anthropogenic) of atmospheric greenhouse gases (mainly focused on CO_2) in order to prevent a potential dangerous impact on the global climate system.

The idea of CO_2 sequestration is to take emitted CO_2, from sources such as power plants, without it entering the atmosphere, and storing it away. The biggest question (after it is captured from the emission source) is how to store this CO_2 safely and effectively. There have been a number of approaches and pilot projects launched with this goal (IPCC 2005). The IPCC identified three main areas where geological storage could be:

1) *Depleted oil and gas reservoirs*. Pumping CO_2 into depleted reservoirs is advantageous because a natural geological seal exists (the reason oil and gas was trapped there to being with) to keep the CO_2 in place. Additionally, the

CO_2 can act as an enhanced oil recovery agent to stimulate further oil and gas production.

2) *Unused coal mines*. These mines offer large volumes underground that are easily accessible. Some of the CO_2 will adsorb on the surface of the coal, displacing methane already there. The released methane can be extracted and exploited.
3) *Deep saline aquifers*. Large salty ground water zones exist at great depths. They offer the ability to store large volumes of CO_2. However, it is difficult to predict the degree of gas permeability in the surrounding geological formations.

Another geological storage area to consider is the ocean. Volumes of CO_2 could be injected and dissolved in the oceans. In fact, this is already occurring without any intentional actions. The ocean is a large sink for CO_2 and is continuously removing CO_2 from the atmosphere. Over 30% of the releasing CO_2 is immediately absorbed. This addition of CO_2 into seawater causes an increase in acidity (lower pH). Increasing acidity can be detrimental to a wide variety of marine life, including corals.

It is known that CO_2 is denser than seawater below around 2,700 m depth. Proposals existed for pumping liquid CO_2 below these depths creating large *lakes* of CO_2 at the bottom of the abyss (IPCC 2005). Hydrate would also form on the interface between the CO_2 and the seawater. In reality, because water currents over the CO_2 would result in dissolving of the hydrate and the CO_2 into the water, this is more of a delayed-release approach. In eloquent experiments by a team from the Monterey Bay Aquarium Research Institute, a remote-operated vehicle was used to release controlled amounts of CO_2 into a beaker on the seafloor at over 3,600 m depth [3]. As shown in Fig. 10.8, the CO_2 in the beaker expanded rapidly as large amount of hydrate formed. It was estimated that a pool of injected CO_2 would expand to over four times its original volume due to hydrate formation and then dissolve away into the ocean. The self-generated fluid dynamic instability as the CO_2 was expelled from the beaker hints at the difficulty that can arise in such a CO_2 disposal approach. Based on the non-permanent storage of CO_2, complex fluid behavior, and the potential catastrophic impact on the local ecology due to increased ocean acidity, open ocean storage is not likely a viable option.

When considering any CO_2 sequestration method, a major concern is the unintended release of CO_2 and potential harm to life it poses. When thinking of CO_2 storage at the bottom of a body of water, we must mention the *Killer Lakes* of Cameroon [8]. Lake Monoun in 1984 and Lake Nyos in 1986 released huge quantities of CO_2 into the atmosphere. The gas, which is heavier than air, spread to surrounding valleys, killing people and animals (more than 1,700 people died in the Lake Nyos event). These violent and deadly de-gasification events in these lakes were caused by a gradual increase in CO_2 from the volcanic subsoil. The pressure at the bottom of the lakes allowed more CO_2 to enter the water than on the surface. When the water in the lake turned over, the water now at the surface was

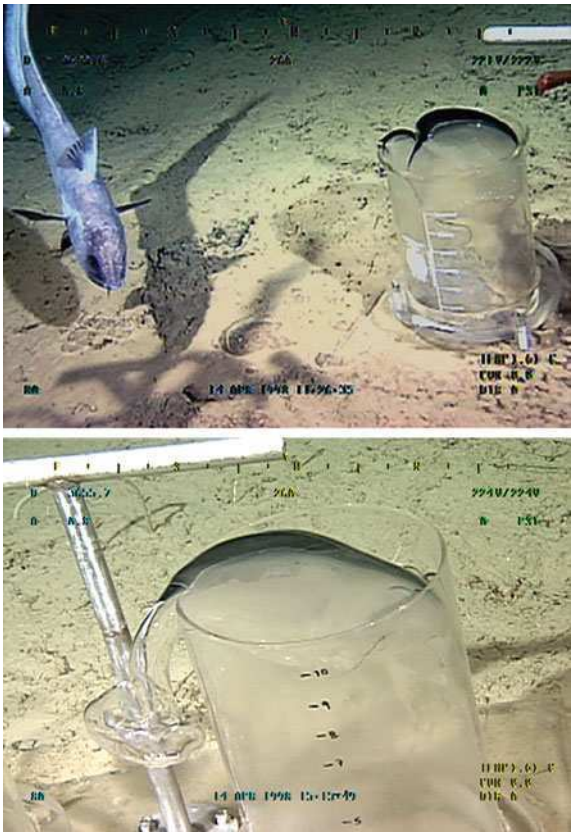

Fig. 10.8 Controlled experiments on the direct disposal of CO_2 on the seafloor at 3,600 m depth. Hydrate quickly formed, causing expansion and forcing the liquid CO_2 to rise and be expelled from the beaker [3]

suddenly super-saturated with CO_2 and released the excess CO_2 in an eruption of gas. These killer lakes are natural phenomena but should be considered when planning any sequestration involving CO_2 injection in deep water.

10.6 Hydrates in Outer Space

And finally we come to the solar system. For the moment, the existence of hydrates on plants, moons, and other solar bodies is based on our knowledge of their pressure and temperature conditions and gases present around them [19]. It is known that the process of magma cooling produces gases such as methane, CO_2, and water. The conditions for hydrate stability exist in both the atmospheres and subsurface for a number of planets and moons in our solar system. Particularly in the gas giant planets (e.g., Jupiter, Saturn, Uranus, and Neptune) gas hydrates are likely more abundant then rocky materials or all of the different crystalline compounds of ice combined [14]. This would make the amount of gas in the form

of hydrates in our solar system second only to gaseous helium and hydrogen. The hydrate formation mechanisms in the solar system have been proposed to be:

1) Direct precipitation from the solar nebula. This process would be responsible for hydrate formation in comets and the Kuiper asteroid belt and would create CO_2, CO, and N_2-rich hydrates;
2) Heating of condensation products of the solar nebula in comets, on Pluto, Charon, Triton, and Plutino. This would form N_2, CO, and methane-rich hydrates;
3) Direct precipitation from circumplanetary nebulae of the outer planets, Callisto, and the moons of Saturn, Uranus, and Neptune. This would create N_2, CO, and methane-rich hydrates;
4) Formation in the primordial hydrosphere of Earth, Mars, Europa, Ganymede, and Callisto. This would create SO_2, CO_2, and N_2-rich hydrates;
5) Formation in plants with more evolved hydrospheres (Permafrost of Mars and cryosphere of Europa). This would create SO_2 and CO_2-rich hydrates.
6) Formation from biogenic sources of methane. This forms methane-rich hydrate on the permafrost and marine sediments on Earth and possibly on Mars and Europa.
7) Formation from thermogenic gas related to oil and gas deposits on Earth. This would create hydrates rich in CH_4, C_2H_6, C_3H_8, and C_4H_{10}.

The Martian atmosphere is composed of 90% CO_2. The remaining 10% is water vapor, nitrogen, and other gases. CO_2 hydrates can exist just below the Martian surface due to the very cold temperatures (from −127°C to −40°C). It is thought that seasonal changes in temperature on surface cause continuous variations of atmospheric composition due to hydrate formation and dissociation [17]. It is believed that CO_2 hydrates exist on the surface of Mars in impressive polar caps and in the atmosphere in the form of clouds. It is also estimated that the gas hydrate stability zone extents over 1 km below the surface. The possibility of obtaining in situ resources such as water derived from hydrates could help stimulate attempts at human colonization of Mars [22].

References

1. Aharon P, Graber ER, Roberts HH (1992) Dissolved carbon and 13C anomalies in the water column caused by hydrocarbon seeps on the northwestern Gulf of Mexico. Geo-Marine Lett 12:33–40
2. Blunier T, Chappellaz J, Schwander J (1995) Variations in atmospheric methane concentration during the Holocene epoch. Nature 374:46–49
3. Brewer PG, Friederich G, Peltzer ET, Orr FM Jr (1999) Direct experiments on the ocean disposal of fossil fuel CO_2. Science 284:943–945
4. Brook EG, Sowers T, Orchardo J (1996) Rapid variations in atmospheric methane concentration during the past 110,000 years. Science 273:1087–1091

5. Bryn P, Berg K, Forsberg CF et al (2005) Explaining the Storegga slide. Mar Petrol Geol 22:11–19
6. Camerlenghi A, Panieri G (2007) Aspetti ambientali. In: Giavarini C (ed) Energia immensa e sfida ambientale. Gli idrati del metano. Editrice La Sapienza, Roma, Italy (in Italian)
7. Chapellaz J, Barnola J, Raynaud D et al (1990) Ice core record of atmospheric methane over the past 160,000 years. Nature 345:127–131
8. Clarke T (2001) Taming Africa's killer lake. Nature 409:554–555
9. Dickens GR (2004) Hydrocarbon-driven warming. Nature 429:513–515
10. EPICA Members (2004) Eight glacial cycles from an Antarctic ice core. Nature 429:623–628
11. Hesselbo SP, Grocke DR, Jenkyns HC et al (2000) Massive dissociation of gas hydrate during a Jurassic oceanic anoxic event. Nature 406:392–395
12. IPCC (2001) Climate change: the scientific basis. Contribution of working group I to the third assessment report of the intergovernmental panel on climate change. In: Houghton JT, Ding Y, Griggs DJ, Noguer M, van der Linden PJ, Dai X, Maskell K, Johnson CA (eds). Cambridge University Press, Cambridge
13. Jahren AH (2002) The biogeochemical consequences of the mid-Cretaceous Superplume. J Geodyn 34:177–191
14. Kargel JS (2001) Formation, occurrence, and composition of gas hydrates in the solar system. Earth system processes—global meeting. Session No. T9: the role of natural gas hydrates in the evolution of planetary bodies and life. Edinburgh, 24–28 June 2001
15. Kennett JP, Cannariato KG, Hendy IL, Behl RJ (2000) Carbon isotopic evidence for methane hydrate instability during quaternary interstadials. Science 288:128–133
16. Kennett JP, Cannariato KG, Hendy IL, Behl RJ (2003) Methane hydrates in quaternary climate change: the clathrate gun hypothesis, vol 54. AGU Special Publication
17. Makogon YF (1997) Hydrates of hydrocarbons. PennWell Books, Tulsa
18. Maslin M, Owen M, Day S, Long D (2004) Linking continental-slope failures and climate change: testing the clathrate gun hypothesis. Geology 32(1):53–56
19. Miller SL (1961) The Occurrence of gas hydrates in the solar system. Proc Natl Acad Sci U S A 47(11):1798–1808
20. Nagakubo S, Arata N, Yabe I et al (2011) Environmental impact assessment study on Japan's methane hydrate R&D program. Fire in the ice, 4–11 January
21. Paull CK, Ussler W III, Holbrook WS (2007) Assessing methane release from the colossal Storegga submarine landslide. Geophys Res Lett 34:L04601
22. Pellenbarg RE, Max MD, Clifford SM (2003) Methane and carbon dioxide hydrates on Mars: potential origins, distribution, detection, and implications for future in situ resource utilization. J Geophys Res. doi:10.1029/2002JE001901
23. Reagan MT, Moridis GJ (2007) Oceanic gas hydrate instability and dissociation under climate change scenarios. Geophys Res Lett 34:L22709
24. Reagan MT, Moridis GJ (2008) Dynamic response of oceanic hydrate deposits to ocean temperature change. J Geophys Res 113:C12023
25. Schaefer H, Whiticar MJ, Brook EJ et al (2006) Ice Record of d13C for atmospheric CH_4 across the younger Dryas-Preboreal transition. Science 313(5790):1109–1112
26. Solheim A, Berg K, Forsberg CF, Bryn P (2005) The Storegga slide complex: repetitive large scale sliding with similar cause and development. Mar Petrol Geol 22:97–107
27. Sowers T (2006) Late quaternary atmospheric CH_4 isotope record suggests marine clathrates and stable. Science 311(5762):838–840
28. Wignall PB (2001) Large igneous provinces and mass extinctions. Earth-Sci Rev 53:1–33
29. Woller MJ, Ruppel C, Pohlman JW et al (2009) Permafrost gas hydrates and climate change: lake-based seep studies on the Alaskan north slope. Fire in the Ice, 6–9, Summer

Index

C. Giavarini and K. Hester, *Gas Hydrates*, Green Energy and Technology,
DOI: 10.1007/978-0-85729-956-7,